# DIFFERENTIAL GLOBAL POSITIONING SYSTEM NAVIGATION: A GEOMETRICAL ANALYSIS

S. P. MERTIKAS

April 1983

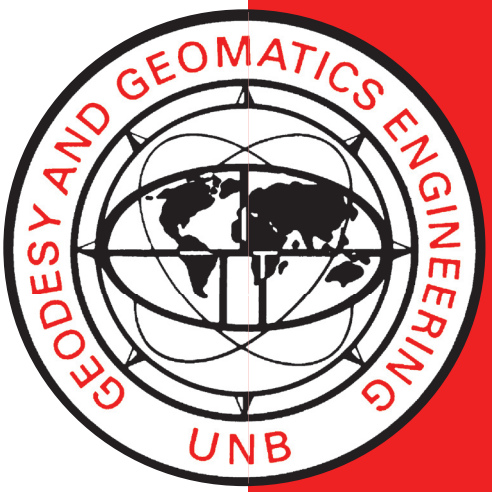


TECHNICAL REPORT
NO. 95

# PREFACE

In order to make our extensive series of technical reports more readily available, we have scanned the old master copies and produced electronic versions in Portable Document Format. The quality of the images varies depending on the quality of the originals. The images have not been converted to searchable text.

# DIFFERENTIAL GLOBAL POSITIONING SYSTEM NAVIGATION: A GEOMETRICAL ANALYSIS

Stelios P. Mertikas

Department of Surveying Engineering
University of New Brunswick
P.O. Box 4400
Fredericton, N.B.
Canada
E3B 5A3

April 1983

Latest Reprinting June 1993

# PREFACE

This report is an unaltered version of the author's M.Sc.E. thesis submitted to this Department under the same title.

The thesis advisor for this work was Professor David E. Wells and financial assistance was in part from the Natural Sciences and Engineering Research Council of Canada, the Bedford Institute of Oceanography and the University of New Brunswick.

The assistance rendered by others is detailed in the acknowledgements.

## ABSTRACT

This thesis examines and evaluates some geometrical aspects of a method called "differential navigation", which is used as a means of real time calibration for a navigation system. Particularly, the evaluation and analysis is applied to a new satellite-based radionavigation system, known as NAVSTAR-GPS (NAVigation Satellite Timing And Ranging system-Global Positioning System).

The NAVSTAR-GPS, being developed by the United States Department of Defense, is scheduled to be fully operational by the end of the decade and is capable of providing realtime continuous positions accurate to 10 metres. Field test results using some of the current prototype GPS satellites have manifested these capabilities.

These early results and other studies led the United States, for national security reasons, to intentionally curtail the GPS capabilities to the general public and provide accuracies of the order of 200 metres.

The need for better accuracies required by a large class of "unauthorized users" prompted us to extend the conventional performance capabilitity of the GPS to the differential one. Differential GPS navigation provides an opportunity to thousands of unauthorized users, unable to gain the full benefit of the GPS system, to effectively make use of the system under intentionally degraded conditions and retrieve the original signals.

Under certain assumptions and through a simulation computer program, this study evaluated and demonstrated the validity and feasibility of the above concept, with main emphasis on the investigation of various geometrical aspects related to the differential

operation. Inferences correspond only to marine applications (two dimensional) of the GPS 18-satellite constellation considering hypothetical intentional degradations.

Recommendations for the continuation of this research are also given.

TABLE OF CONTENTS

LIST OF FIGURES

LIST OF TABLES

## NOTATION

1. Position vector and Cartesian coordinates of the jth ground station (receiver):

$$\underline{R}_j = [X_j, Y_j, Z_j]^T \quad .$$

2. Position vector and Cartesian coordinates of the ith satellite at some epoch $t_k(\tau)$:

$$\underline{r}_i[t_k(\tau)] = [x_i(t_k(\tau)), y_i(t_k(\tau)), z_i(t_k(\tau))]^T \quad .$$

3. Geometric (true) range vector from jth receiver to ith satellite:

$$\underline{\rho}_{ij} = [\xi_{ij}, n_{ij}, \zeta_{ij}]^T \quad .$$

4. Pseudorange vector from jth receiver to ith satellite:

$$\underset{\sim}{\underline{\rho}}_{ij} \quad .$$

5. Magnitude of geometric (true) range:

$$\rho_{ij}(t_k) = \sqrt{\{X_j - x_i(t_k)\}^2 + \{Y_j - y_i(t_k)\}^2 + \{Z_j - z_i(t_k)\}^2} \quad .$$

6. Superscript zero in parenthesis indicates preliminary values:

$$\rho_{ij}^{(o)} \quad .$$

7. Observation vector of pseudoranges from jth receiver to four satellites:

$$\underline{L} = [\tilde{\rho}_{1j}, \tilde{\rho}_{2j}, \tilde{\rho}_{3j}, \tilde{\rho}_{4j}]^T \quad .$$

8. Misclosure vector:

$$\underline{W} = F(\underline{X}^{(o)}, \underline{L}^{(o)}) \quad .$$

9. Design matrices:

$$A = \{\frac{\partial F}{\partial \underline{X}_j}\Big|_{\underline{X}_j}(o)\} \quad ; \quad B = \{\frac{\partial F}{\partial \underline{L}}\Big|_{\underline{L}}(o)\}$$

10. Correction vector:

$$\underline{\delta X} = \underline{X}_j - \underline{X}_j^{(o)} \quad .$$

11. Vector of residuals:

$$\underline{V} = \underline{L} - \underline{L}^{(o)} \quad .$$

12. Receiver's solution:

$$\underline{X}_j = [X_j, Y_j, Z_j, \Delta t_{u_j}]^T \quad .$$

13. Unit vector from the user position (j) to the ith satellite:

$$\underline{U}_i = [u_i, v_i, w_i]^T \quad .$$

ACKNOWLEDGEMENTS

I am particularly grateful to John L. Lyall, Chief of the Navigation Department of the Defense Mapping Agency; to LCDR Gerald B. Mills of the Naval Postgraduate School at Monterey, CA; to Dr. Jacques Beser of Intermetrics Inc.; to Richard J. Anderle of the Naval Surface Weapons Center; to Brad Montgomery of Texas Instruments Incorporated; to Rudolph Kalafus of the U.S. Department of Transportation; and to Dr. Charles C. Counselman III of The Massachusetts Institute of Technology for providing invaluable help and information concerning differential GPS navigation.

I wish to express my deep thanks to my supervisor, Professor David E. Wells, for enabling me to foster a spirit of better insight into thinking, learning, listening and judging, and above all for being a good friend of mine. Being a perfectionist, he could not be satisfied with anything that seemed to him to fall below the highest standard either in the choice of precise words or the careful and orderly arrangements of the context.

Special thanks are also due to Dr. D. Delikaraoglou for his tremendous help with the simulation computer program.

The penetrating wisdom and ample knowledge of Dr. Y.Q. Chen contributed toward the clarification of the difficult concepts in this study. A benevolent scientist who attaches great importance to his reputation as a scholar, both in respect of personal esteem and because it determines his livelihood.

Professor George Veis of the National Technical University of Athens, the leading spirit of satellite geodesy, has done much to

nourish the idea of inquiry for different applications of the Surveying Engineer. New tendencies and interests of his pupils will always contain a strong element of his views.

Another acknowledgement of a debt too great to be satisfied by a few words goes to Marinos Kavouras and Costas Armenakis. Common sufferings and common hopes for a brighter future have united us and have led to a lasting and sincere friendship. Without them, my stay in the little university town of Fredericton would have been exceedingly difficult for me.

Special thanks are also given to Professor P. Vanicek of the Department of Surveying Engineering, to Professor D. Livesey of the Physics Department and to Dr. G. Lachapelle of Nortech Surveys (Canada) Inc. for their constructive criticism of the manuscript.

I am deeply indebted to Wendy Wells for her excellent word processing and for translating my ungrammatical way of thinking into readable and functional English.

I also express my appreciation to my colleagues of the Surveying Engineering Department for their exhilarating cooperation.

This work was supported in part by operating and strategic grants from the Natural Sciences and Engineering Research Council of Canada, and in part by the Bedford Institute of Oceanography.

# 1

# Introduction

This thesis examines and evaluates some geometrical aspects of a method called "differential navigation", which is used as a means of real time calibration for a navigation system. Particularly, this evaluation and analysis is applied to a new satellite-based radionavigation system, known as NAVSTAR-GPS (NAVigation Satellite Timing And Ranging system-Global Positioning System).

NAVSTAR-GPS is currently under development by the United States Department of Defense (USDOD). The GPS provides continuous, all weather, worldwide, accurate, three-dimensional navigation and has the potential to replace many existing radionavigation systems [Milliken and Zoller, 1978; Stansell, 1978; USDOD, 1982].

It should be noted that although NAVSTAR-GPS is designed to satisfy the positioning and navigation requirements of any type of vehicle (air-borne, ship-borne, land-based), this study considers only the marine applications of the system.

Field test results using some of the current prototype GPS satellites have indicated that accuracies of the order of a few metres can be achieved [Parkinson, 1979; Lachapelle et al., 1982; Payne, 1982]. These early results and other studies led the U.S.A. to establish a special working group of people from the Department of Defense and the

Department of Transportation (USDOT), whose purpose is to study and plan the policies for all radionavigation systems under U.S. government control. Every year this group publishes a document called the Federal Radionavigation Plan (e.g., USDOD [1982]). According to this document, it is proposed that the performance of the GPS be intentionally degraded to 200 metres CPE (Circular Probable Error). The term CPE is one of the adopted accuracy measures for a radionavigation system, and represents the radius of a circle containing 50% of the fixes being made [Burt et al., 1967]. Therefore the full accuracy of the GPS system will not be available to unclassified civil users.

Denial of accuracy, or Selective Availability as the USDOD calls it, may be implemented in the late 1980s, when GPS will be fully operational. If so, then this policy will represent a disappointment and a great problem to a large number of civil users who need accuracies of the order of a few tens of metres. Offshore oil exploration, seismic surveys, marine gravity and magnetic measurements, hydrographic surveys, physical oceanography operations, fishing, collision avoidance, harbour and harbour approach navigation, delineation of oil reserves, pipeline laying, etc., are some of the marine applications requiring better accuracies than those which will be provided after the implementation of the Selective Availability. Table 1.1 gives an overview of the accuracy requirements for those marine operations that cannot be satisfied by GPS after it has been intentionally degraded.

The need to provide better accuracies than would be available from GPS if degraded for Selective Availability, prompted us to consider the differential GPS navigation concept as described by Teasley et al. [1980], Cardal and Cnossen [1980], Beser and Parkinson [1981], and

| Type | | Accuracy |
|---|---|---|
| Conventional Seismic Surveys | Position repeatability | 150 m CPE |
| | Position absolute accuracy | 150 m CPE |
| | Sequential positions | 15 m CPE |
| Well site Surveys | Position repeatability | 50 m CPE |
| | Position absolute accuracy | 100 m CPE |
| Drilling vessel Positioning | Approach to location | 50 m CPE |
| | In place position confirmation | 5 - 10 m CPE |
| Offshore hydrography | 1:100 000 scale | 100 m CPE |
| Inshore hydrography | 1:10 000 scale or greater | 10 m CPE |
| 3D Seismic Surveys | Position repeatability | 20 m CPE |
| | Sequential positions | 5 m CPE |
| Harbour, harbour approach | Position repeatability | 4 - 5 m CPE |

TABLE 1.1

Accuracy Requirements that Cannot be Satisfied After the Implementation of the Selective Availability (after Radio Technical Commission for Marine Services [1981]).

Cnossen et al. [1981].

A receiver, called a differential monitor station located on a well-surveyed site, serves as a means of calibration for the navigation system (see Figure 1.1). This receiver continuously receives radionavigation signals and compares them with values estimated from its known position. The differences between computed and known positions become the differential corrections and are sent to nearby users to correct their position. Therefore, a data link is required between the users and the differential monitor station.

Differential GPS navigation is a possible solution to the Selective Availability problem, since the effects of any common errors or intentional degradation to both receivers (monitor and user) will be reduced when using a differential technique. Any degradation techniques applied to GPS will appear to both the user and the differential monitor station with a similar structure. Therefore it is likely that the undegraded accuracy can be partially retrieved by using differential GPS navigation.

As stated previously, the objective of this thesis is to analyse, evaluate and test some geometrical parameters which affect differential GPS navigation when Selective Availability is present.

Differential GPS navigation has already been investigated by other people. Ruedger [1981] studied the properties of the upper layer of the ionosphere using differential techniques; Howel et al. [1980] examined the update rate of the differential corrections; Cardal and Cnossen [1980], Teasley et al. [1980], and Cnossen et al. [1981] described the various types of differential techniques and their implementation. All the above studies refer to a close-range (10 km approximately)

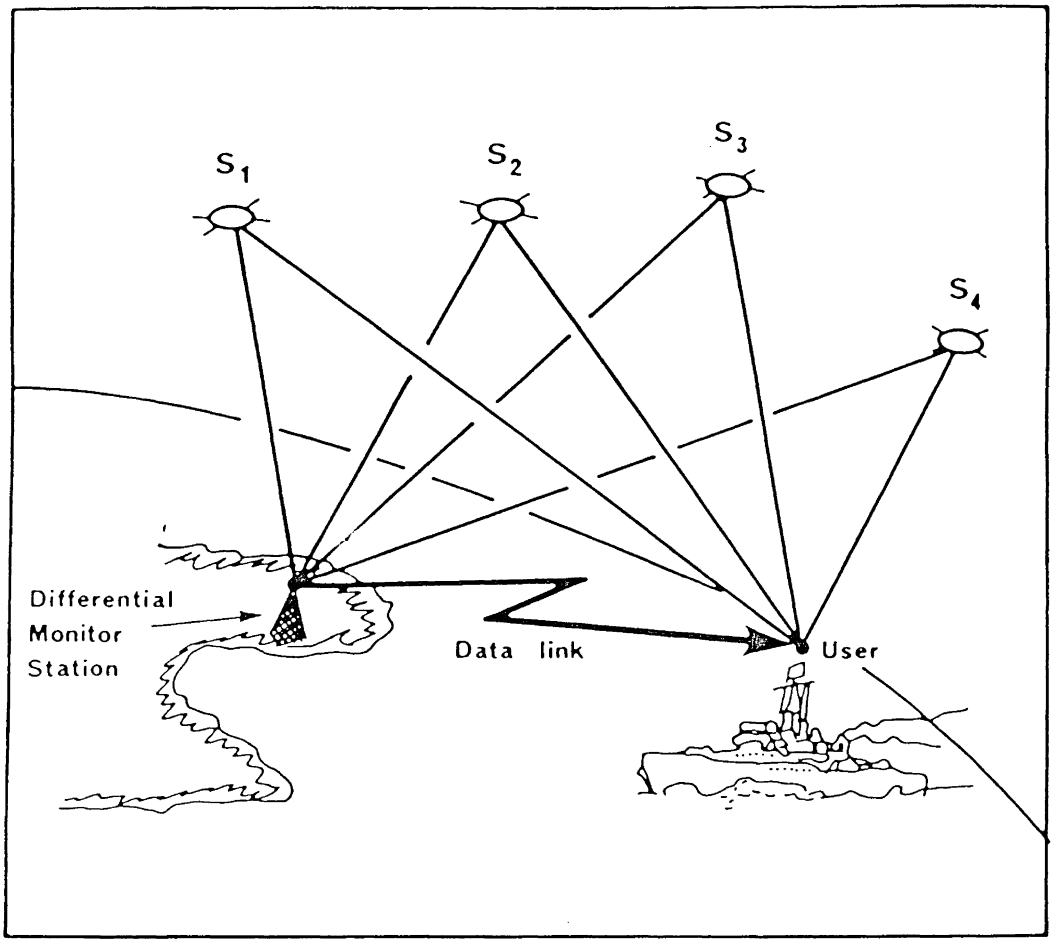


FIGURE 1.1
Differential GPS Navigation.

application of differential GPS navigation. Beser and Parkinson [1981] evaluated the degradation of accuracy of differential GPS navigation due to distance from the monitor.

A lot of parameters are playing an important role when one tries to evaluate the differential GPS navigation concept. The update rate of the differential corrections (monitor correction broadcast rate), the location of the differential monitor station, the distance of the user from the monitor, the actual implementation (if any) of the Selective Availability, the type of differential corrections, etc., are some of the parameters which affect differential GPS navigation. A lot of them have been examined before by other people, and a brief description of what has been done so far was given previously.

This thesis contains the following contributions:

1) The development of various models for the Selective Availability.
2) The development of models for differential corrections.
3) The development of simulation software to implement and test both the above points.
4) Determination of answers to some specific points, such as
   a) How close to undegraded point positioning can we come by using differential techniques? Is it possible to recover most of the undegraded accuracy after the application of the Selective Availability in the form represented by the various models developed?
   b) Is it possible to apply differential corrections to a user at very large distances from the monitor?
   c) If the user moves in various directions away from the differential monitor station, does this play a role in the

performance of the differential GPS navigation?

d) The period of revolution of the GPS satellites about the earth is approximately 12 hours. This means that over 24 hours different satellites will be seen above the horizon and there will be variations in the satellite-monitor or satellite-user geometry. In obtaining a navigation fix, this geometry will be sometimes stronger than at other times. Does this variation affect differential GPS navigation?

e) One of the contributions of this thesis, as mentioned before, is the development of various models for the implementation of the Selective Availability. Is the differential GPS concept more effective in recovering the actual GPS signals from some kinds of degradation than from others?

This thesis is divided into several parts and a brief description of them follows.

At the outset the backbone of the whole study is established. A general description of the new satellite NAVSTAR-GPS system is given, with emphasis on the system's accuracy, its diverse applications for marine operations, the present and future satellite constellations, etc. A detailed description can be found elsewhere [Milliken and Zoller, 1978; Payne, 1982, Wells et al., 1982]. The development of GPS receivers is the most changing theme and therefore we will not dwell on it.

The chapter on the "Accuracy Measures for Navigation" deals with the most common and most frequently adopted accuracy measures. Various accuracy estimates are described which provide an accuracy assessment for a navigation system. Circular Probable Error (CPE), 2drms,

Geometric Dilution of Precision (GDOP), error ellipse, and accuracy deviations expressed in percentiles, are described.

Differential GPS navigation is examined in Chapter 4. Questions considered include the importance of differential GPS navigation, the kinds of differential corrections, the types of differential GPS navigation which can be implemented, and the major factors that affect differential navigation.

In order to evaluate the validity of the differential GPS navigation concept with respect to various parameters, such as distance from the monitor, type of intentional degradation, kinds of differential corrections, etc., a simulation computer program was written. The function, the assumptions made, and the principles of this simulation are explained in Chapter 5, "Simulation Description".

Chapter 6 is devoted to the evaluation and explanation of the obtained results, whereas the last chapter gives the conclusions along with some recommendations for future plans.

The difficulties encountered in finding a complete reference when one tries to understand how a navigation fix is computed using GPS observations, gave rise to Appendix I on "User Navigation Solution". This appendix is divided into two segments: The first one gives a description of how to compute satellite positions given a navigation message, and the second develops the observation equations used for the solution.

# 2

# Present Status of GPS

## 2.1 General Description

A very rudimentary introduction to the GPS system was given in the previous chapter. Exactly what it is, what it does, how it works, why use GPS, what are the important civil navigation applications, are some of the questions that still need to be answered here. Thus this chapter will further explore the potential of the GPS system.

The NAVSTAR-GPS originated through a consolidation and coordination of efforts from all the components of the U.S. Department of Defense. Although this new radionavigation system was conceived mainly for military appplications, today it is proposed for numerous civil applications as well.

As mentioned previously, GPS will provide suitably equipped users with worldwide, accurate, all-weather, three-dimensional navigation information (position, velocity) and time. The GPS is presently scheduled to be fully operational by 1988. In the interim, six prototype satellites have been placed in orbit, with four additional launches planned before 1985 [Wells et al., 1981]. These satellites serve as a means of validating and establishing the operability of the system. The final operational satellite constellation will consist of

18 satellites in six orbital planes, with three satellites equally spaced in each plane at an inclination of $55^{o}$ and a nominal period of a satellite revolution T = 11 hr, 57 min, 57.26 sec [Payne, 1982]. The above constellation will be possibly extended to a 24-satellite constellation [USDOD, 1982]. Although this 18-satellite constellation (Figure 2.1) will ensure a minimum of four visible satellites to a user at all times [USDOD, 1982], it may experience occasional outages. An outage is either when a user can only obtain data from less than four satellites (standard definition), or when a three-dimensional error fix is about three times the three-dimensional root-mean-square (RMS) error of the high performance user (more or less arbitrary definition, Jorgensen [1980]).

The GPS comprises three major segments: the space segment, the control segment, and the user segment. These segments are shown in Figure 2.2, and a complete account can be found in Milliken and Zoller [1978], Parkinson [1979], and Payne [1982].

## 2.2 GPS Navigation Signals

Navigation using GPS can be performed by the satellites transmitting radionavigation signals and the user receiving them. Each GPS satellite transmits navigation signals on two frequencies, the primary $L_1$ (1575.42 MHz) and the secondary $L_2$ (1227.6 MHz), which enable corrections for ionospheric delays [Ward, 1981]. These frequencies are multiples of the 10.23 MHz (mega bits per second (Mbps)) reference frequency of the satellite's atomic (Cesium, Rubidium or crystal) clock, that is

$L_1$ = 1575.42 MHz = 154 × 10.23 MHz, and

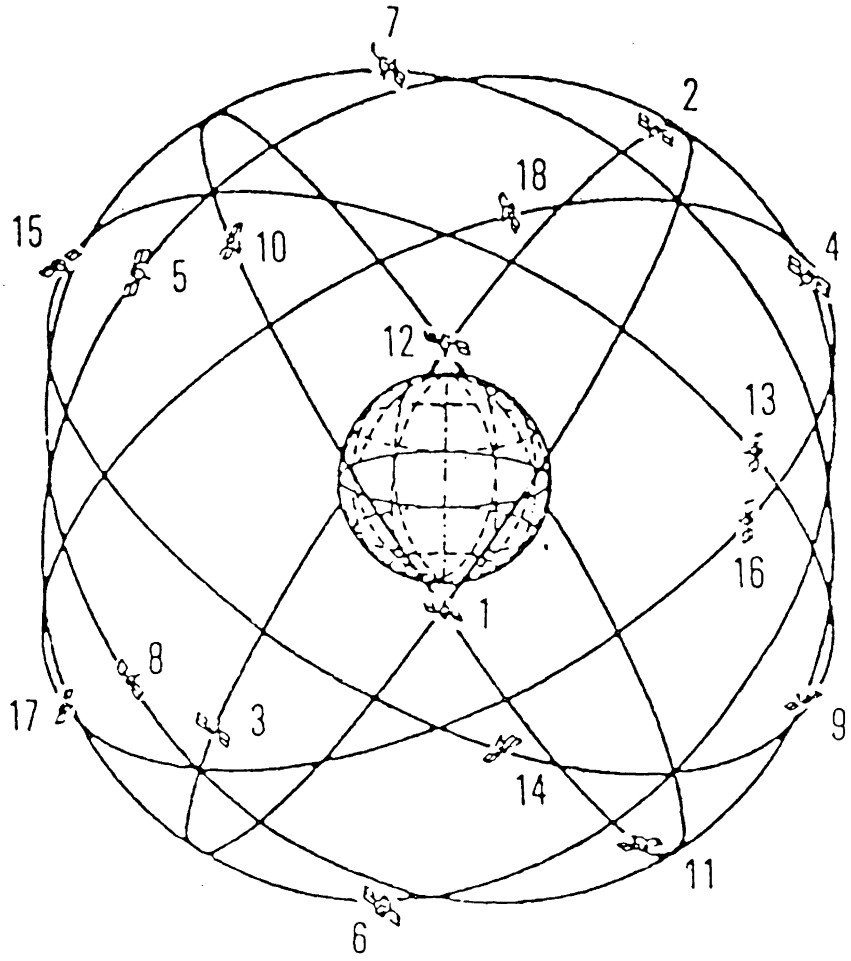


FIGURE 2.1

18-Satellite Constellation (after Jorgensen [1980]).

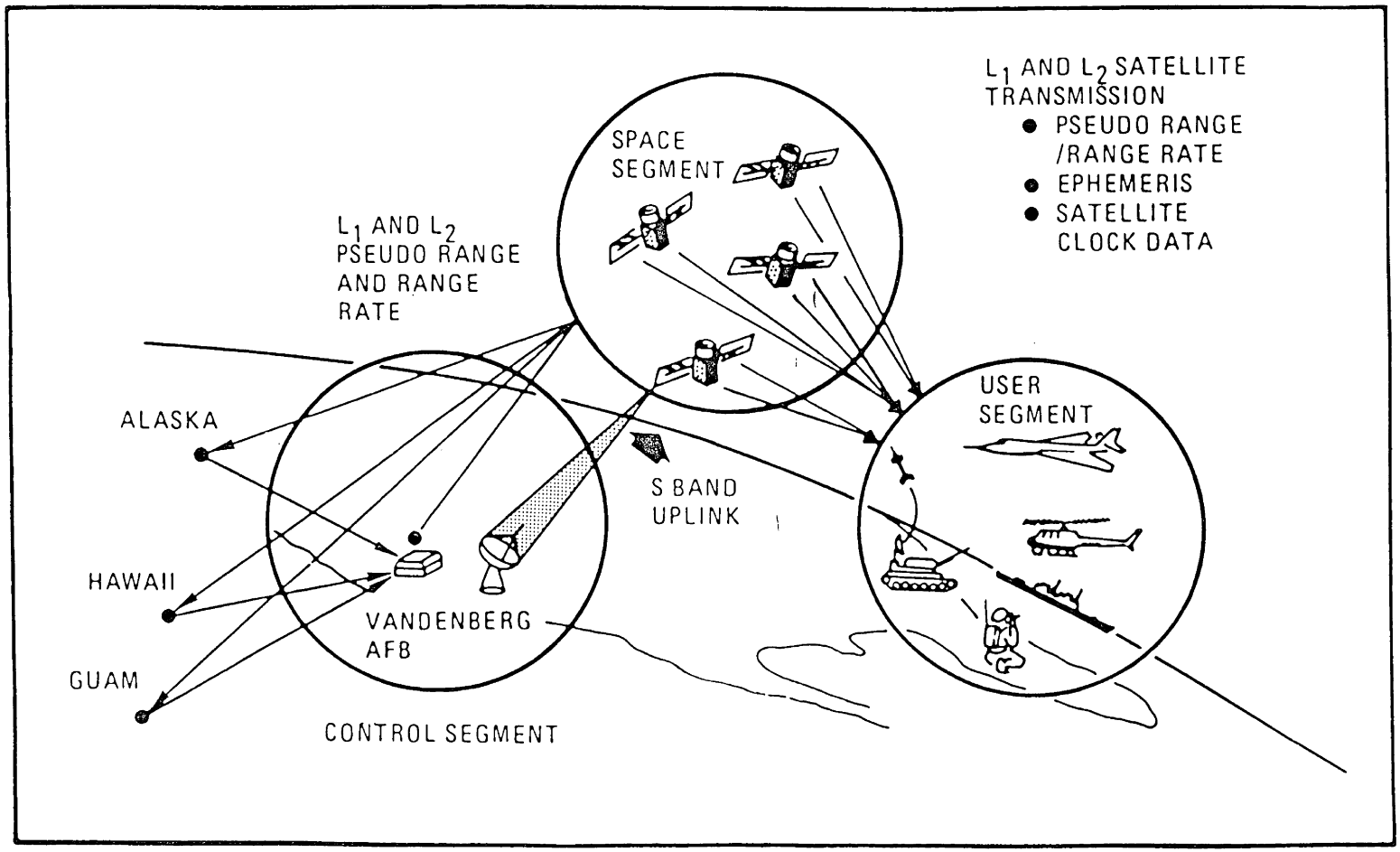


FIGURE 2.2

GPS Segments (after Cardall and Cnossen [1981]).

$L_2$ = 1227.6 MHz = 120 × 10.23 MHz.

The stability of these clocks is better than a few parts in $10^{-13}$ during several hours (approximately 12 hours).

The $L_1$ and $L_2$ signals reaching the receiver (user) at any given instant left the transmitter (satellite) some time before. If time marks are embedded in the signals, which at the receiver (user) would identify the instant of transmission, then the time spent by the signal to cover the distance from the satellite to the user can be determined. By multiplying this time by the speed of light, the user can determine his distance or range from the satellite. These time marks can be implemented by shifting the phase of the carrier by an instantaneous value of a sequence of ones and zeros (zero means phase-shift whereas one does not). This is illustrated in Figure 2.3. The above modulation is made through a technique of code sequence called spread spectrum [Harris, 1973; Dixon, 1975]. In this case time marks are the code sequence modulation (also called the Pseudo-Random-Noise (PRN) code) which act as a noiselike (but deterministic) carrier of information [Spilker, 1978].

If the receiver is synchronized to the satellite clock and if it generates an exact replica of the emitted signal, then the travel time from the satellite to the user can be determined. The receiver matches its internal code against the code modulation on the signal it is receiving and measures the number of bits of code delay (time marks) between the received signals and its internal reference code. This defines the time difference between transmission and reception, or in other words the time spent by the signal to travel from the satellite to the receiver (user), see Figure 2.4.

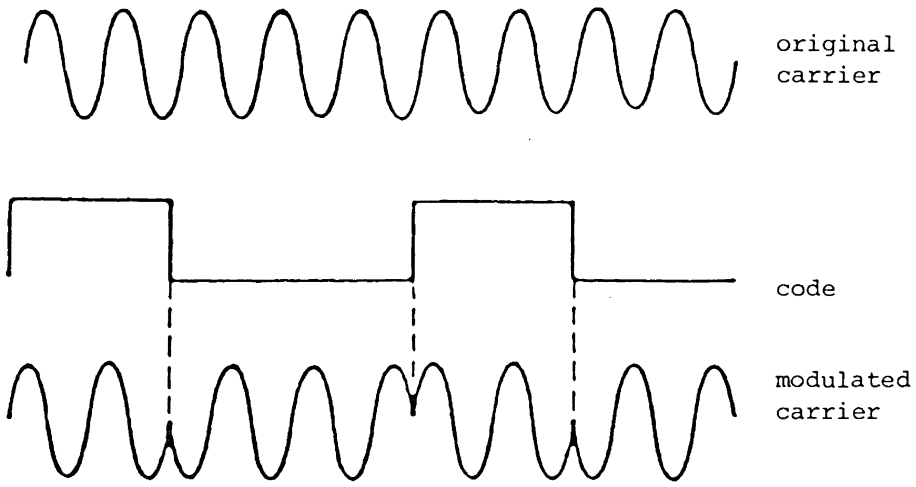


FIGURE 2.3

GPS Coded Phase Modulation.

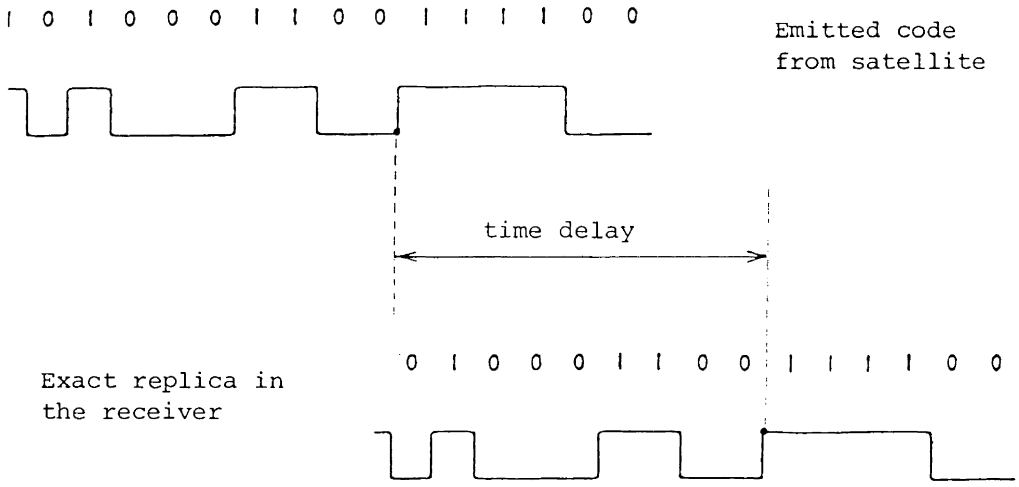


FIGURE 2.4

Determination of Time Delay in the Receiver.

Three kinds of PRN-codes are superimposed on the GPS satellite radionavigation signals: A 1.023 MHz (Mbps clock rate) Coarse/Acquisition (C/A) code, a 10.23 MHz (Mbps) Precision (P) code, and a 50 Hz (bps) Data (D) code.

The C/A-code is modulated only on the $L_1$ frequency and provides a coarse ranging signal. It repeats itself every millisecond and therefore failure to identify the proper millisecond entails an uncertainty in range of

$$K\{1 \text{ millisecond} \times (\text{speed of light})\} =$$

$$= K\{1 \text{ millisecond} \times (300{,}000 \text{ km/sec})\} =$$

$$= K\{10^{-3} \text{ sec} \times (300{,}000 \text{ km/sec})\} =$$

$$= K\{300 \text{ km}\}$$

where K is an integer number. The C/A-code also serves as an acquisition aid to gain access to the precise (P) code by providing appropriate information [van Dierendonck et al., 1978].

The P-code is normally very difficult to match because of its very long length. It has a period of 267 days but only 7-day portions of it are assigned to different satellites. Therefore we have 37 different P-codes, since the one-week signals assigned do not overlap with the P-code of any other satellite.

Navigation information and other data are modulated on the carrier at a rate of 50 bits per second. This is termed the D-code. This message contains information on the satellite ephemeris, satellite identification, satellite-clock parameters, status of the GPS, system time, etc. Table 2.1 gives a summary of the characteristics of the GPS signals.

| Parameter | C/A-code | P-code | Data |
|---|---|---|---|
| Code rate | 1.023 Mbps | 10.23 Mbps | 50 bps |
| Code length | 1023 bits (= 1 millisecond) | $\approx 6 \times 10^{12}$ bits (= 7 days = 1 week) | 1500 bits (30 secs) |
| Transmission frequency | $L_1$, may be $L_2$ as well [Payne, 1982] | $L_1$ and $L_2$ | $L_1$ and $L_2$ |

TABLE 2.1

Summary of GPS Signal Parameters
(after Spilker [1978]).

## 2.3 GPS Measurements

Knowing the positions of the GPS satellites at any time as well as the associated clock errors provided by the D-code, and measuring the range from the user to the satellite we can deduce that the user's position will lie on the surface of a sphere centred at the satellite. By measuring three ranges to three satellites simultaneously, the user's position can be determined by the intersection of three spheres centred at each satellite.

Since the user does not usually carry a precision atomic clock (but a fairly inexpensive crystal clock) another unknown is added to the computations, that is, the user clock bias from GPS system time (offset) [USDOD, 1982]. Therefore three range measurements are required for the position determination (X, Y, Z or $\phi$, $\lambda$, h) and one for the user clock bias ($\Delta t_{uj}$). One should at least observe four satellites simultaneously to compute a complete (X, Y, Z, $\Delta t_u$) three-dimensional fix by solving a system of four equations with four unknowns (four-parameter solution)

(see Figure 2.5).

This absolute three-dimensional position can be referred to any appropriate selected coordinate system. One fundamental geocentric system applicable to satellite positioning is the earth-fixed, earth-centred reference system called the World Geodetic System 1972 (WGS-72). The WGS-72, as shown in Figure 2.6, is characterized by the following properties (details can be found in Appendix I):

1. The X-axis passes through the intersection of the equator and the Greenwich meridian.
2. The Z-axis passes through the north pole.
3. The Y-axis completes the right-handed coordinate system.

The condition of simultaneity of range measurements requires that there is no mutual interference of the GPS satellite signals. This is one of the properties of the spread spectrum techniques, and this is one of the major reasons used for the selection of this type of signal [Dixon, 1975; Spilker, 1978].

In reality, the basic GPS measurement is not a direct geometric distance from the user to the satellite but a range in terms of raw receiver measurement which includes atmospheric delays (tropospheric, ionospheric) and user clock bias. This is termed a pseudorange observation ($\tilde{\rho}_{ij}$) and is illustrated in Figure 2.7. Because the satellites themselves are in motion, the system allows us to measure another inherently complementary quantity, that is, integrated Doppler data [Jorgensen, 1980; Hatch, 1982]. Hence, two types of navigation data are available through the GPS system: pseudoranges and integrated Doppler data (pseudorange rate). This allows the user to compute a three-dimensional position velocity and time information (user clock

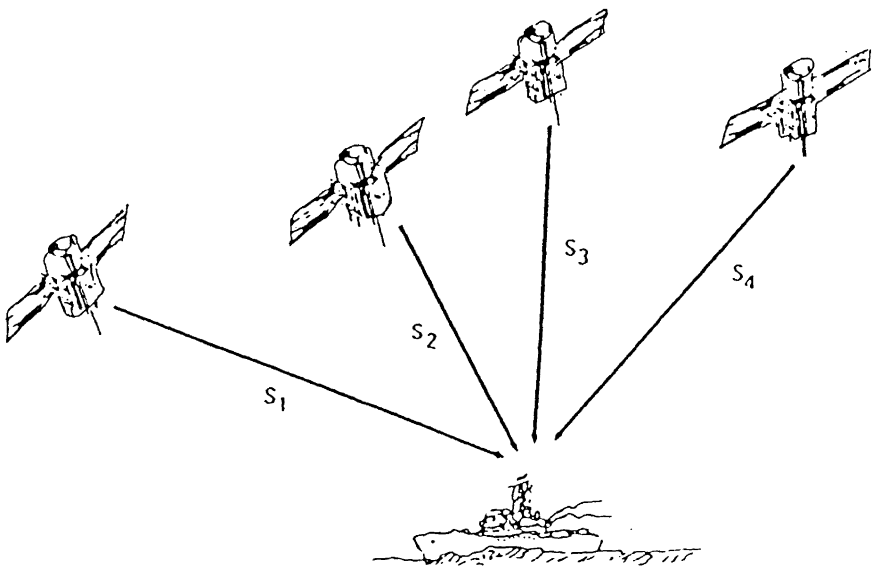


FIGURE 2.5

Navigation Fix.

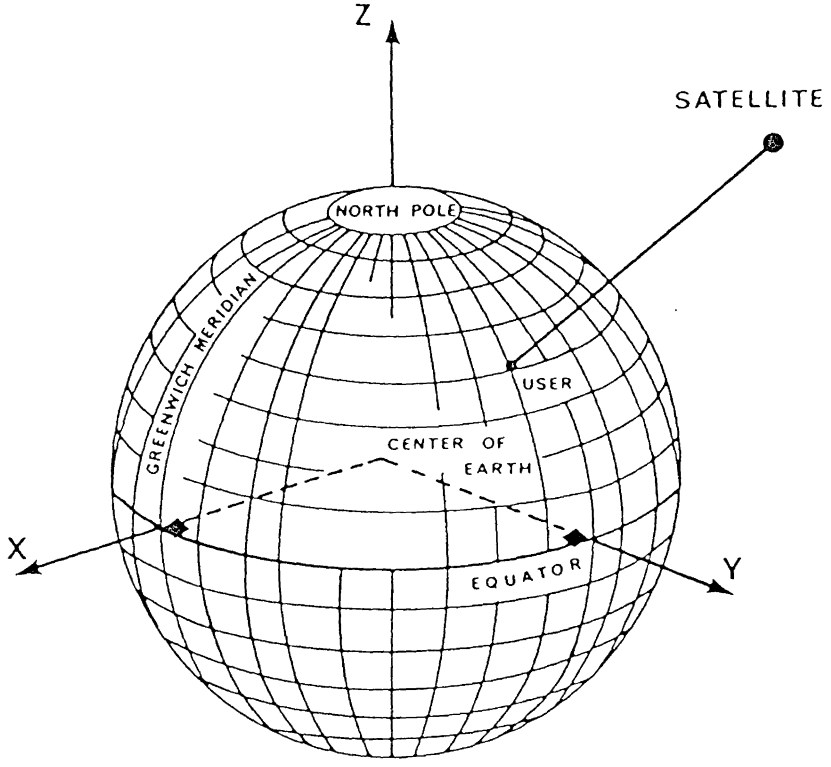


FIGURE 2.6

WGS-72 Reference System.

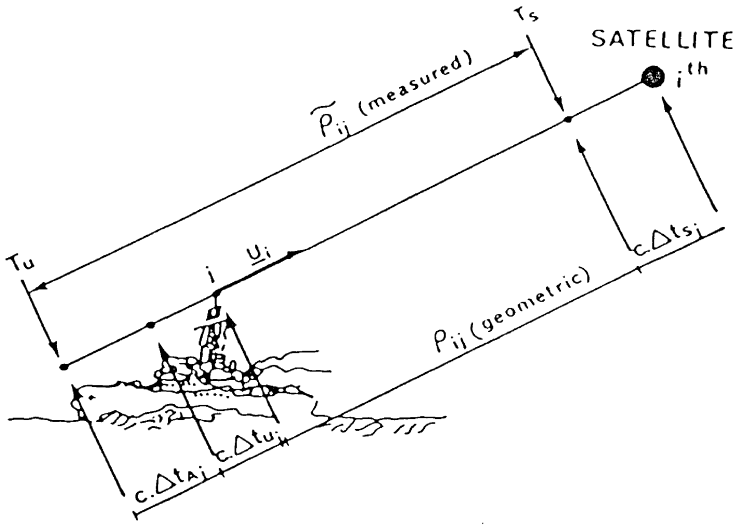


$c \cdot \Delta t_{A_j}$ = atmospheric delays

$c \cdot \Delta t_{u_j}$ = user clock time bias

$c \cdot \Delta t_{S_i}$ = satellite i clock time bias

$\rho_{ij}$ = geometric range

$c(T_u - T_s) = \tilde{\rho}_{ij}$ = pseudorange

FIGURE 2.7

Pseudorange Observation.

bias) [Wolfe, 1976].

At present, horizontal accuracies of 20 metres CPE have been obtained using the C/A-code only [Lachapelle et al., 1982], and less than 10 metres CPE using the P-code [Montgomery and Johnson, 1982]. By 1987, 18 satellites will be placed in orbit and a two-dimensional accuracy of 25 metres or less with a 95 percent probability, or 10 metre CPE, will be provided continuously [USDOD, 1982]. The U.S. Department of Defense plans to degrade the accuracy of both the P-code and the C/A-code signals. According to the Federal Radionavigation Plan [USDOD, 1982] two kinds of accuracies will be provided to unauthorized civil users: the Precise Positioning Service (PPS), and the Standard Positioning Service (SPS). The PPS will provide two-dimensional accuracies of 18 metres (2drms), whereas the SPS accuracies will be 500 metres (2drms). The accuracy figure 2drms is a multiple of the CPE. According to the definition given in the Federal Radionavigation Plan [USDOD, 1982], 2drms is two and a half times greater than CPE (2drms = 2.5 * CPE).

## 2.4 Comparison with other Radionavigation Systems

The GPS actually evolved in response to a need for a worldwide, all-weather, accurate radionavigation system and as a constraint to the proliferation of radionavigation systems [Milliken and Zoller, 1978; Parkinson, 1979]. Let us review some of the major radionavigation systems that exist today and compare them with GPS.

Table 2.2 shows some of the existing radionavigation systems used for marine applications of positioning and navigation with their maximum coverage and accuracy. It was difficult to construct a table that would

| System | Maximum Coverage | Position Accuracy |
|---|---|---|
| TRANSIT (NNSS) | world | 40 - 500 m |
| OMEGA | world | 2000 m |
| LORAN-C | 2000 km | 50 - 500 m |
| TRIDENT III | 250 km (LOS)* | 3 m |
| LORAC | 480 km (day)<br>165 km (night) | 15 - 40 m |
| DECCA LAMBDA | 650 km (day)<br>350 km (night) | 36 - 100 m |
| DECCA HI-FIX | 300 km | 5 m |
| ARGO | 200 - 400 km | 1.5 m |
| SYLEDIS | 350 km | 1 m |
| AUTOTAPE | 150 km | 10 - 30 m |
| TRISPONDER | 80 km | 3 m |
| RAYDIST | 480 km (day)<br>280 km (night) | 3 m |

* = line-of-sight

TABLE 2.2

Examples of Radionavigation Systems.

express the accuracy figures on the same probability level, i.e., 50 metres with 95% probability. Table 2.2 represents the most recent available information.

Generally all short-range radionavigation systems are confined to line-of-sight operation and, in addition, require the installation of several shore stations. Hence they are not useful for distant offshore work. Worldwide coverage is not fulfilled.

Let us briefly discuss three long range navigation systems which can or almost can provide worldwide coverage. These systems are the LORAN-C [Ingham, 1974; Laurila, 1976; U.S. Coast Guard, 1978], the OMEGA [Kasper and Hutchinson, 1978; International Omega Association, 1978], and the TRANSIT [Stansell, 1971]. Some factors influencing the performance of these systems, their limitations, and the additional capabilities of GPS that cannot be fulfilled by the above systems are examined.

LORAN-C is primarily a ground-based navigation system [Ingham, 1974]. Because of the atmosphere one major problem arises, that is, propagation errors. Propagation errors are due to a variation in the propagation velocity of the signals. The velocity is actually slowed down by the physical and electrical properties of the earth's surface (ground conductivity). These propagation errors amount to 120 m to 900 m [Laurila, 1976]. LORAN-C coverage is up to 2000 km and therefore only a small part of the world is provided with positioning. Weather also affects the proper functioning of LORAN-C. Precipitation or mist contribute errors in the overall accuracy of the system [Laurila, 1976]. A description of some other sources of significant errors, such as positional reliability, interference, etc., can be found in Stansell

[1978] and the U.S. Coast Guard [1978].

OMEGA is also a ground-based navigation system but it can satisfy the need for worldwide navigation. Worldwide coverage is provided by the eight ground transmitting stations, but again the system suffers from propagation errors [Kasper and Hutchinson, 1978]. In particular ionospheric and solar radiation (sudden ionospheric disturbances, polar cap disturbances) render serious errors in the performance of the system [IOA, 1978]. Position errors amount to approximately 2000 m [Laurila, 1976]. Even though this system provides extensive coverage, its reliability is sometimes doubtful. Errors of 10 miles, 30 miles, and 100 miles have been noticed [Stansell, 1978]. Weather conditions and positional repeatability cause a problem in the performance of the system as well.

TRANSIT, also known as the U.S. Navy Navigation Satellite System (NNSS), is a satellite-based system. It determines the user's position by measuring the Doppler frequency shift of satellite radio signals [Wells, 1969]. A comparison of the TRANSIT system with GPS is given in Table 2.3. There are basically three drawbacks in the TRANSIT system: The rate of fixes, the large uncertainties in position determination when the ship's velocity is unknown, and the interference and jamming of the TRANSIT signals themselves.

A user requires about 10 to 15 minutes to establish his position, and the maximum fix rate becomes about five fixes per hour [Wells et al., 1981]. Consequently the TRANSIT system provides intermittent (not continuous) coverage. The system does not appear very useful when the user is moving. An uncertainty of about 1 knot (1 mile/hour) of the ship's velocity may render an error of about 500 metres in positioning

| | TRANSIT | GPS |
|---|---|---|
| Satellite height | 1100 km | 20 183 km |
| Broadcast satellite position error ($1\sigma$) | 25 m tangential<br>10 m normal<br>5 m radial | 2 m tangential<br>2 m normal<br>2 m radial |
| Number of satellites | 6 | 18 |
| Orbital period | 110 min | 12 hours |
| Transmission frequency | 150 MHz<br>400 MHz | 1227.6 MHz<br>1575.42 MHz |
| Basic observable | Doppler shift | Time-of-arrival<br>Doppler shift |

TABLE 2.3

Comparison of TRANSIT with GPS.

[Wells, 1980]. Since no provisions were taken to avoid interference among signals from other TRANSIT satellite signals, jamming occurs at high latitudes (close to the north pole). This is happening because more than one TRANSIT satellite appear above the user's horizon due to the satellite's polar orbit.

Figure 2.8 recapitulates the capabilities of the four navigation systems in terms of accuracy and coverage. It seems clear that GPS will offer unique capabilities in positioning and navigation and will fulfill the need of worldwide, continuous, accurate requirements that other radionavigation systems cannot cover. The GPS promises an outstanding value in navigation. According to the Federal Radionavigation Plan redundant navigation systems will be phased out and only a small number of them will remain in use to cover all navigational requirements [USDOD, 1982].

The importance of and need for a new navigation system on a

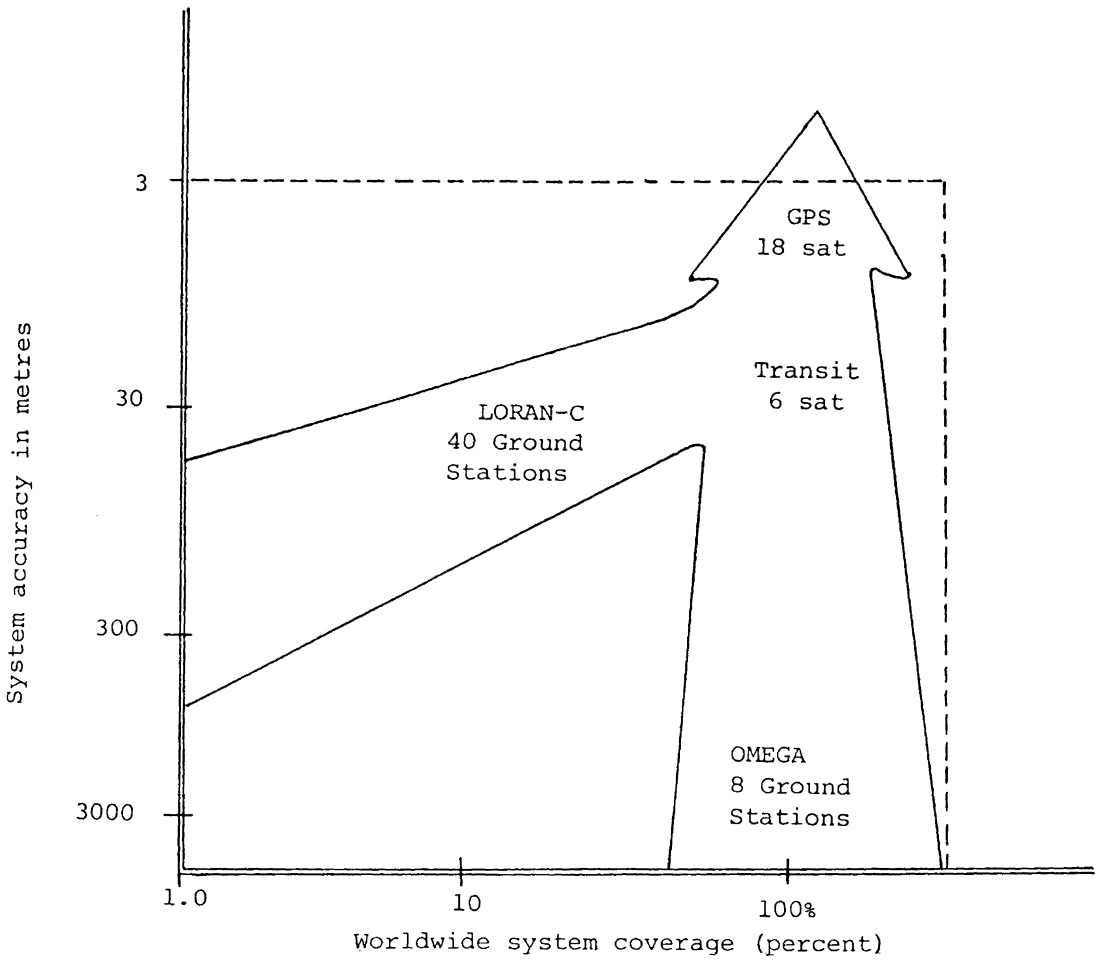


FIGURE 2.8

Capabilities of All-Weather Navigation Systems.
(after McDonald [1975]).

worldwide basis has prompted not only the United States but also the European community (whose internationally managed system is called NAVSAT [Rosetti, 1982]) and the U.S.S.R. [Klass, 1982a; 1982b] to develop a global system.

The GPS may look like a panacea for navigation and positioning but it has two limitations. It cannot provide relative positioning, and visibility is sometimes an impediment in acquiring GPS signals. There are times when relative navigation is very important. The GPS, however, can supply only an absolute position, although the differential GPS concept may help in relative positioning. In the GPS, visibility is an important aspect. Because of the very high frequency ($L_1$ = 1575 MHz; $L_2$ = 1227 MHz) of the GPS signals, visibility is limited to the line of sight. Therefore shielded or underwater positioning cannot be provided.

## 2.5 Marine Applications

There are a number of marine navigation and positioning requirements that can be satisfied with the advent of NAVSTAR-GPS. These requirements stem from a wide range of present and future human activities in off-shore oil exploitation, fishing, safe navigation, marine seismic exploration, approach to harbours, hydrographic surveys, etc. Table 2.4 shows some of the accuracy requirements for marine operations. The GPS will solve the global coverage, the instantaneous fix, and the accuracy problems not satisfied by other systems. Precise navigation by GPS in remote areas, where the coverage of navigation aids is non-existent or weak, would be of great benefit to the civilian society.

| Requirements for | Accuracy ($1\sigma$) |
|---|---|
| Ocean navigation | 1000 m |
| Safety-rescue operations | 200 m |
| Commercial fishing | 200 m |
| Resource exploitation | 20-40 m |
| Detailed geophysical surveys<br>3-D surveys | 20-40 m (3 m by the year 2000) |
| Drilling platform locations<br>(actual drilling) | 5-10 m (0.5 m by the year 2000) |
| Critical harbour approach<br>(e.g., fog), inland<br>navigation | 5-10 m (0.5 m by the year 2000) |

TABLE 2.4

Some Accuracy Requirement for Marine Operations
(after Beser and Parkinson [1981]; Gay [1982]).

Post-mission analysis of GPS data will be possible because of the obtained intrinsic time information to all positioning and velocity data. More details on the GPS applications can be found in Stansell [1978] and Johnson and Ward [1979].

## 2.6 Denial of Accuracy

As stated previously, the GPS signals will be degraded such that the GPS will result in a positional error of 200 metres CPE (500 m 2drms). This will be achieved by denying civil users access to the Precise code (P-code) and by imposing degradation on the Coarse/Acquisition code (C/A-code). At any rate, access to the P-code is not so essential for marine applications since accuracies of 20 metres have already been obtained using the C/A-code only [Lachapelle et

al., 1982].

This policy of the denial of the GPS accuracy to civil users was motivated by the U.S. Department of Defense such that no access to a potential positioning system would be available to an enemy for national security reasons [USDOD, 1982]. This policy will be implemented during the first year of full GPS operation (i.e., 1987) with subsequent accuracy improvements as time passes. Until then, the full GPS accuracy will be provided to civil users with no restrictions. It is expected that the Selective Availability concept will continue to be implemented by the Department of Defense, and no changes will be made to this policy prior to 1990 [Beser and Parkinson, 1981; Kalafus, 1982].

There is a number of consequences which will follow after the imposition of the Selective Availability policy. Many marine accuracy requirements essential to some user groups (see Table 1.1) cannot be met by using the conventional degraded GPS system. The full benefit of the GPS cannot be gained.

Since only the C/A-code will be available, reductions for ionospheric delays cannot be made based on the double frequency principle [Ward, 1981]. The C/A-code is superimposed only on the $L_1$ frequency. Therefore, ionospheric reduction can be made only by using the ionospheric coefficients provided through the navigation message [van Dierendonck et al., 1978].

# 3

# Accuracy Measures for Navigation

## 3.1 General

The accuracy measures used to assess the performance of navigation systems are vague and ambiguous and they do not carry the same meaning as they do on land. This is so because assessment of the accuracy of a position fix faces a lot of problems at sea. The lack of comparison of position fixes with fixed survey control monuments, the difficulty to repeat an observation because of ship movement, the marking of a position at sea are the major problems that one usually encounters at sea.

In view of these problems, accuracy measures for navigation may be much simpler than the conventional ones available on land associated with error ellipses, ellipsoids of constant probability, etc. [Mikhail, 1976; Vanicek and Krakiwsky, 1982]. However, because the nature of various sources of errors is to be distributed in an elliptical fashion (see Vanicek and Krakiwsky [1982]) a brief notion of the error ellipse will be made here too. It should be also mentioned that on the sea surface we are concerned primarily with two-dimensional error measures, such as the Circular Probable Error (CPE), the 2drms, the deviations in positioning expressed in percentiles, etc. All the above and two

factors which particularly affect the GPS user accuracy in terms of range error (User Equivalent Range Error (UERE)) and satellite-user geometry (Geometric Dilution of Precision (GDOP)) will be described in this chapter.

## 3.2 Error Ellipse

Rigorous mathematical methods show that after making some observations (e.g., ranges to satellites) to determine a position fix and considering that these observations are normally distributed [Vanicek and Krakiwsky, 1982] the true position of the fix is situated within an error ellipse described by a probability confidence level (e.g., 39%). This is illustrated in Figure 3.1. If the probability of a fix being within an error ellipse is 39% then this particular ellipse is called the standard error ellipse. The size, shape and orientation of an error ellipse are described by the semi-major axis ($\alpha$), the semi-minor axis ($\beta$), and the angle ($\theta$). Derivations of the above quantities are given in Mikhail [1976]. In order to establish different confidence levels (e.g., 95%, 90%, 80%, etc.) the semi-axes of the standard error ellipse should be multiplied by the values shown in Table 3.1. This table is constructed by considering the property that the sum of the squares of the normalized variables ($x'/\sigma_{x'}$) and ($y'/\sigma_{y'}$) follow a $\chi^2$ distribution with two degrees of freedom when the observations are normally distributed, that is

$$\Pr[\{(\frac{x'}{\sigma_{x'}})^2 + (\frac{y'}{\sigma_{y'}})^2\} < \xi] = \Pr[\chi_2^2 < \xi] = 1 - \alpha \quad . \qquad (3.1)$$

More details can be found in Vanicek and Krakiwsky [1982].

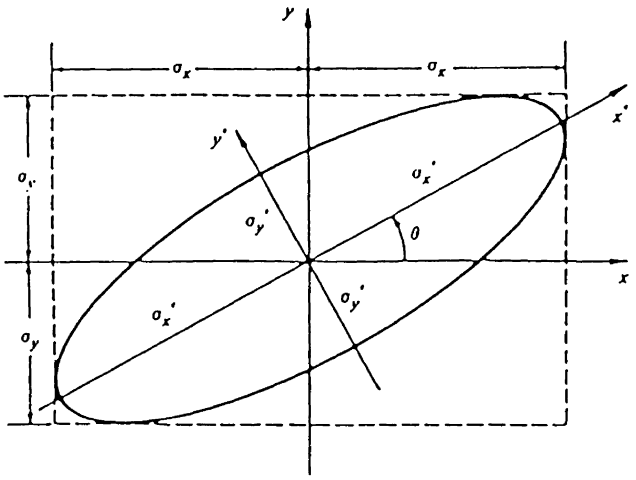


$\alpha = \sigma'_x$ = semi-major axis

$\beta = \sigma'_y$ = semi-minor axis

$\theta$ = orientation angle

FIGURE 3.1

Error Ellipse (from Mikhail and Gracie [1981]).

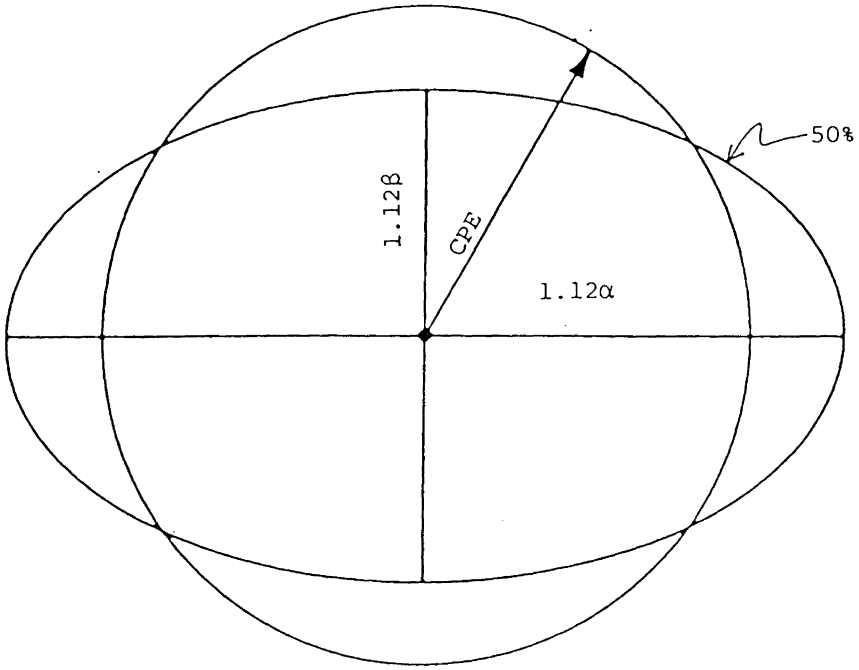


FIGURE 3.2

Circle and the Equivalent Probability Error Ellipse (from Burt er al. [1967]).

| Multiple of a Standard Error Ellipse Dimensions ($\xi$) | Probability of a Fix Being Within the Derived Error Ellipse (Percent) ($1 - \alpha$) |
|---|---|
| 2.45 | 95 |
| 2.00 | 86 |
| 1.12 | 50 |
| 1.00 | 39 |
| 0.80 | 28 |
| 0.67 | 20 |

TABLE 3.1

Probability for Various Error Ellipses
(from Surveys and Mapping [1975]).

## 3.3 Circular Probable Error, 2drms, drms

Instead of using error ellipses, it is often convenient to use circles with certain probability confidence levels. The Circular Probable Error (CPE), is one of those circular probabilistic error measures. As previously defined, it is the radius of a circle which contains 50% of all possible fixes that can be obtained with a navigation system at any place [USDOD, 1982].

The concept of the CPE figure actually originated from military applications in weapons delivery, where the main interest was to calculate the probability of damage to a target (you are either on or off the target). The same notion was applicable to navigation. Navigators were interested in the probability of being located within a circle of constant radius. Figure 3.2 illustrates the CPE circle with its associated error ellipse of equivalent probability (50%).

The joint probability function of the two orthogonal variables x' and y' which are normally distributed, each with zero mean and with

standard deviations $\sigma_{x'}$ and $\sigma_{y'}$, respectively, is given by

$$f(x', y') = \frac{1}{2\pi\sigma_{x'}\sigma_{y'}} \exp\{-\frac{1}{2}[(\frac{x'}{\sigma_{x'}})^2 + (\frac{y'}{\sigma_{y'}})^2]\} \quad . \qquad (3.2)$$

The probability that a point (x', y'), whose coordinates are chosen randomly and independently from this joint distribution, will lie within a circle of radius $K\sigma_{x'}$ (where $\sigma_{x'} > \sigma_{y'}$) is

$$P(K, \sigma_{x'}, \sigma_{y'}) = \iint_{\sqrt{(x'^2 + y'^2)} < K\sigma_{x'}} f(x', y') \cdot dx' \cdot dy'. \qquad (3.3)$$

Introducing polar coordinates by letting $x'/\sigma_{x'} = \rho\cos\theta$ and $y'/\sigma_{x'} = \rho\sin\theta$, this probability takes the form

$$P(K,\sigma_{x'},\sigma_{y'}) = \frac{\sigma_{x'}}{2\pi\sigma_{y'}} \int_{\theta=0}^{\theta=2\pi} \int_{\rho=0}^{\rho=K} \exp\{-\frac{1}{2\rho^2}[\cos^2\theta + (\frac{\sigma_{x'}}{\sigma_{y'}})^2 \sin^2\theta]\}\rho d\rho d\theta. \qquad (3.4)$$

Letting $c = \frac{\sigma_{y'}}{\sigma_{x'}}$ and $2\theta = \phi$, we obtain

$$P(K,c) = \frac{1}{2\pi c} \int_{\phi=0}^{\phi=\pi} \int_{\rho=0}^{\rho=K} \exp\{-(\frac{\rho^2}{4c^2})[(1+c^2)-(1-c^2)\cos\phi]\}\rho d\rho d\phi \quad . \qquad (3.5)$$

If one sets $z = \rho^2/4c^2$ the above becomes

$$P(K,c) = \frac{2c}{\pi} \int_{\phi=0}^{\phi=\pi} \int_{z=0}^{z=K^2/4c^2} \exp\{-z[(1+c^2)-(1-c^2)\cos\phi]\}dz d\phi \quad . \qquad (3.6)$$

Upon integration with respect to z, one obtains

$$P(K,c) = \frac{2c}{\pi} \int_0^{\pi} \frac{1-\exp\{-(\frac{K^2}{4c^2})[(1+c^2)-(1-c^2)\cos\phi]\}}{(1 + c^2) - (1 - c^2)\cos\phi} d\phi \quad . \qquad (3.7)$$

The development of the above is based on Harter [1960]. Ways for the numerical integration of equation (3.7) are given in Harter [1960] as

well as a table of computed probabilities as a function of K and c.

When one sets the probability P(K,c) equal to 50% (e.g., P(K,c) = 0.5) then the sought radius of $K\sigma_{x'}$ is the CPE radius (CPE = $K\sigma_{x'}$). Figure 3.3, taken from Burt et al. [1965], shows a graphical representation of K = CPE/$\sigma_{x'}$ as a function of c = $\sigma_{y'}/\sigma_{x'}$ with several other approximations for comparison with the exact curve.

It should be mentioned that the area of the CPE circle is always greater than the area of the error ellipse of equivalent probability [Burt et al., 1965]. The CPE value is simpler than an error ellipse since it does not require three quantities ($\alpha$, $\beta$, $\theta$) as the error ellipse does to be specified. Nevertheless, it has some disadvantages [Roeber, 1982]:

1) It ignores the nature of the distribution of errors. All possible fixes should lie within an error ellipse rather than a circle when the observations are normally distributed.
2) Nothing is known about the fixes outside of the circle in terms of probability and magnitude.

If $\phi_i$ (computed) and $\lambda_i$ (computed) are the latitude and longitude as computed from a navigation fix, the true errors $\Delta\phi_i$ and $\Delta\lambda_i$ are:

$$\Delta\phi_i = \phi_i \text{ (computed)} - \phi_i \text{ (actual)} \tag{3.8}$$

$$\Delta\lambda_i = \lambda_i \text{ (computed)} - \lambda_i \text{ (actual)} \tag{3.9}$$

where $\phi_i$ (actual) and $\lambda_i$ (actual) are the true latitude and longitude of this position.

After making n observations the root-mean-square (rms) and correlation values of the latitude and longitude can be expressed as:

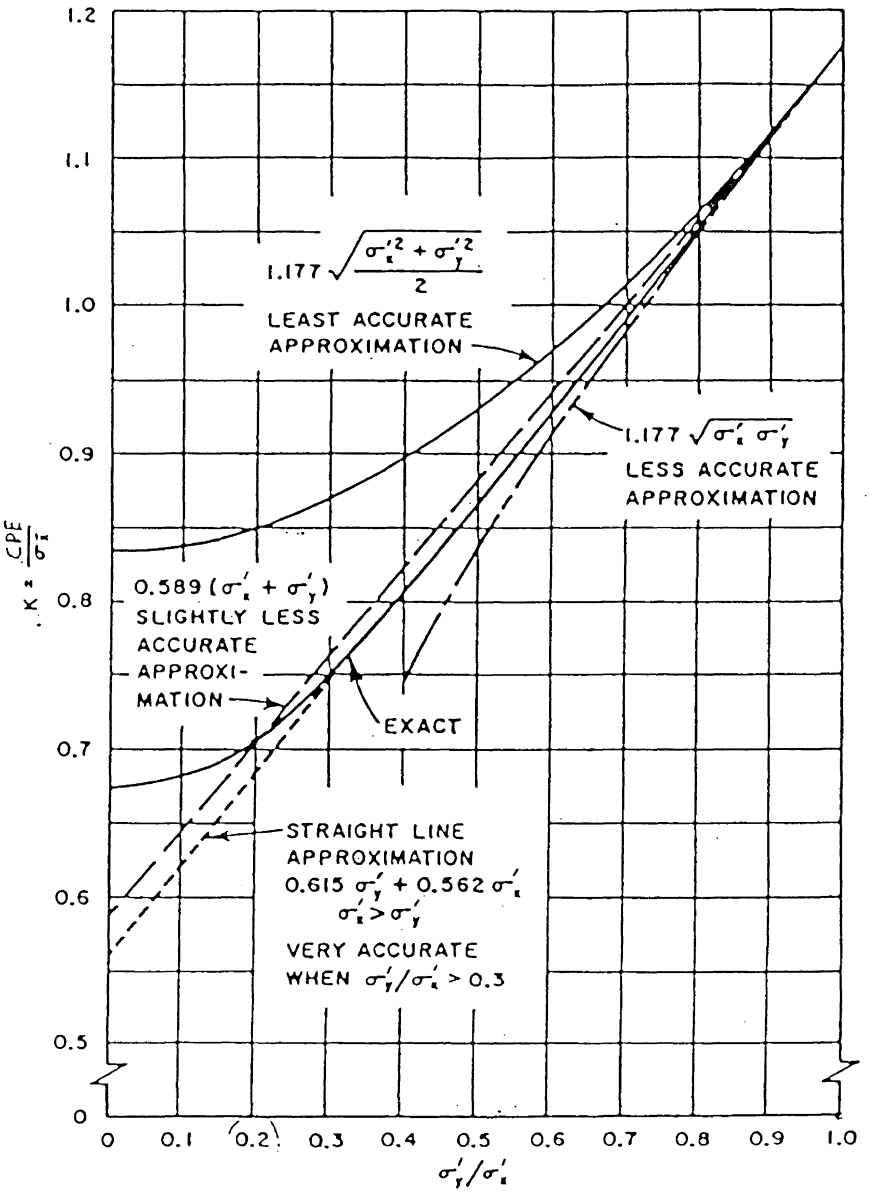


FIGURE 3.3
Relationship of $K=CPE/\sigma'_x$ with $c=\sigma'_y/\sigma'_x$

$$\sigma_{\phi,rms} = \sqrt{\frac{\sum_{i=1}^{n} \Delta\phi_i^2}{n}} \qquad (3.10)$$

$$\sigma_{\lambda,rms} = \sqrt{\frac{\sum_{i=1}^{n} \Delta\lambda_i^2}{n}} \qquad (3.11)$$

$$\sigma_{\phi\lambda} = \frac{\sum_{i=1}^{n} (\Delta\phi_i \ \Delta\lambda_i)}{n} \qquad (3.12)$$

A transformation of the above values to the semi-major and semi-minor axes of an ellipse [Mikhail 1976] would give

$$\alpha = \sqrt{\frac{1}{2}(\sigma^2_{\phi,rms} + \sigma^2_{\lambda,rms}) + \sqrt{\frac{1}{4}(\sigma^2_{\phi,rms} - \sigma^2_{\lambda,rms})^2 + \sigma^2_{\phi\lambda}}} \qquad (3.13)$$

$$\beta = \sqrt{\frac{1}{2}(\sigma^2_{\phi,rms} + \sigma^2_{\lambda,rms}) - \sqrt{\frac{1}{4}(\sigma^2_{\phi,rms} - \sigma^2_{\lambda,rms})^2 + \sigma^2_{\phi\lambda}}} \qquad (3.14)$$

The CPE can be calculated from rigorous mathematical formulae [Harter, 1960; Burt et al., 1965]. Nevertheless, the following approximation for the CPE value can be used (see Figure 3.3):

$$CPE = 0.589\ (\alpha + \beta), \text{ especially for } 0.2 \leq \beta/\alpha \leq 1.0 \ . \qquad (3.15)$$

An approximate formula for the radii ($R_i$) of circles which include a specified probability of a normal bivariate distribution is given as [Oberg, 1947]:

$$R_i = (\alpha + \beta)\sqrt{(\tfrac{1}{2})\ \ln(\frac{1}{1 - Pr_i})} \quad . \qquad (3.16)$$

Hence, if one wants to calculate the factor with which the value of CPE should be multiplied to obtain another circle with probability, say 75%, we have

$$\frac{R_{75}}{R_{50}} = \frac{R_{75}}{CPE} = \frac{(\alpha + \beta)\sqrt{(\frac{1}{2})\ \ln(\frac{1}{1 - 0.75})}}{(\alpha + \beta)\sqrt{(\frac{1}{2})\ \ln(\frac{1}{1 - 0.5})}} = 1.414 \quad , \qquad (3.17)$$

or

$$R_{75} = 1.414\ CPE \quad . \qquad (3.18)$$

Table 3.2 shows the relationship between CPE and various radii of other probability circles.

| Multiply Value of CPE by | To Obtain Radius of Circle of Probability |
|---|---|
| 1.150 | 60% |
| 1.318 | 70% |
| 1.414 | 75% |
| 1.524 | 80% |
| 1.655 | 85% |
| 1.823 | 90% |
| 2.079 | 95% |
| 2.578 | 99% |

TABLE 3.2

Relationship Between CPE and Radii of Other Probability Circles (from Burt et al. [1965]).

It is noteworthy that the error figure 2drms, described in the Federal Radionavigation Plan [USDOD, 1982] as the circle containing at least 95% of all possible fixes, is derived multiplying CPE by 2.5.

The drms (distance, rms) is defined as the square root of the sum of the squares of the semi-major and semi-minor axes of a probability ellipse (see Figure 3.4), that is:

$$drms = \sqrt{\alpha^2 + \beta^2} \quad . \qquad (3.19)$$

The quantity drms is a rather confusing error measure since it provides no information about the probability associated with each single value

of it [Burt et al., 1965].

## 3.4 Accuracy Measures Using Percentiles

Maintaining circular error measures for the evaluation of the accuracy of a navigation system, another procedure using rank statistics [Hogg and Craig, 1978] could also be described. We shall adopt the radial quantity $\Delta R_i$ represented by the following relation (see Figure 3.5):

$$\Delta R_i = \sqrt{\Delta\phi_i^2 + \Delta\lambda_i^2} \tag{3.20}$$

as a numerical deviation of a random position fix from its actual position. If this position fix is repeated n times then a set of n $\Delta R_i$ values can be obtained:

$$\{\Delta R_i\} \text{ where } i = 1,2,3,\ldots,n \quad . \tag{3.21}$$

When the above set is ordered the 50th percentile (median) and the 95th percentile can be computed. The (100p)th percentile of a sample is defined as a value $\xi_p$ of the sample for which a certain percentage (e.g., 50%, 95%) of the values of the sample are less than or equal to that particular value ($\xi_p$).

The 50th percentile and the 95th percentile should be close to the CPE (50%) value and 2drms (95%), as specified in the Federal Radionavigation Plan, when the sample of radial deviations is large. The primary advantage of using percentiles is that they are straightforward to calculate, regardless of the shape of the distribution of the observed values and that they are easy to interpret. The disadvantage is that percentiles could lead to inaccurate conclusions when the sample is very small.

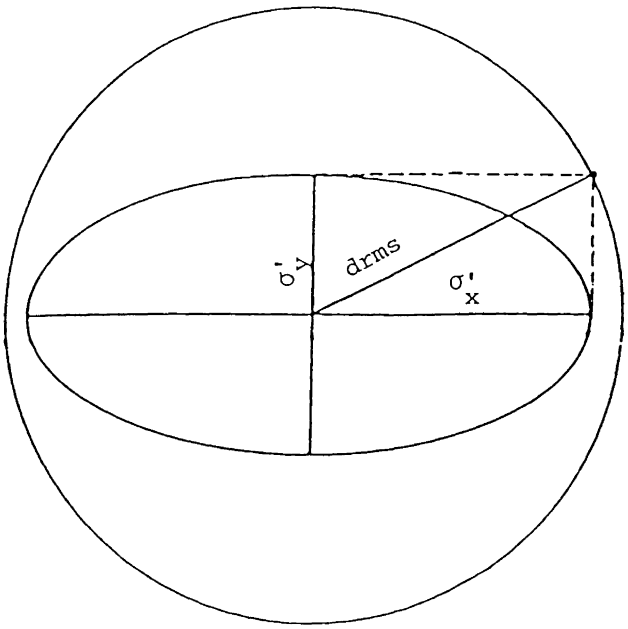


FIGURE 3.4

drms Radial Error (drms = $\sqrt{\sigma_x'^2 + \sigma_y'^2} = \sqrt{\alpha^2 + \beta^2}$).

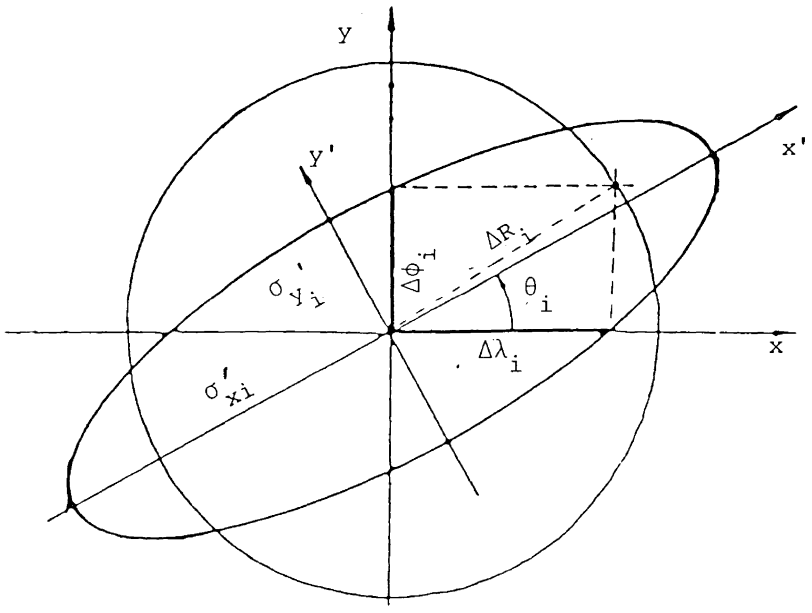


FIGURE 3.5

Radial Deviation $\Delta R_i$.

## 3.5 Accuracy Measures for GPS Performance

This section is devoted to the establishment of a meaningful accuracy statement of the GPS performance for a uniform interpretation. The GPS user accuracy is dependent upon various factors [Martin, 1980]; however there are two primary ones: the range error and geometry. The former is expressed by the User Equivalent Range Error (UERE), and the latter by the Geometric Dilution of Precision (GDOP).

UERE is based on the assumption that there is no correlation between satellite measurements. It represents the combined accuracy parameter of the observed satellite measurements and reflects the total error contribution of the GPS system. UERE involves "system" errors, such as uncertainties of the ephemeris data, propagation errors, clock errors, etc. In other words, each pseudorange observation towards a specific satellite is associated with an observed range error, known as UERE. The UERE is often expressed in terms of standard deviations ($\sigma$). The relationship between accuracy expressions and probability when the underlying distribution of errors is normal (Gaussian) [Hogg and Craig, 1978] is shown in Table 3.3.

| Accuracy Expression | Error Level | Probability % |
|---|---|---|
| Two sigma | $2\sigma$ | 95 |
| One sigma standard deviation | $1\sigma$ | 67 |
| Average error | $0.80\sigma$ | 58 |
| Probable error | $0.67\sigma$ | 50 |

TABLE 3.3

Normal Distribution of Errors
(from Surveys and Mapping [1975]).

The use of GDOP value was originally developed in LORAN navigation systems [Swanson, 1978]. It is a quantity which is used extensively in determining the information content due to satellite geometry and results in a measure of the overall geometrical strength to the navigation solution. It provides a method of quantitatively determining whether a particular satellite geometry is good or bad.

It can be found in Appendix I that the linearized observation equations are given as

$$A\ \delta\underline{X} + B\ \underline{V} + \underline{W} = 0 \quad . \tag{3.22}$$

An estimate of the correction vector $\delta\underline{X}$ of the solution is given as

$$\delta\underline{X} = \underline{X}_j - \underline{X}_j^{(0)} = (A^T P A)^{-1}\ A^T\ P\ \underline{W} \quad . \tag{3.23}$$

The correction vector $\delta\underline{X}$ represents corrections $(\delta X_j,\ \delta Y_j,\ \delta Z_j,\ \delta\Delta t_{uj})$ that the user will make to his current estimate of position $X_j^{(0)} = [X_j^{(o)},\ Y_j^{(o)},\ Z_j^{(o)},\ \Delta t_{uj}^{(o)}]$. The derivation of equation (3.23) and the complete description of the quantities involved are again given in the appendices.

The cofactor matrix [Vanicek and Krakiwsky, 1982] of the estimate $\delta\underline{X}$ is given by

$$Q_{\delta\underline{X}} = (A^T\ PA)^{-1} = \begin{vmatrix} q_x^2 & q_{xy} & q_{xz} & q_{x\Delta t_u} \\ q_{yx} & q_y^2 & q_{yz} & q_{y\Delta t_u} \\ q_{zx} & q_{zy} & q_z^2 & q_{z\Delta t_u} \\ q_{\Delta t_u x} & q_{\Delta t_u y} & q_{\Delta t_u z} & q_{\Delta t_u}^2 \end{vmatrix} \tag{3.24}$$

Geometric Dilution of Precision is defined as the square root of the

trace of the above cofactor matrix after setting the weight matrix P equal to identity matrix, that is

$$GDOP = \sqrt{\text{trace } (A^T A)^{-1}} = \sqrt{q_x^2 + q_y^2 + q_z^2 + q_{\Delta t_u}^2}. \qquad (3.25)$$

Other quantities of interest, along with the Geometric Dilution of Precision, are the horizontal, the vertical, the positional, the time and the horizontal time dilution of precision defined as follows:

$$\begin{aligned} HDOP &= \sqrt{q_\phi^2 + q_\lambda^2} \\ VDOP &= \sqrt{q_z^2} = q_z \\ PDOP &= \sqrt{q_x^2 + q_y^2 + q_z^2} \\ TDOP &= q_{\Delta t_u} \\ HTDOP &= \sqrt{q_\phi^2 + q_\lambda^2 + q_{\Delta t_u}^2} \end{aligned} \qquad (3.26)$$

For a complete three-dimensional position fix (X, Y, Z, $\Delta t_u$) the covariance matrix of the estimate $\underline{\delta X}$ is

$$C_{\underline{\delta X}} = \sigma_o^2 Q_{\underline{\delta X}} = \begin{vmatrix} \sigma_x^2 & \sigma_{xy} & \sigma_{xz} & \sigma_{x\Delta t_u} \\ \sigma_{yx} & \sigma_y^2 & \sigma_{yz} & \sigma_{y\Delta t_u} \\ \sigma_{zx} & \sigma_{zy} & \sigma_z^2 & \sigma_{z\Delta t_u} \\ \sigma_{\Delta t_u x} & \sigma_{\Delta t_u y} & \sigma_{\Delta t_u z} & \sigma_{\Delta t_u}^2 \end{vmatrix} \qquad (3.27)$$

where $\sigma_o^2$ is the variance factor [Vanicek and Krakiwsky, 1982].

By setting the weight matrix P equal to the identity matrix, equation (3.27) gives

$$C_{\underline{\delta X}} = \sigma_{range}^2 Q_{\underline{\delta X}} = (UERE) Q_{\underline{\delta X}} \quad . \qquad (3.28)$$

From the above relationship an approximate measure in the total user

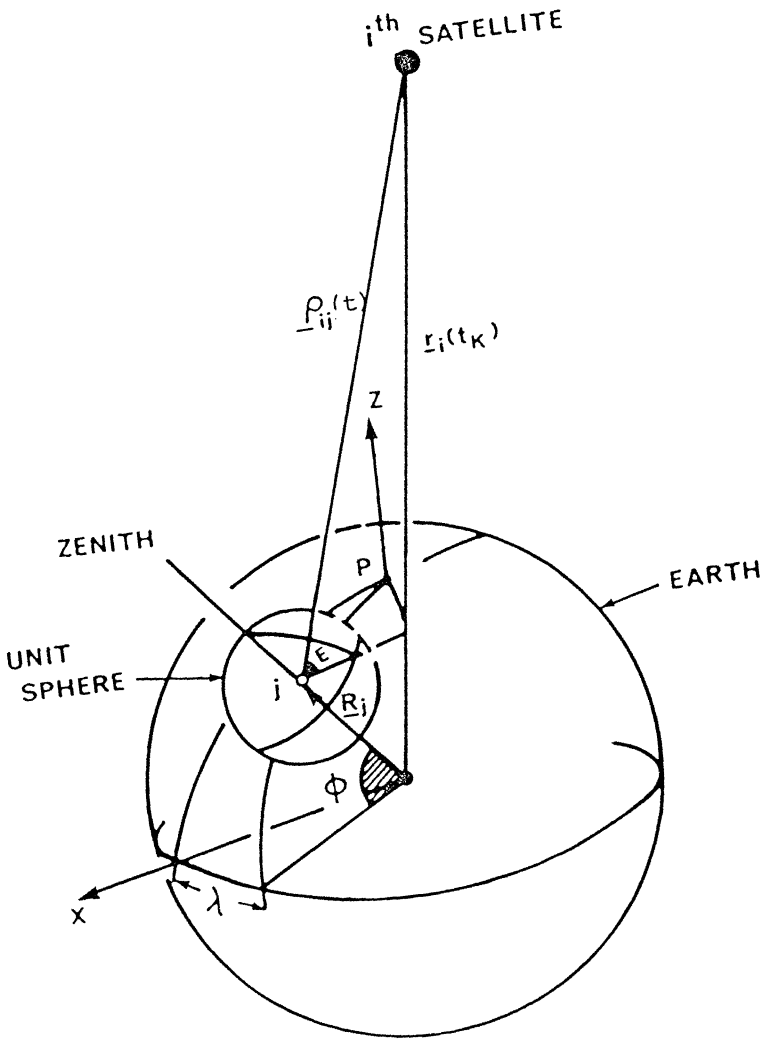


FIGURE 3.6
Elevation Angle E of the ith Satellite.

error would be:

$$\text{user error} = \sqrt{\sigma_x^2 + \sigma_y^2 + \sigma_z^2 + \sigma_{\Delta t_u}^2} = (\text{UERE})\sqrt{q_x^2 + q_y^2 + q_z^2 + q_{\Delta t_u}^2} \quad (3.29)$$

The product of the DOP factors by an estimate in the range measurements ($\sigma_{range}$ = UERE) results in a user error such that

$$\text{user error} = (\text{UERE})(\text{GDOP}) \quad . \quad (3.30)$$

The same is true for the other DOP factors. For example, a PDOP value of 2.5 and a UERE of ± 4 metres (1σ) would result in a user position error (1σ) of

$$(\text{PDOP}) \times (\text{UERE}) = 2.5(\pm 4\text{m}) = \pm 10 \text{ metres.}$$

It is mentioned in Ward [1981] that a PDOP value of 3 or less is expected in the full 18-satellite constellation.

Geometric dilution of precision values can be described as a measure of the navigator's position uncertainty per unit of measurement noise. It has been conceded that GDOP values are statistically distributed in a non-Gaussian fashion [Jorgensen, 1980].

So far, GDOP has been defined in an analytical way. Another way for the determination of GDOP is based on the computation of the volume of a special tetrahedron formed by the satellites and the user's location.

Let $\underline{\rho}_{ij}(t_k)$ be the geometric range vector, $\underline{R}_j$ the position vector of the jth user, and $\underline{r}_i(t_k)$ the position vector of the ith satellite, as shown in Figure 3.6.

The magnitude of the cross-product of the pair $\underline{R}_j$ and $\underline{\rho}_{ij}$ is defined as follows:

$$|\underline{R}_j \times \rho_i| = |\underline{R}_j||\underline{\rho}_{ij}| \sin(90^\circ + E) \quad , \quad (3.31)$$

whereas the dot product for the same vectors is

$$\underline{R}_j \cdot \underline{\rho}_{ij} = |\underline{R}_j||\rho_{ij}| \cos(90^\circ + E) \quad . \quad (3.32)$$

Dividing (3.31) by (3.32), we obtain:

$$\frac{\cos(90^\circ + E)}{\sin(90^\circ + E)} = \frac{-\sin E}{\cos E} = \frac{-\dfrac{\underline{R}_j \cdot \underline{\rho}_{ij}}{|\underline{R}_j| \; |\underline{\rho}_{ij}|}}{\dfrac{|\underline{R}_j \times \underline{\rho}_{ij}|}{|\underline{R}_j| \; |\underline{\rho}_{ij}|}} \quad . \tag{3.33}$$

Therefore the elevation angle E of the ith satellite can be obtained by

$$\tan E = \frac{-\dfrac{\underline{R}_j \cdot \underline{\rho}_{ij}}{|\underline{R}_j| \; |\underline{\rho}_{ij}|}}{\dfrac{|\underline{R}_j \times \underline{\rho}_{ij}|}{|\underline{R}_j| \; |\underline{\rho}_{ij}|}} = -\frac{\underline{R}_j \cdot \underline{\rho}_{ij}}{|\underline{R}_j \times \underline{\rho}_{ij}|} \quad . \tag{3.34}$$

An allowable elevation angle for the determination of whether a satellite is considered visible is

$$E \geq 5^\circ \quad . \tag{3.35}$$

Therefore, candidate satellites to be considered for visibility are those whose elevation angle E is greater or equal to $5^\circ$. Any satellite with an elevation angle of less than $5^\circ$ is masked out by terrain, antenna limitations, foliage, obstructions, etc. Based on the criterion of (3.35) one can determine the number of visible satellites for a particular user (j) and time ($t_k$).

Let $\underline{U}_i$ be the unit vector from the user (j) to the ith visible satellite, as shown in Figure 3.7. When the full 18 satellites are in operation, four to seven satellites will be visible, on a continuous basis, at any site on the globe [USDOD, 1982]. All unit vectors $\underline{U}_i$ are centred at the user's location (j) and enclosed within a unit sphere. If we calculate all the combinations of unit vectors $\underline{U}_i$ of four satellites, we end up with a set of four unit vectors each time. It can be seen from Figure 3.8 that a special tetrahedron (e.g., 1-2-3-4) is formed by those four tips of unit vectors.

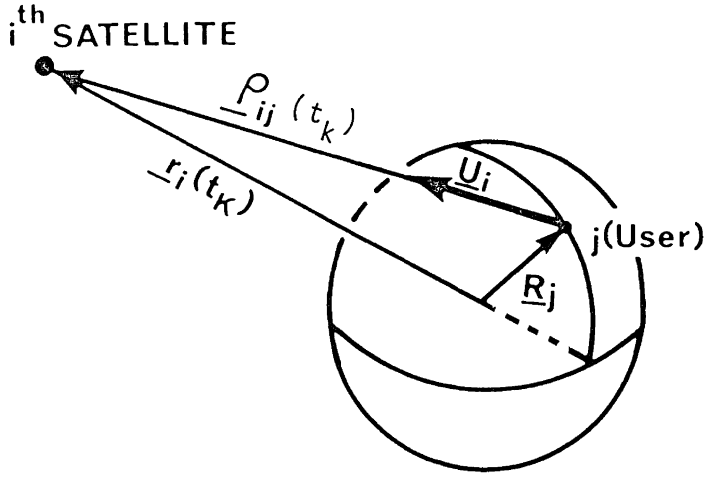


FIGURE 3.7

Unit Vector $\underline{U}_i$ to ith Satellite.

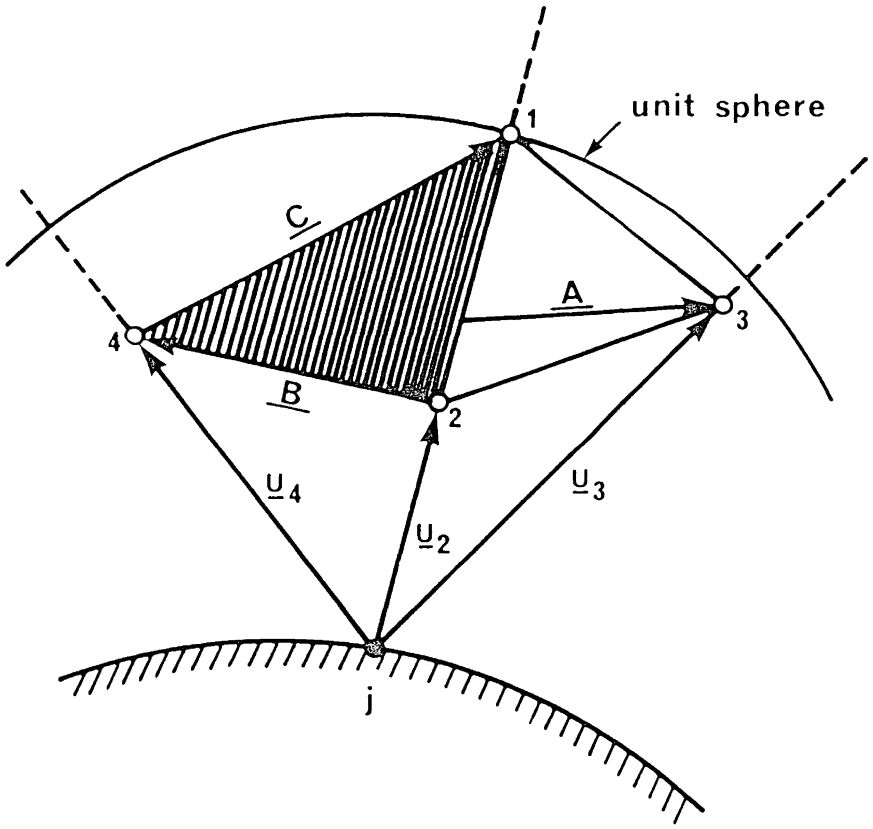


FIGURE 3.8

Tetrahedron Formed by the tips of Four Vectors $\underline{U}_i$

Variability of satellite geometry depends on the orientation of the four satellite positions available. This is, in turn, a function of the user's location (j) and time ($t_k$) because of satellite motion and earth rotation. It has been shown that the GDOP value is inversely proportional to the volume of this special tetrahedron (1-2-3-4) [Bogen, 1974]. Hence, the largest volume yields the smallest value of GDOP and vice versa.

Determination of the maximum volume of a tetrahedron among all other volumes formed by all the other combinations of four satellites also implies the determination of those satellites with the best navigation performance. The best navigation performance relies on the geometry of the four satellites and the smallest value of GDOP.

The volume (V) of the tetrahedron (1-2-3-4) can be computed using the scalar triple product

$$V = 1/6\ \underline{C}(\underline{A} \times \underline{B}) \quad . \tag{3.36}$$

The previous account takes into consideration geometrical aspects related to satellite geometry and the user's location, which has as a final goal the selection of satellites with the best navigation performance. It can be seen that the geometrical interpretation is easier to understand and visualize.

The minimum number of observations constitutes the necessary and sufficient elements for a unique set of estimates for the solution. Any additional observations, which are said to be redundant with respect to the model (four-parameter, three-parameter, two-parameter solution), should always be taken into consideration for a more precise and reliable solution [Mikhail, 1976; Vanicek and Krakiwsky, 1982]. In this case, the corresponding GDOP value will not only incorporate four

satellites but all those used for the solution (multi-dimensional GDOP). Some diagrams of the GDOP distribution are presented in Chapters 5 and 6.

# 4

# Differential GPS Navigation

## 4.1 General

The fundamental concept of differential navigation was presented in the introduction. Differential methods have already been applied to other radionavigation aids, such as LORAN-C [Goddard, 1973; Johler et al., 1976], OMEGA [Swanson, 1977], and TRANSIT [Westerfield and Worsley, 1966], to significantly improve the accuracy of the conventional (non-differential) systems.

As previously described, the differential monitor station, installed at a fixed known location, is responsible for four functions:

1) the reception of raw radionavigation signals;

2) the computation of a position fix;

3) the determination of differential corrections; and

4) the transmission of differential corrections to nearby users.

These differential corrections are the differences between the correct (known) values and the actual measured ones.

The differential concept implies that a communication link exists between the differential monitor station and the users. This data link ensues from the need to transfer the differential information from the monitor to the user's location. Bias errors, propagation errors,

transmitter imperfections, etc., common at both the differential monitor station and the user's location will be alleviated by the application of differential mode. The degree of reduction depends on the correlation between the errors at the differential monitor station and the user.

The same idea of differential navigation is also applicable to the GPS satellite system [Cardal and Cnossen, 1980; Dunn and Rees, 1980; Howell et al., 1980; Teasley et al., 1980; Cnossen et al., 1981; Beser and Parkinson, 1981; Kalafus, 1982; Montgomery and Johnson, 1982]. Provided that differential GPS navigation techniques are technically feasible (i.e., assuming that a data link exists), the GPS navigation performance appears to improve through differential mode (see previous references).

It should be noted that there is a distinction between differential GPS navigation and differential GPS techniques used for precise geodetic applications. The two methods should not be confused since the second one is not a real time process which is used to measure the interstation vector between two stations to an accuracy of a few centimetres over thousands of kilometres [Herman, 1981; Counselman et al., 1982].

Tests and studies [Teasley et al., 1980; Newell and Winter, 1981; Beser and Parkinson, 1981] have shown that differential GPS navigation can improve the accuracy of the conventional GPS system. Based on the fact that common bias errors are reduced in the differential mode, either the undegraded C/A-code accuracy can be retrieved during signal degradation periods or the performance of the system will be even further enhanced when signal degradation is absent [Cnossen et al., 1981; Kalafus, 1982].

## 4.2 Models for Differential Corrections

There are three types of differential GPS navigation. They are described in Cnossen and Cardal [1980], Cnossen et al. [1981], and Beser and Parkinson [1981]. The basic difference is in the nature and the way of processing the differential correction data.

Here we review their main points only.

1) Data link. The differential corrections are sent to a user in the form of simple additions such as ( $\delta\phi(t)$, $\delta\lambda(t)$, $\delta\Delta t(t)$).

2) Pseudolite. The differential monitor station plays the role of a satellite which generates and transmits its own pseudorandom signal, along with correction data. The correction data, in the form of range errors ( $\delta\rho_i(t)$) to all visible satellites, is superimposed on the navigation satellite message.

3) Translator. No processing of data takes place in the differential monitor station. The information coming from a satellite is merely relayed to a user set where it is processed.

There are two forms of differential corrections. Either the user is applying the differential corrections prior to calculating his navigation fix ( $\delta\rho_i(t)$) or he is adding them directly to the final solution in the form of simple additions ( $\delta\phi(t)$, $\delta\lambda(t)$, $\delta\Delta t(t)$).

It is noteworthy that when differential corrections, in the form of simple additions ( $\delta\phi(t)$, $\delta\lambda(t)$, $\delta\Delta t(t)$) are applied then the differential monitor station and the user should track exactly the same set of satellites.

Any measured deviations ( $\delta\phi(t)$, $\delta\lambda(t)$, $\delta\Delta t(t)$) at the differential monitor station correspond to the particular selected set of satellites used for the navigation solution. These deviations should also agree

with the deviations that the same set of satellites will yield at some distance from the differential monitor station, i.e., at the user's site.

In the case where range corrections ( $\delta\rho_i(t)$) are applied, three alternatives can be chosen:

1) Range corrections can be determined using the same set of satellites that the user and the monitor can track. Therefore, the choice of satellites will be restricted to those satellites common to the monitor and the user only. The monitor solves for a two-dimensional fix and time (three-parameter solution).

2) Range corrections can be determined using all visible satellites to the differential monitor station. The advantage is that range corrections can be transmitted for all GPS satellites in view. This permits the user to be flexible to select the best set of satellites for his solution. This kind of satellite selection can be achieved by using a satellite alert program [Mertikas, 1982]. Again the solution for the monitor will be for three unknowns ( $\phi$, $\lambda$, $\Delta t$) (three-parameter solution).

3) Range corrections will be determined using all visible satellites but the navigation solution of the monitor will be with the clock bias constrained (two-parameter solution). An external synchronization of the monitor's clock to the GPS system time is required. No restriction will be imposed on the user's satellite selection.

For marine navigation, a two-dimensional fix only is necessary since the ellipsoidal height (h) [Vanicek and Krakiwsky, 1982] can be considered known. Thus the navigation solution can be confined to the determination of three unknowns (X, Y, $\Delta t$ or $\phi$, h, $\Delta t$) or only two (X, Y

or $\phi$ $\lambda$) when external time synchronization is provided.

The position corrections, shown in Figure 4.1 are

$$\phi^U(t) = \phi^U_{Deg}(t) - \delta\phi^M(t) \qquad (4.1)$$

$$\lambda^U(t) = \lambda^U_{Deg}(t) - \delta\lambda^M(t) \quad , \qquad (4.2)$$

where

$\phi^U(t)$, $\lambda^U(t)$ are the corrected latitude and longitude at the user's location;

$\phi^U_{Deg}(t)$, $\lambda^U_{Deg}(t)$ are the user's latitude and longitude obtained through degraded GPS signals;

$\delta\phi^M(t)$, $\delta\lambda^M(t)$ are the position corrections detected at the differential monitor station.

A geometrical description of the range correction is given in Figure 4.2. The range correction will be

$$\tilde{\rho}^U_i(t) = \tilde{\rho}^U_{i,Deg}(t) - \delta\rho^M_i(t) \quad , \qquad (4.3)$$

where

the index i refers to the satellites;

$\tilde{\rho}^U_i(t)$ is the corrected pseudorange at the user's location;

$\tilde{\rho}^U_{i,Deg}(t)$ is the degraded pseudorange at the user's location;

$\delta\rho^M_i(t)$ is the range correction detected at the differential monitor station.

The range correction $\delta\rho^M_i(t)$ determined at the differential monitor station is

$$\delta\rho^M_i(t) = \rho^M_{i,Deg}(t) - \rho^M_i(t) \quad . \qquad (4.4)$$

where

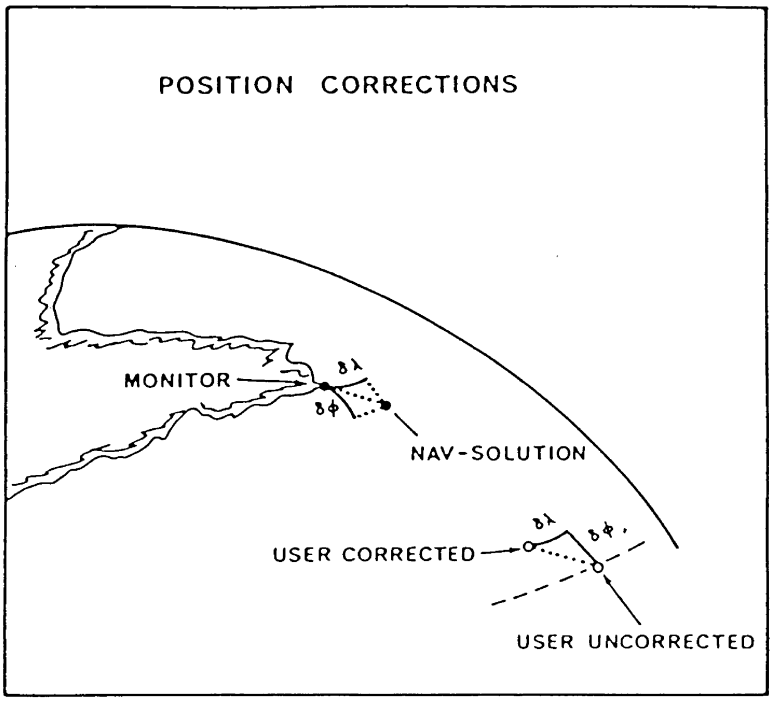


FIGURE 4.1
Position Corrections.

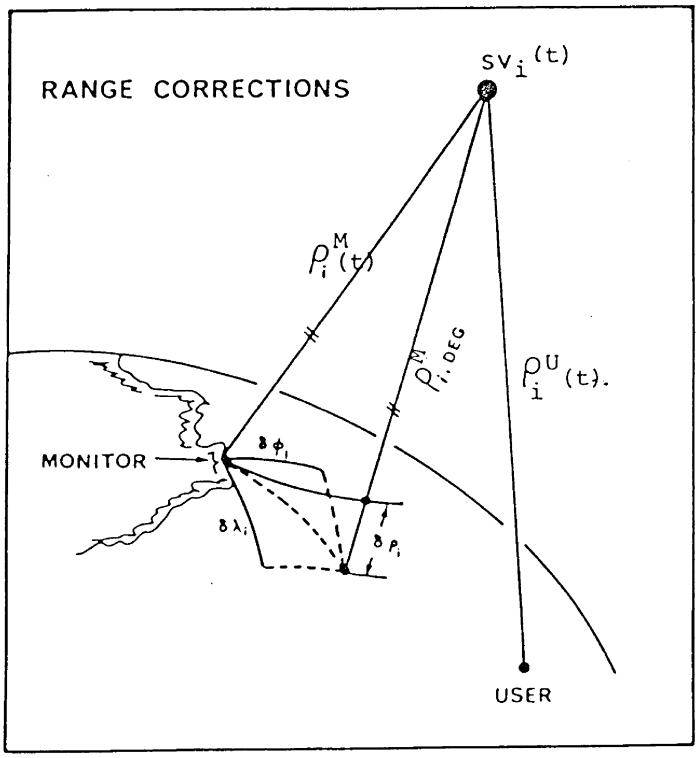


FIGURE 4.2
Range Corrections.

$\rho^M_{i,Deg}(t)$ is the degraded range to the ith satellite as observed by the monitor station, and

$\rho^M_i(t)$ is the correct (known) range from the monitor to the ith satellite.

## 4.3 Models for the GPS Signal Degradation

For the purpose of this thesis, we assume that the GPS degradation will consist of adding false biases to some of the broadcast GPS satellite ephemeris and/or clock parameters. We assume that no physical clock noise will be used to implement the degradation. These parameter biases are assumed to change slowly enough that the differential monitor stations can detect and communicate them to the user before they have changed significantly.

In previous simulation studies for differential GPS evaluation, the intentional degradation has been implemented in various ways. For example, in Cnossen et al. [1981], the degradation is generated by including a hypothetical bias of 80 metres in the range such that a 200 m CPE error in the navigation solution results. In this study, the generation of the intentional degradation is implemented for three cases:

1) degradation via time,
2) degradation via orbit parameters,
3) combined.

In the time degradation, we add a random component to the $a_o$ coefficient of the representation model for the space vehicle clock corrections (see van Dierendonck et al. [1978]), that is

$$a_{o,Deg}(t) = a_o + \sigma_{TIM} \cdot W_{TIM}(t) \qquad (4.5)$$

where

$a_{o,Deg}(t)$ = degraded time offset coefficient (seconds)

$a_o$ = undegraded time offset coefficient (seconds)

$W_{TIM}(t)$ = random number coming out of a Gaussian random number generator with zero mean and unit variance (unitless)

$\sigma_{TIM}$ = standard deviation of the imposed noise (seconds).

This type of intentional degradation entails a degradation not only in the pseudorange but also in the space vehicle position. The true position of the satellite will be different from that described in the navigation message, and the computed range will be spurious since it includes a time bias in the GPS time (see Figure 4.3).

The orbit degradation will again involve a random component to the satellite Cartesian coordinates $(x_i(t_k), y_i(t_k), z_i(t_k))$ applied to each satellite, that is

$$x_{i,Deg}(t_k) = x_i(t_k) + \sigma_{SAT} \cdot W_x(t_k) \tag{4.6}$$

$$y_{i,Deg}(t_k) = y_i(t_k) + \sigma_{SAT} \cdot W_y(t_k) \tag{4.7}$$

$$z_{i,Deg}(t_k) = z_i(t_k) + \sigma_{SAT} \cdot W_z(t_k) \tag{4.8}$$

where

$[x_i(t_k); y_i(t_k); z_i(t_k)]$ are the undegraded satellite coordinates,

$[x_{i,Deg}(t_k); y_{i,Deg}(t_k); z_{i,Deg}(t_k)]$ are the degraded satellite coordinates,

$W_x(t_k)$, $W_y(t_k)$, $W_z(t_k)$ are random numbers with N(0,1) (unitless),

$\sigma_{SAT}$ is the standard deviation of the imposed noise (metre).

Therefore the satellite position will be different than its true one. In this case, although the satellite position would be false, SV (false), the range is undegraded (see Figure 4.4).

The third case is a combination of the above two degradations. The

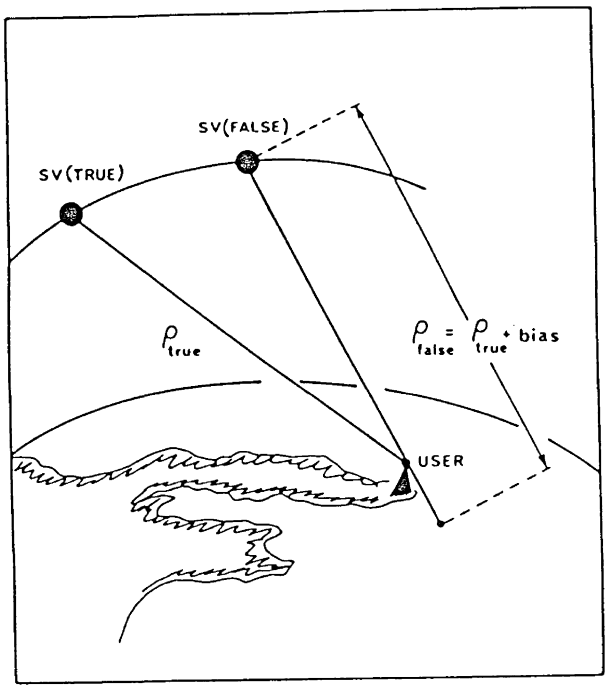


FIGURE 4.3

GPS Time Degradation.

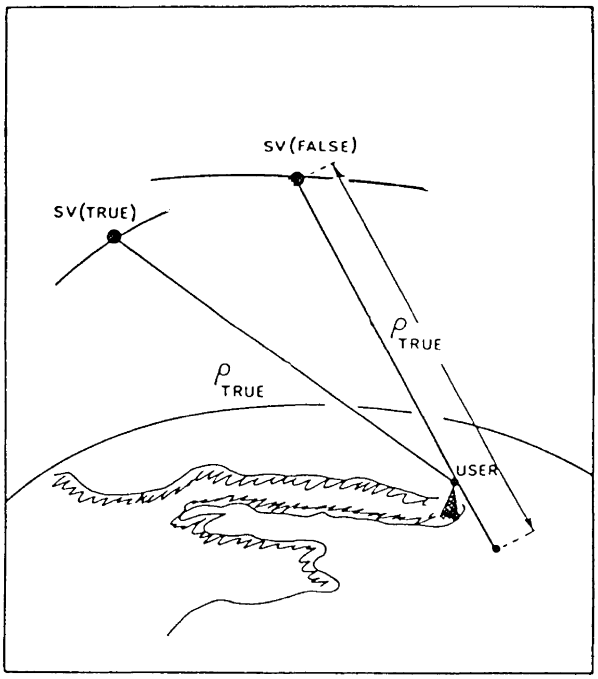


FIGURE 4.4

GPS Ephemeris Parameter Degradation.

intentional degradation should be such that a navigation error of 200 m CPE (500 m 2drms), specified in the Federal Radionavigation Plan, results.

## 4.4 Parameters Affecting the Differential GPS Navigation

There are a lot of factors that may affect the performance of the differential GPS navigation. These include:

1) The correlation of the differential corrections with distance from the differential monitor station.
2) The update rate of differential corrections (monitor correction broadcast rate).
3) The selection of site for installation of the differential monitor station.
4) The variations in geometry of satellite constellations.
5) The form of the intentional degradation employed.
6) The type of differential corrections.
7) The orientation of the user-monitor line.
8) Miscellaneous factors, such as the navigation algorithms, the ionospheric properties, the earth's curvature, etc. (see Ruedger [1981], Kalafus [1982]).

One major aspect which should be examined to evaluate the differential GPS concept, is the range of effectiveness of the differential corrections. The investigation of distance as a significant parameter would be a significant factor for the development of not only a ground-based network of differential monitor stations but probably a satellite-based one as well. Limitations in the data communication link, such as line of sight, propagation, etc., problems,

may be a determining factor that will probably restrict the application of differential corrections at very large distances. Relay satellites, which retransmit received signals down to earth without altering them, may help in overcoming some of the transmission problems for the differential corrections.

The update rate of the corrections is another important factor for the evaluation of the differential GPS. The determined differential corrections should be representative of the GPS bias errors and transmitted to nearby users fast enough so that no significant error variations will occur during their application. The update of the differential corrections at an improper rate (too slow) may deteriorate the behaviour of the differential mode. Previous studies [Howel et al., 1980] have already examined the update rate aspect. They have indicated that differential errors increased with decreasing update rate. Kalafus [1982], using real degraded signals, points out that differential corrections would be useless, if they are transmitted every minute or so.

As previously mentioned, the revolution of the GPS satellites is approximately 12 hours. Therefore, for a particular user on earth the same satellite configuration will repeat itself every 24 hours. The geometric variation of the satellite constellations over a day will influence the performance of the differential GPS navigation. Sometimes, the satellite-receiver geometry will favour the differential mode, but sometimes it will not. To get a better appreciation of the behaviour of the differential mode, an analysis of the parameters influencing the differential GPS performance should be extended over 24 hours to include different satellite configurations.

The introduction of Selective Availability errors into the GPS will determine the navigational accuracy of not only the point positioning but also the differential mode. So far, no final plans have been reported by the U.S. Department of Defense. Evaluation of the differential mode under a would-be intentional degradation prompted us to develop models, as previously explained in Section 4.4. It should be noted again, that results in this study are only indicative of the differential GPS performance since the intentional degradation employed may or may not be the contemplated one.

The way of implementing correction terms is another important factor. Some types of differential corrections may result in a better navigation performance than others, and may also be valid over large areas. For example, position corrections applied to distant users may not let the users be flexible for processing different algorithms for satellite selection and navigation solution, since they should conform to the differential monitor processes for the satellite selection e.g., common satellites. The above condition will be an impediment in providing position corrections over large distances.

The differential GPS performance is expected to vary with direction. This is due primarily to the variability of satellite-receiver geometry along various directions (azimuths).

Our knowledge about the propagation properties of the upper layers (e.g., 20 000 km height) of the ionosphere is quite scanty. The GPS signals will propagate through different ionospheric paths for the monitor and user and, therefore, the ionosphere may play an important role in affecting the differential GPS performance.

Visibility problems due to the earth's curvature and mask angle is

another consideration in the evaluation of the differential GPS concept. A more complete explanation of these miscellaneous factors is given in Ruedger [1981] and Kalafus [1982].

However, the bias errors may be reduced by using the differential mode, the receiver random noise becomes an obstacle in the further improvement of the differential C/A-code performance. Sometimes, it dominates over other random errors [Ward, 1981; Kalafus, 1982]. This receiver noise effect can be solved by improvements in the receiver's design.

# 5

# Simulation Description

Differential GPS navigation using the degraded C/A-code is investigated in a computer simulation program. A simplified block diagram of the simulation program, a flow chart, and an explanation of the geometry involved, are given in Figures 5.1, 5.2, and 5.3, respectively. A list of the subroutines employed is given in Appendix II.

This simulation consists of

1. a trajectory generation;
2. selection of differential monitor station and user test sites;
3. imposition of intentional degradation;
4. alert algorithms;
5. generation of GPS pseudoranges;
6. navigation solution for the differential monitor station and the user;
7. application of differential corrections;
8. interpretation of the results; statistical summary.

The satellite constellation used is that of 18 satellites in 6 orbital planes, with three satellites equally spaced in each plane at an inclination of $55^{o}$ and a nominal period of a satellite revolution

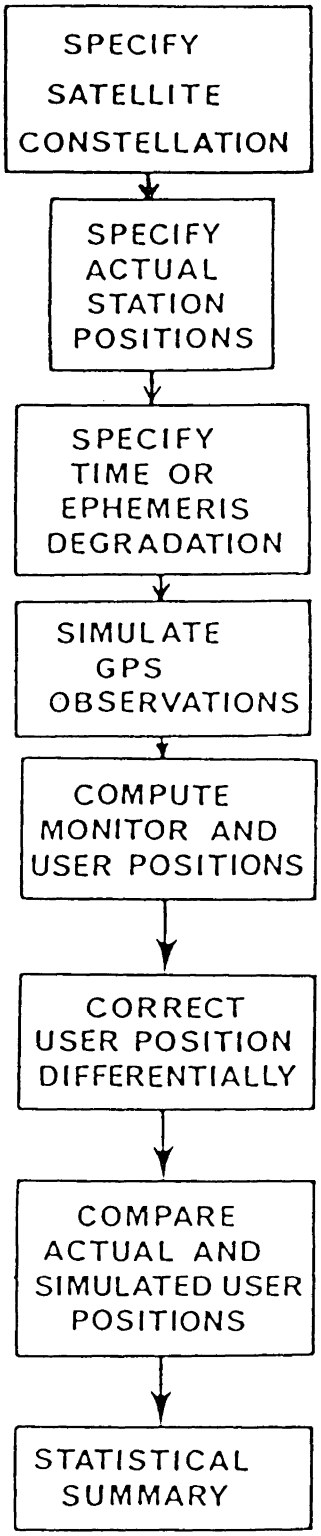


FIGURE 5.1

Simulation Block Diagram.

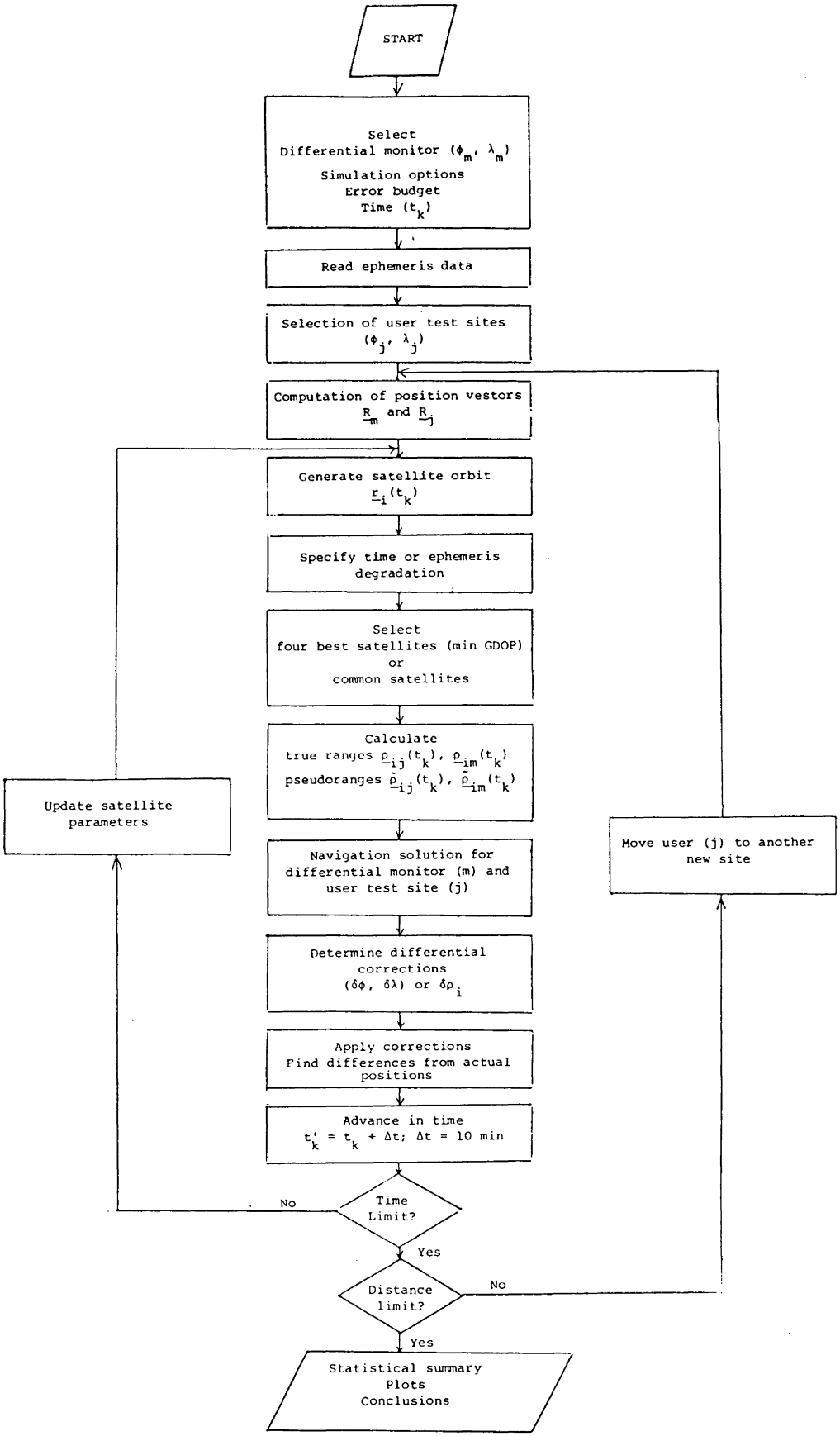


FIGURE 5.2
Simulation Flow Chart

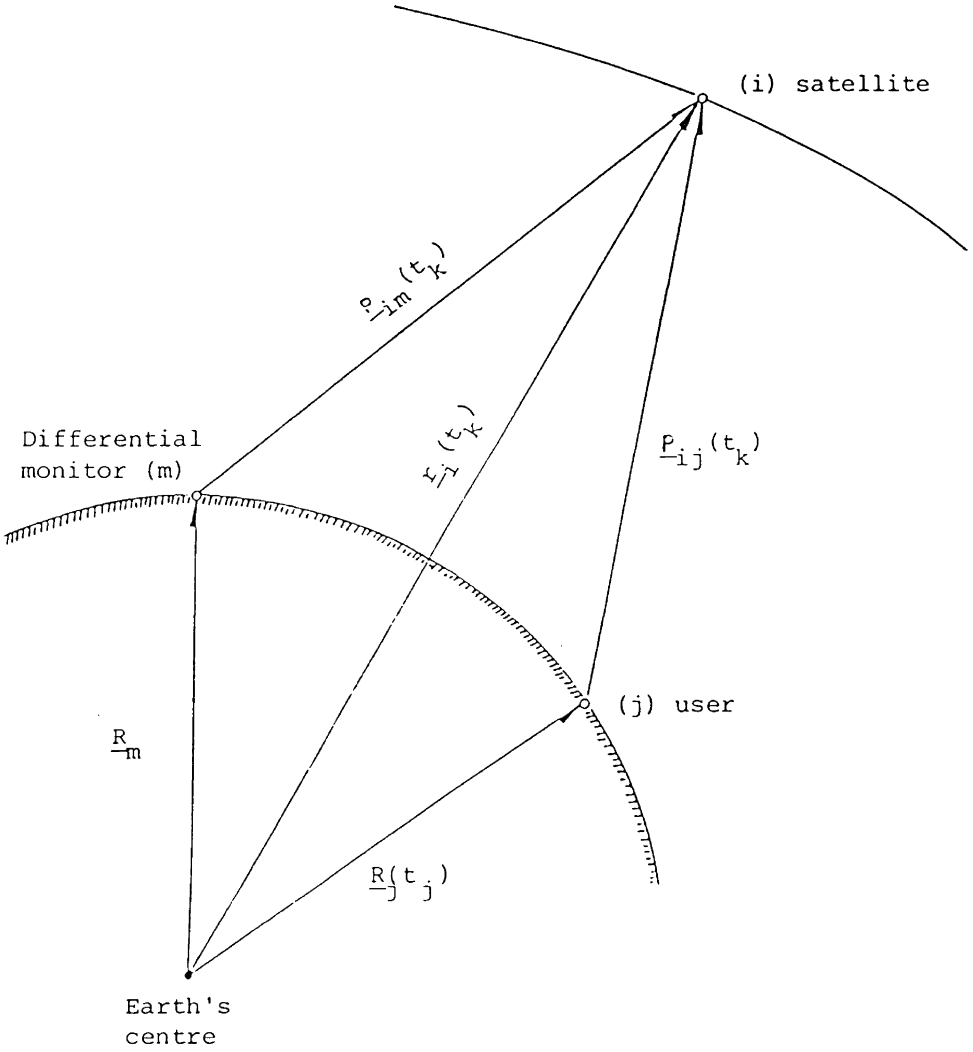


FIGURE 5.3

Geometry of Differential GPS Navigation.

T = 11 h, 57 min, 57.26 sec [Payne, 1982].

The differential monitor station selected is Cape Race, Newfoundland ($\phi$ = 46-46-30N, $\lambda$ = 53-10-30W), as shown in Figure 5.4. This position was selected for the following reasons:

1. it can provide an extensive coverage in the Atlantic Ocean;
2. it has been used as a transmitting station by other radionavigation aids, such as LORAN-C. With some modifications, the signals from this kind of station may be used as carriers of differential GPS corrections to users at distant locations.

The user test sites are changing positions and are moving away from the differential monitor station such that the accuracy performance with respect to distance can be evaluated. The user test sites are distributed in three different ways: along a parallel circle; along a meridian; and diagonally, as shown in Figures 5.4 and 5.5. Figures 5.6 and 5.7 depict the distribution of the GDOP values with time when a four-parameter solution (X, Y, Z, $\Delta$t) is performed by selecting the best set of four satellites. These two diagrams correspond to Cape Race and to a user 1000 km away along the diagonal, respectively. The above distribution is based on samples taken every 10 minutes for 24 hours.

The intentional degradation is implemented by using equations (4.5), (4.6), (4.7), (4.8), and combinations of them, as previously explained in Section 4.4. Table 5.1 shows the standard deviations of the imposed degradation that result in an approximately 200 m CPE error in the navigation solution over 24 hours (10 minute fix) using the best satellites for the solution.

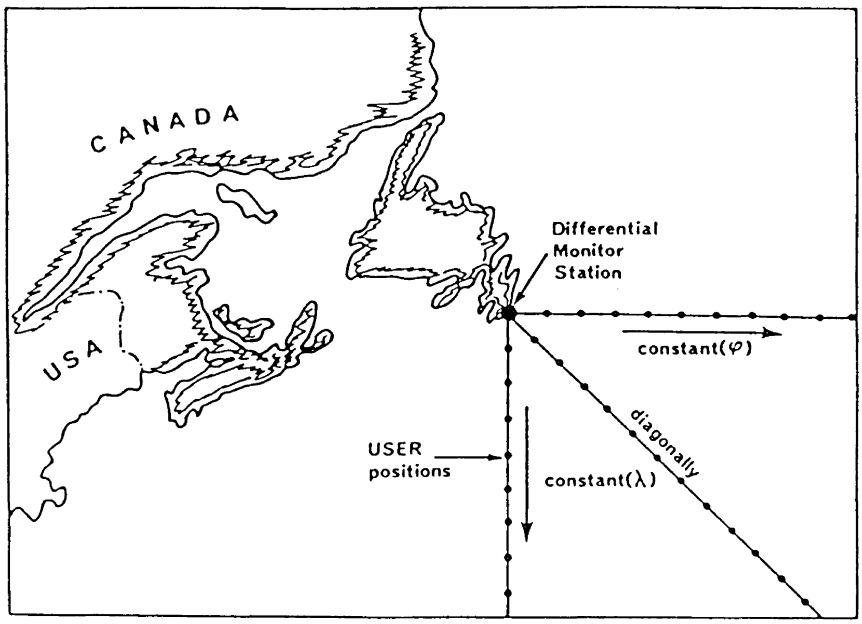


FIGURE 5.4

Simulation Geometry.

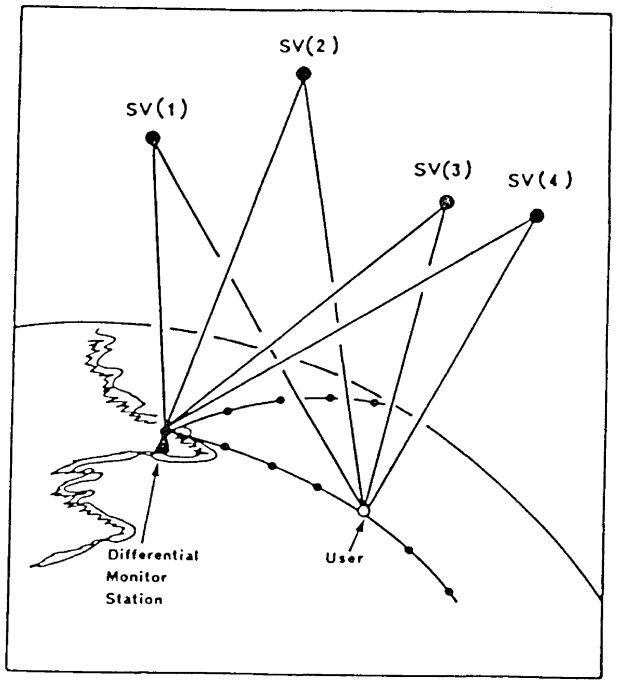


FIGURE 5.5

Effect of Monitor-User Separation.

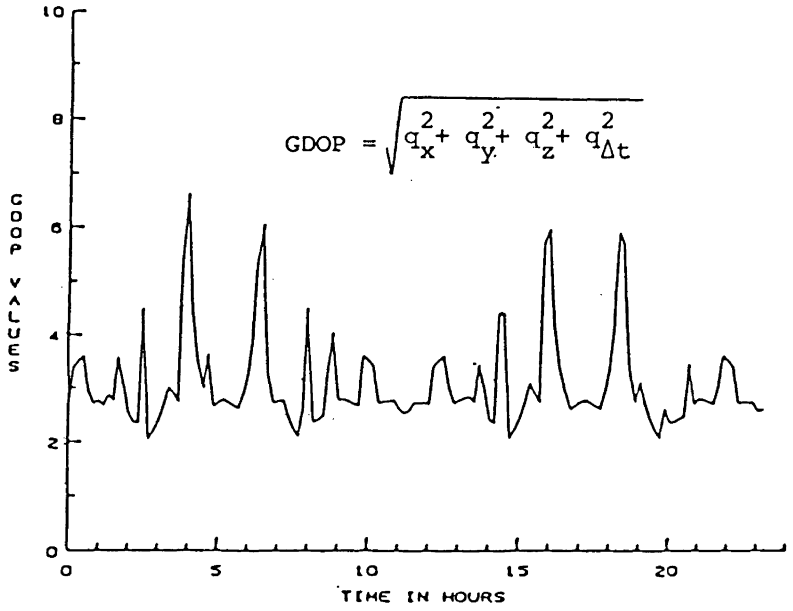


FIGURE 5.6

GDOP Distribution with Time at Cape Race, Newfoundland(four best satellites).

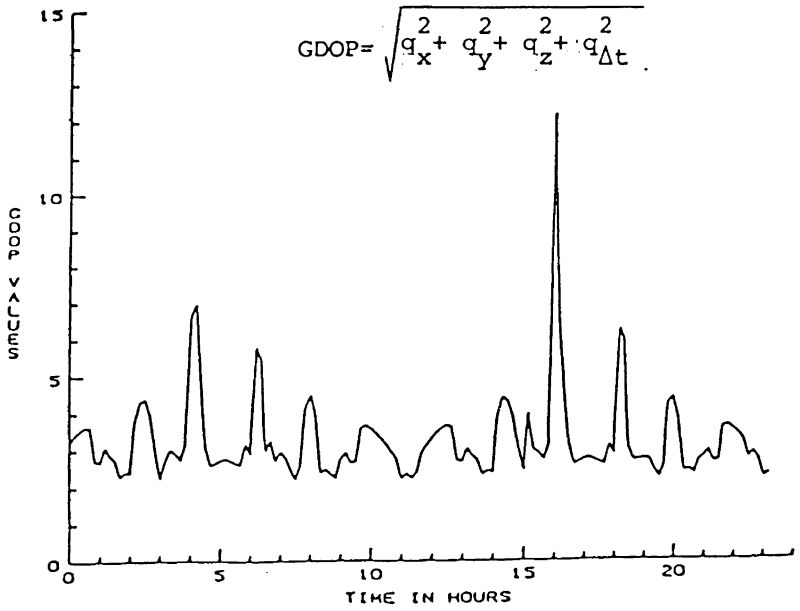


FIGURE 5.7

GDOP Distribution with Time at a User's Location ($\phi$=40-6-30,$\lambda$=313-19-30) (four best satellites).

| Type of Intentional Degradation | Standard Deviation of the Imposed Noise |
|---|---|
| Satellite position degradation | $\sigma_{SAT} = \pm$ 145 metres |
| Time degradation | $\sigma_{TIM} = \pm$ 430 nsec |
| Combined degradation | $\sigma_{SAT} = \pm$ 80 metres |
| | $\sigma_{TIM} = \pm$ 355 nsec |

TABLE 5.1

Intentional Degradation.

In order to determine which satellite measurements yield the best information for determining a receiver's location, a set of GPS satellites must be selected based on some criterion. This is done by using alert algorithms. When position corrections ($\delta\phi(t)$, $\delta\lambda(t)$, $\delta_{\Delta}t(t)$) are applied (see Figure 5.8), the program itself will search for the satellites visible to both the differential monitor station and the user (e.g., SV(2), SV(3), SV(4), SV(5), SV(6), and the navigation solution is performed using only these satellites. If less than three common satellites are available, the program will stop by itself.

The degree of improvement in the differential performance over the conventional one, and/or the termination of the simulation due to the lack of adequate common satellites for a unique navigation solution (less than three), are indications of the range of effectiveness of the differential position corrections.

When range corrections ($\delta\rho_i(t)$) are implemented, the algorithm for the selection of satellites could be either the previously explained procedure (see Figure 5.9) or it could be more flexible when all visible

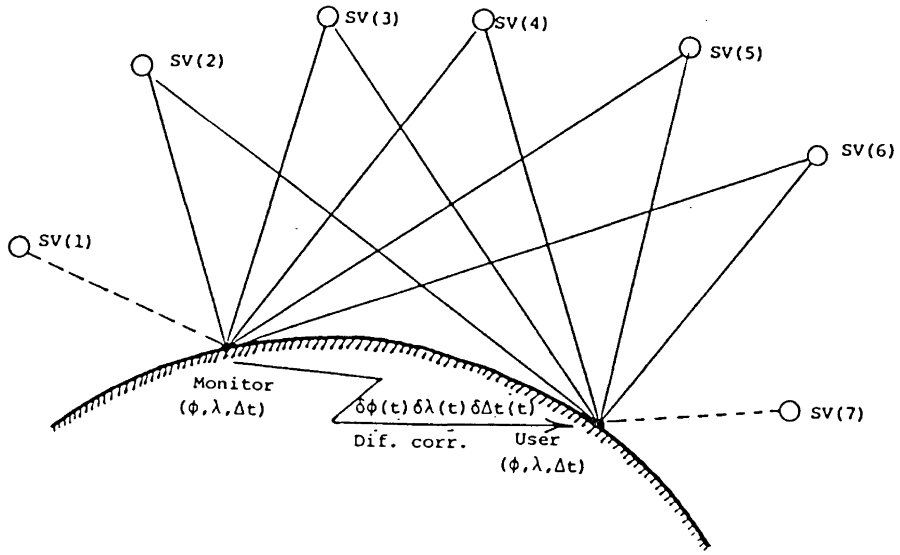


FIGURE 5.8
Position corrections;Common Satellites

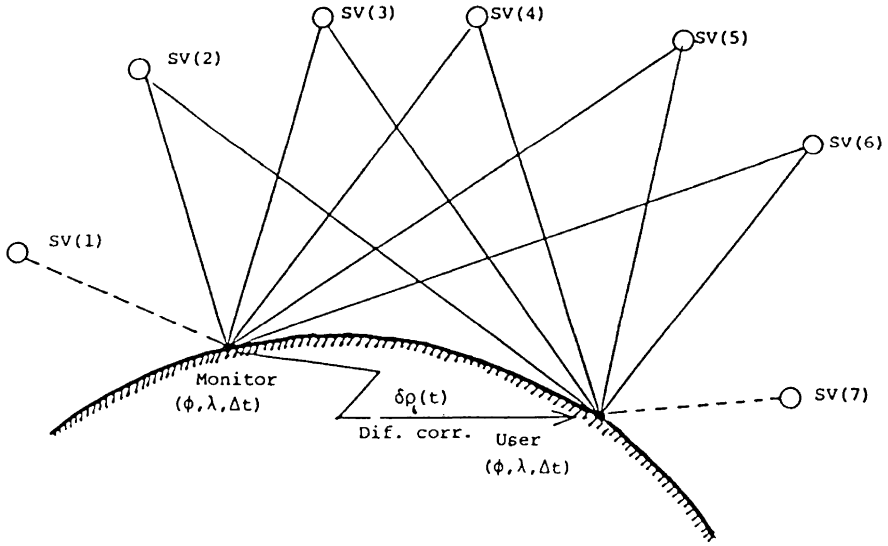


FIGURE 5.9
Range corrections;Common Satellites

GPS satellites are included in the monitor's solution (see Figures 5.10, 5.11). In the latter case, the selection of satellites for the user test sites is based on an algorithm which determines those four satellites that yield the best navigation performance (minimization of the tetrahedron's volume). The GDOP is kept to its minimum value. It is noteworthy that if a satellite, from the best set of four (e.g., SV(7)-Best), is not included in the set of all satellites visible to the monitor, no range corrections are applied to these particular satellite measurements, and they are not included in the user's solution. A summary of the differential corrections is given in Table 5.2.

GPS measurements are generated by using the following equation:

$$\tilde{\rho}_{ij}(t) = \rho_{ij}(t) + e_{SV}(t) + e_{RCV}(t) + e_{REF}(t) + e_{SCLK}(t) + e_{RCLK}(t), \quad (5.1)$$

where

$\tilde{\rho}_{ij}(t)$ = pseudorange from the jth receiver to the ith satellite (metres)

$$\rho_{ij}(t) = \text{true range} = \sqrt{(x_i - X_j)^2 + (y_i - Y_j)^2 + (z_i - Z_j)^2} \quad . \quad (5.2)$$

The terms $e_{SV}$, $e_{RCV}$, $e_{REF}$, $e_{SCLK}$ and $e_{RCLK}$ are again expressed in metres and are error terms which correspond to satellite (SV), receiver (RCV), refraction (REF), satellite clock (SCLK), and receiver clock (RCLK), respectively. These are generated using the following equations:

$$e_{SV}(t) = \sigma_{SV} \cdot W_{SV}(t) \quad , \quad (5.3)$$

$$e_{RCV}(t) = \sigma_{RCV} \cdot W_{RCV}(t) \quad , \quad (5.4)$$

$$e_{REF}(t) = \Delta\rho_{ION}(t) + \Delta\rho_{TRO}(t) \quad , \quad (5.5)$$

$$e_{CLK}(t) = \alpha_0 + a_1(t - t_{oc}) + a_2(t - t_{oc})^2 + (\sigma_{CLK}\, W_{CLK}(t)), \quad (5.6)$$

where

$W_{SV}(t)$ and $W_{RCV}(t)$ and $W_{CLK}(t)$ are numbers coming out of a Gaussian random number generator with zero mean and unit variance;

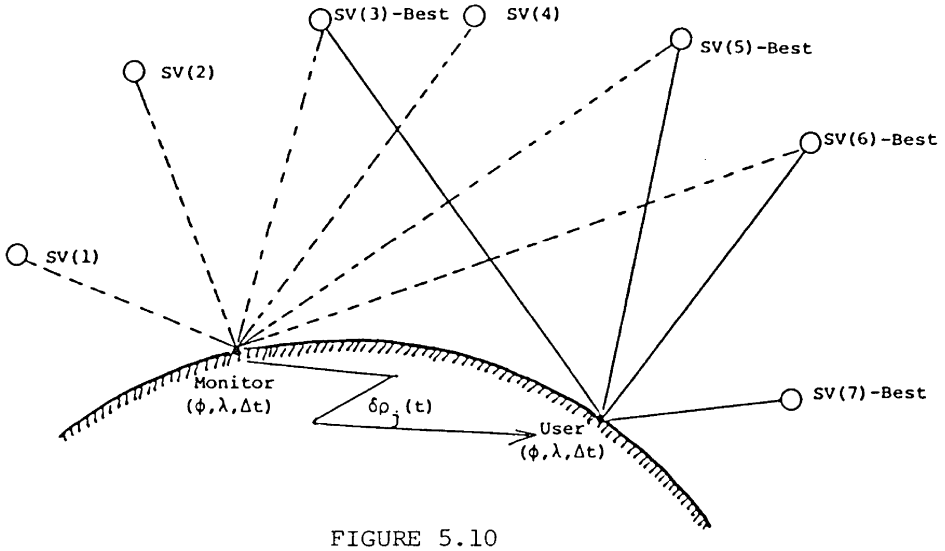


FIGURE 5.10
Range Corrections;All Visible Satellites

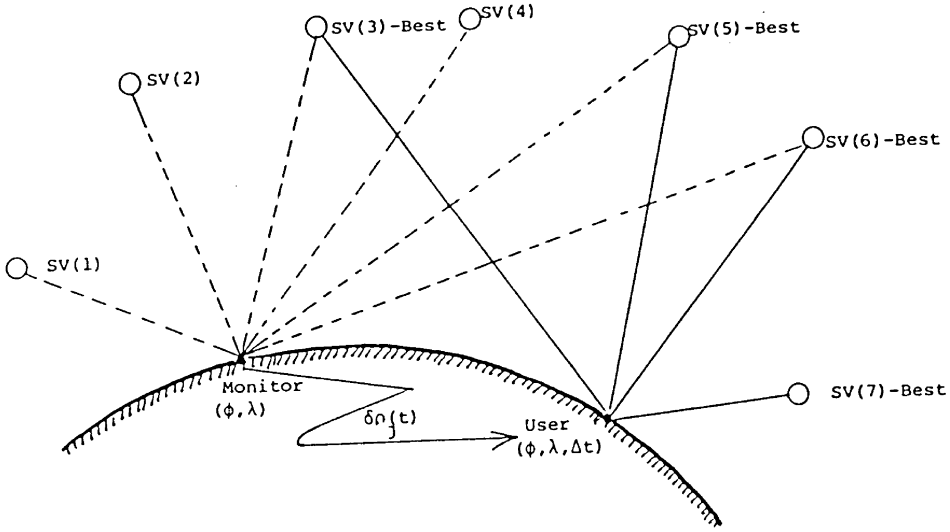


FIGURE 5.11
Range Corrections;All Visible Sat.;Clock Constrained.

| Model of Differential Corrections | Navigation Solution: Monitor | Navigation Solution: User | Description of Selected Set of Satellites | Form of Differential Corrections |
|---|---|---|---|---|
| Position Corrections | $\phi$, $\lambda$, $\Delta t$ Common satellites | $\phi$, $\lambda$, $\Delta t$ Common satellites | same common satellites between all-in-view at monitor and all-in-view at user | $\delta\phi(t)\,\delta\lambda(t)\,\Delta\delta(t)$ |
| Range Corrections | $\phi$, $\lambda$, $\Delta t$ Common satellites | $\phi$, $\lambda$, $\Delta t$ Common satellites | same common satellites between all-in-view at monitor and all-in-view at user | $\delta\rho_i(t)$ |
| Range Corrections | $\phi$, $\lambda$, $\Delta t$ all-in-view satellites | $\phi$, $\lambda$, $\Delta t$ Common satellites | same common satellite between all-in-view at monitor and best four at user (usual case: common $\equiv$ best four) | $\delta\rho_i(t)$ |
| Range Corrections and Clock Constrained | $\phi$, $\lambda$ all-in view satellites | $\phi$, $\lambda$, $\Delta t$ Common satellites | same common satellites between all-in-view at monitor and best four at user (usual case: common $\equiv$ best four) | $\delta\rho_i(t)$ |

TABLE 5.2

Summary of Differential Corrections.

$\sigma_{SV}$ was taken as 1.5 metres and $\sigma_{RCV}$ as 10 metres for the C/A-code;

$\Delta\rho_{ION}$ and $\Delta\rho_{TRO}$ are range errors due to ionospheric and tropospheric delay [Martin, 1980; Hopfield, 1972];

$e_{CLK}(t)$ is a deterministic clock model with a random noise ($\sigma_{CLK} = 2.10^{-11}$ sec) incorporated [van Dierendonck et al., 1978; Fell, 1980].

The frequency dependent delay ($\Delta\rho_{ION}$) was computed as [Martin, 1980]:

$$\Delta\rho_{ION}=\Delta\rho_{ij}(t,L_1)=\left[\tilde{\rho}_{ij}(t,L_1)-\tilde{\rho}_{ij}(t,L_2)\right]\frac{(L_2)^2}{(L_2)^2-(L_1)^2}+\sigma_{ION}W_{ION}(t) \quad (5.7)$$

where

i index refers to the satellite;

j index refers to the receiver;

$L_1$ and $L_2$ are the GPS frequencies;

$\tilde{\rho}_{ij}(t,L_1)$ and $\tilde{\rho}_{ij}(t,L_2)$ are ranges affected by refraction at the $L_1$ and $L_2$ frequencies, respectively;

$\sigma_{ION}$ was taken as 0.04 metres;

$W_{ION}(t)$ are random numbers with N(0,1).

The tropospheric delays were calculated using the simplified Hopfield model [Hopfield, 1969]:

$$\Delta\rho'_{TRO} = \frac{K_d}{\sin(E^2+6.25)^{1/2}} + \frac{K_W}{\sin(E^2+2.25)^{1/2}} \quad , \quad (5.8)$$

where

$$K_d = 1.552 \times 10^{-5}\left(\frac{P}{T}\right)((148.72T - 448.3552) - h_j)$$

$$K_W = 7.46512 \times 10^{-2}\left(\frac{e}{T^2}\right)(11000 - h_j)$$

T = temperature in degrees of Kelvin,

P = pressure in mbars,

E = elevation angle to the satellite in degrees,

e = water vapour pressure in mbars,

$h_j$ = height of the station above the geoid in metres.

For our computations, we used T = 5.85°C, P = 1020 mbar, and e = 100%.

The total tropospheric effect incorporated in the simulation included the actual effect adding random and systematic components, such as,

$$\Delta\rho_{TRO} = \Delta\rho'_{TRO} + K_{TRO}(\Delta\rho'_{TRO}) + \sigma_{TRO}\, W_{TRO}(t) \quad , \qquad (5.9)$$

where

$K_{TRO}$ = input factor defining the amount of the actual effect to be added to the tropospheric correction as a systematic error (K = 4%),

$\sigma_{TRO}$ = 0.05 metres,

$W_{TRO}(t)$ = random numbers from N(0,1).

The navigation solution is performed through a least-squares procedure. The sought solution is corrections to approximate values of user longitude, latitude and receiver clock offset ($\delta\phi$, $\delta\lambda$, $\delta\Delta t$; three-parameter solution).

The application of differential corrections is implemented by the models explained in Chapter 4. When position corrections are applied to the user's solution, equations (4.1) and (4.2) are used. When range corrections are applied to pseudoranges prior to calculating the user's solution, equations(4.3) and (4.4) are employed.

In our simulation runs a multi-channel receiver was considered and a single fix was computed every 10 minutes for the differential monitor

station and the user. The simulation was extended over 24 hours (140 fixes) and therefore different satellite configurations were involved in the analysis.

Several plotting subroutines are used to present the results obtained, and they are described in the next chapter.

# 6

# Results

This chapter provides a discussion of the results, and demonstrates the influence of some geometrical aspects, such as direction, separation distance, etc., on differential GPS navigation. All the concepts are applied to marine navigation (two dimensional) only and to intentionally degraded C/A-code signals (Standard Positioning Service), considering the 18-satellite configuration.

We have assumed multi-channel receivers at the differential monitor station and the user test sites that provide continuous tracking of all the GPS satellites. As previously explained, 140 single fixes were computed over 24 hours (10 minute fix) for both receivers.

In this study, we assume the application of differential corrections by the user to be simultaneous with their detection at the monitor station. Other studies have examined the error introduced by the communication delays between user and monitor, as well as the frequency with which updates should be provided (see Howell et al. [1980]).

The user is moved away from the monitor station. Various positions and headings of the user will cause the monitor and the user to observe the GPS satellite signals from a different perspective. The degree of

correlation between the monitor's and the user's errors will determine the monitor's coverage area.

The information transmitted to users from the differential monitor can be summarized as follows:

(a) Position corrections--common satellites

  (i) differential corrections: $\delta\phi(t)$, $\delta\lambda(t)$,

  (ii) number and identifier codes of common satellites among all those in view at the differential monitor and the user.

(b) Range corrections--common satellites

  (i) differential corrections: $\delta\rho_i(t)$,

  (ii) number and identifier codes of common satellites among all those in view at the differential monitor and the user.

(c) Range corrections--all visible satellites

  (i) differential corrections: $\delta\rho_i(t)$,

  (ii) number and identifier codes of tracked visible satellites at the differential monitor.

(d) Range corrections--all visible satellites--clock constrained

  (i) differential corrections: $\delta\rho_i(t)$,

  (ii) number and identifier codes of tracked visible satellites at the differential monitor.

For the cases of (a) and (b) above, the navigation algorithm employed solves for three parameters ($\phi$, $\lambda$, $\Delta t$) and incorporates the common satellites from all those in view at the differential monitor and the user only. This implies that the two receivers require the knowledge beforehand of which common satellites are to be included in the solution. To handle this, the receivers should be "aware" of the approximate position of one another in order to make use of the alert

algorithms. This does not seem to be an easy task. A communication link might be used to communicate the vessel's positions to the monitor. Nevertheless, the technique for the selection of common satellites is suitable for post-processing applications.

The third case (c) incorporates a three-parameter solution ($\phi$, $\lambda$, $\Delta t$), whereas the fourth case (d) only a two-parameter ($\phi$, $\lambda$) solution. It is of interest to note that these last two procedures are more flexible, since they impose no restriction on the user for the selection of satellites. However flexible the user might be, he still has to search for the common satellites between his best set and all those in view at the monitor. The two separated receivers do not usually observe the same set of either visible or best satellites over 24 hours. This search is done in order to exclude satellites from the best set which were not taken into the monitor's solution. Therefore, the navigation solution for the user will utilize these common satellites only. On the other hand, biases experienced by the two receivers will be the same by using the same satellites. In such a case, the differential mode is expected to be efficient.

The selection of those satellites which will yield the "best" navigation performance constitutes an optimization problem, and is beyond the scope of this study. The best set of four satellites for a four-parameter solution or the best set of three, which seems more appropriate for our three-parameter solution, induce a minimization problem. Either one has to minimize certain DOP values, or volumes of special figures, such as the special tetrahendron, and so on. These quantities are, of course, related and aim at the reduction of errors of the navigation solution. Reduction of position error means reduction of

the various factors that influence it. For example, the satellite-receiver geometry is a significant factor. This is related to the GDOP value. A high GDOP value means an unfavourable satellite-receiver geometry and vice versa. Knowledge of the DOP condition will assist us in investigating the errors introduced by the satellite receiver geometry to the system when the differential mode is applied.

Figures 6.1 and 6.2 show time series data of the radial deviation (e.g., $\Delta R_i(t) = \sqrt{\Delta\phi_i^2(t) + \Delta\lambda_i^2(t)}$) at the monitor when intentional degradation of time and satellite position is employed, and without degradation, respectively.

The following diagrams show the DOP distribution over 24 hours at two different locations, e.g., Cape Race, Newfoundland (differential monitor), and a user 1000 km away ($\phi$ = 40-6-30, $\lambda$ = 313-19-30). The masking angle considered was 5 degrees. These diagrams correspond to the previously explained satellite algorithms for differential operation, and they provide a comparison with respect to the geometric influence on the solution.

Figures 6.3 and 6.4 correspond to the HTDOP values obtained for the common satellites for the monitor and the user in a three-parameter solution. Figures 6.5 and 6.6 pertain to all the visible satellites for the monitor and the best set of four satellites for the user, respectively. The average value of HTDOP for the above four cases is around 2.0.

The choice of a two-parameter solution, i.e., the "clock constrained solution", shows a significantly stronger geometry of the system. This is depicted in Figure 6.7, where the mean value of the HDOP is approximately 1.0.

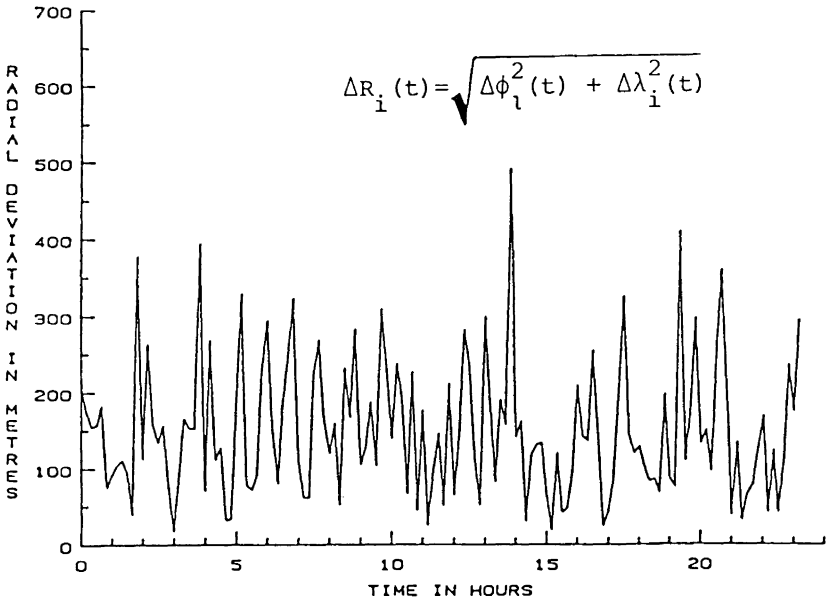


FIGURE 6.1
Variations of the Radial Deviation with Time
Using Common Satellites for the Solution.

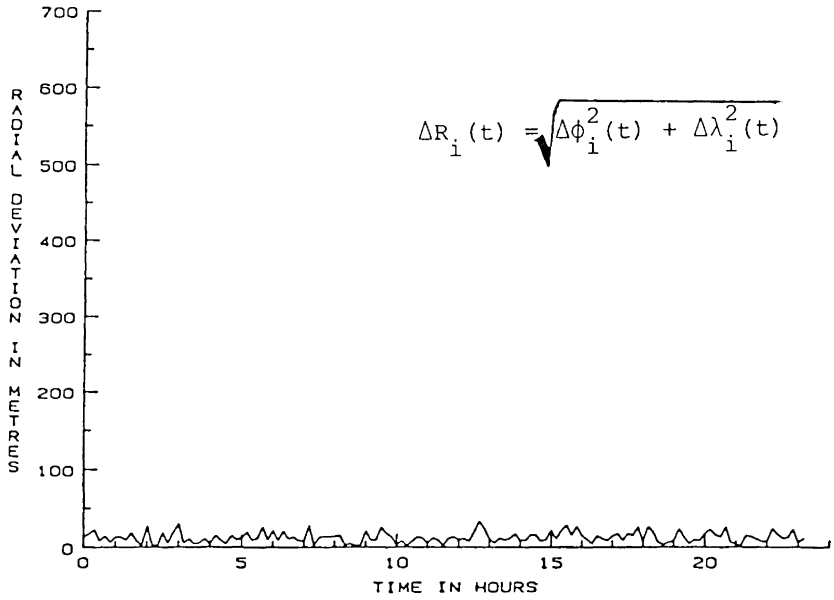


FIGURE 6.2
Variations of the Radial Deviation with time
Using Common Satellites for the Solution.

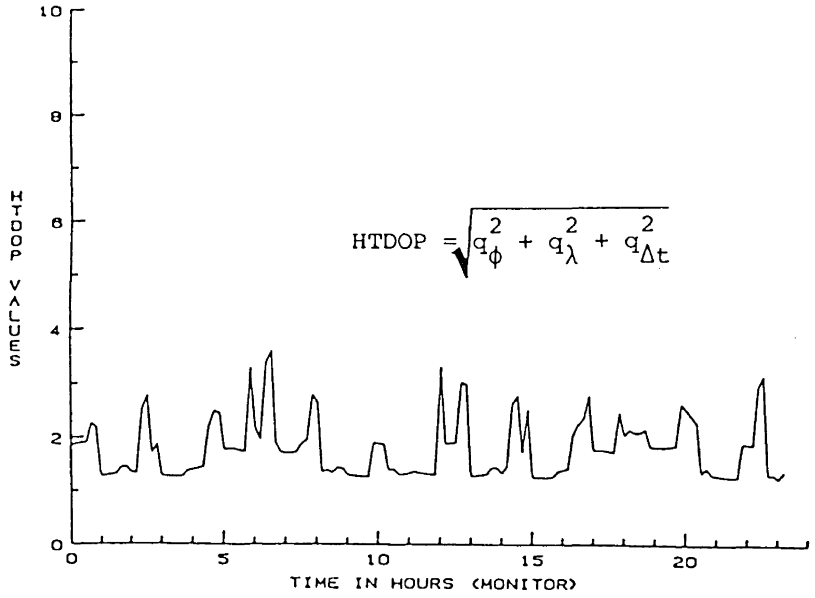


FIGURE 6.3
Common Satellites;Three-parameter Solution

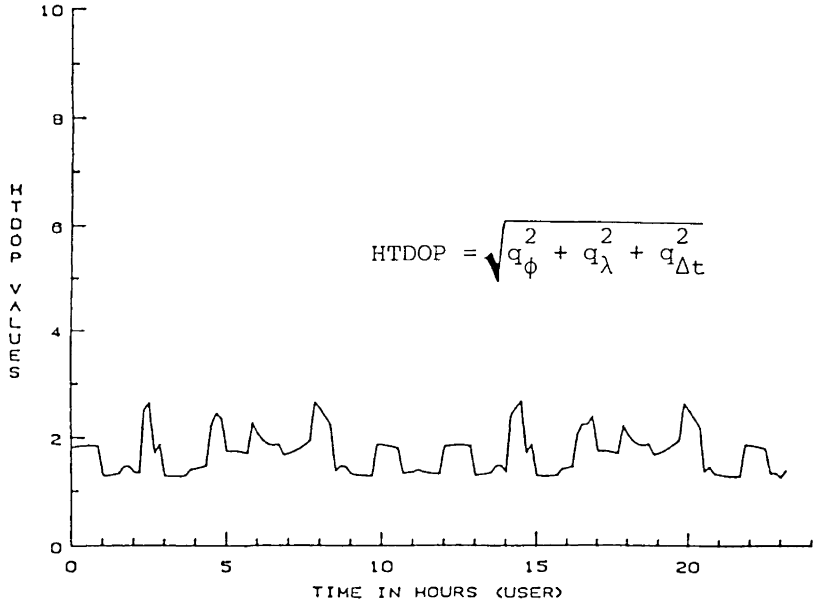


FIGURE 6.4
Common Satellites;Three-Parameter Solution

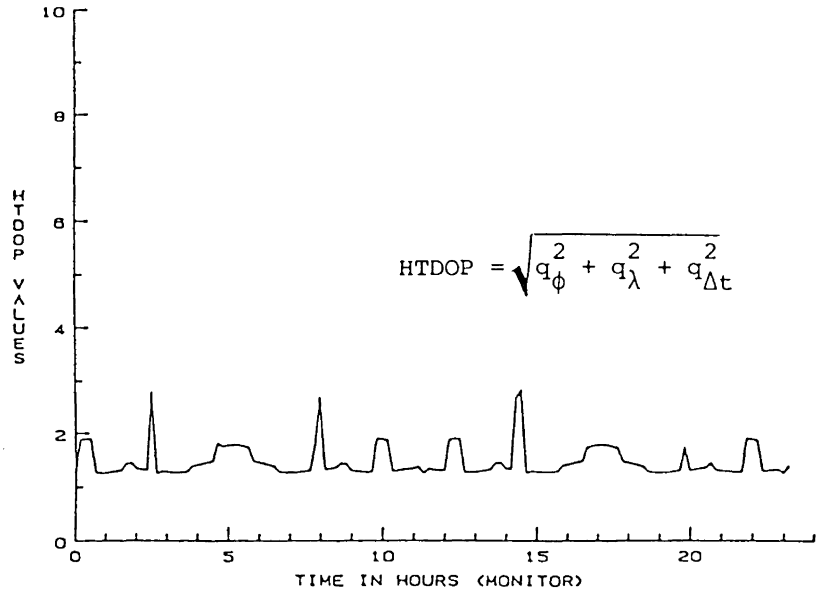


FIGURE 6.5
All Visible Satellites;Three-Parameter Solution.

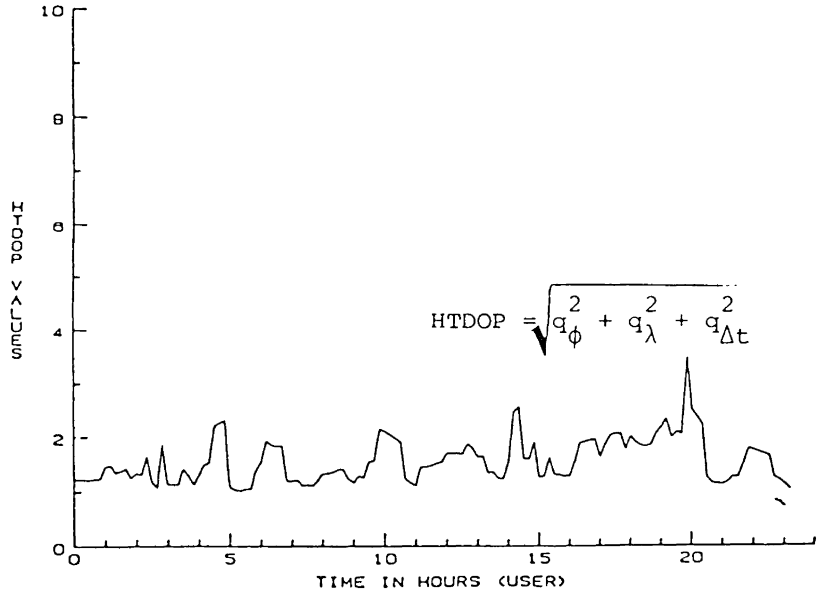


FIGURE 6.6
Best Four Satellites;Three-Parameter Solution.

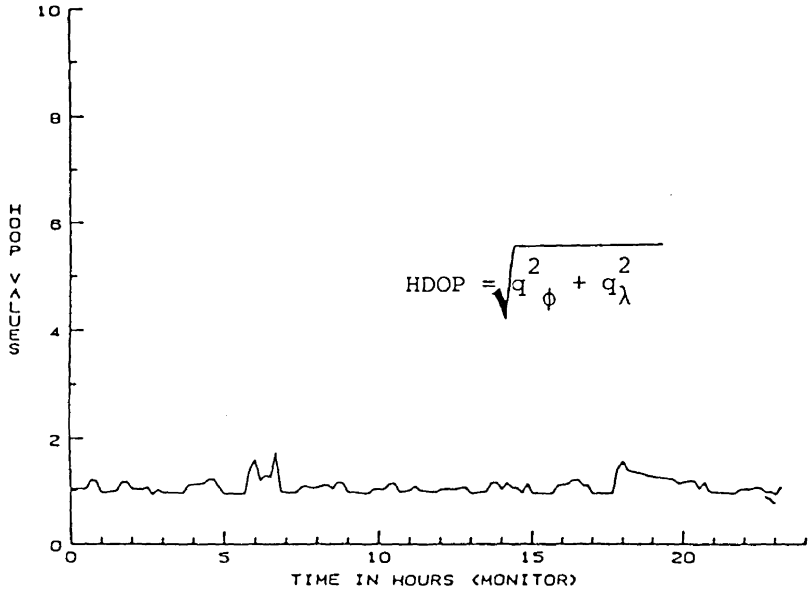


FIGURE 6.7
All Visible Satellites;Two-Parameter Solution.

Table 6.1, 6.2, and 6.3 show a point positioning comparison between the conventional and differential modes. The user is situated 117 km ($\phi$ = 46-1-30, $\lambda$ = 307-34-30) away from the monitor station. The figures represent 140 fixes over 24 hours expressed in CPE and 95th percentile values. The CPE values were calculated by using equation (3.15) and the 95th percentiles by the procedure explained in Section 3.4.

The numbers presented in these tables are indicative only of the degree of relative improvement one might expect from the use of differential GPS navigation. As a first point of interest, note that when the differential operation is chosen, horizontal errors immediately drop to approximately 17 metres CPE, or to 38 metres 95th percentile, certainly a significant improvement of about nine times. The same dramatic improvement is not achieved though when all the visible satellites are included in the monitor's solution and its clock is not constrained. In this case, the improvement factor is about 1.5.

Table 6.4 shows some values of the horizontal accuracies interpreted with the aid of percentiles, CPE (50%) and 2drms (95%) error figures. It should be noted that there is a difference between the results obtained through rank statistics and the ones with CPE and 2drms; still the improvement factor is about the same. This table corresponds to a time and satellite position degradation when position corrections are applied and the user being coincident with the monitor station (0 km away). At any rate, it is obvious that differential GPS navigation alleviates the effects of the degraded C/A-code.

Positional accuracy seems always to be affected by some geometry and some combination of inherent errors of the particular navigation system involved. The same principle holds for the GPS system. The

| Degradation Mode | Correction Mode | Point Positioning CPE (m) | Differential CPE (m) | Improvement Factor |
|---|---|---|---|---|
| Satellite Ephemeris | Position (Common Satellites) | 161.81 | 16.66 | 9.7 |
| | Range (Common Satellites) | 161.81 | 16.23 | 9.9 |
| | Range (Best Satellites) | 227.98 | 141.49 | 1.6 |
| Time | Position (Common Satellites) | 155.42 | 16.37 | 9.5 |
| | Range (Common Satellites) | 155.42 | 16.15 | 9.6 |
| | Range (Best Satellites) | 204.34 | 135.04 | 1.5 |
| Combined Time and Satellite Ephemeris | Position (Common Satellites) | 153.03 | 16.52 | 9.3 |
| | Range (Common Satellites) | 153.03 | 16.20 | 9.4 |
| | Range (Best Satellites) | 199.84 | 130.42 | 1.5 |

TABLE 6.1

Comparison of Conventional Degraded GPS (C/A-code) with Differential at a User 117 km Away from the Monitor (three-parameter solution for the monitor).

| Degradation Mode | Correction Mode | Point Positioning 95th Percentile (m) | Differential 95th Percentile (m) | Improvement Factor |
|---|---|---|---|---|
| Satellite Ephemeris | Position (Common Satellites) | 330.87 | 38.22 | 8.7 |
| | Range (Common Satellites) | 330.87 | 35.92 | 9.2 |
| | Range (Best Satellites) | 526.35 | 340.50 | 1.5 |
| Time | Position (Common Satellites) | 332.73 | 34.55 | 9.6 |
| | Range (Common Satellites) | 332.73 | 36.01 | 9.2 |
| | Range (Common Satellites) | 422.74 | 273.32 | 1.5 |
| Combined Time and Satellite Ephemeris | Position (Common Satellites) | 346.45 | 34.49 | 10.0 |
| | Range (Common Satellites) | 346.45 | 35.89 | 9.7 |
| | Range (Best Satellites) | 440.12 | 296.70 | 1.5 |

TABLE 6.2

Comparison of Conventional Degraded GPS (C/A-Code)
With Differential at a User 117 km away from the Monitor
(three-parameter solution for the monitor).

| Degradation Mode | Correction Mode | Point Positioning | | Differential | | Improvement Factor | |
|---|---|---|---|---|---|---|---|
| | | CPE | 95th Percentile | CPE | 95th Percentile | | |
| Satellite Ephemeris | Range (Best Satellites) | 227.98 | 526.35 | 28.81 | 56.95 | 7.9 | 9.2 |
| Time | | 205.34 | 422.74 | 28.86 | 57.30 | 7.2 | 7.3 |
| Combined | | 199.84 | 440.12 | 28.83 | 57.64 | 7.0 | 7.6 |

TABLE 6.3

Comparison of Conventional Degraded GPS (C/A-Code)
With Differential at a User 117 km Away from the Monitor
(two-parameter solution for the monitor, i.e., clock constrained).

| Accuracy Measure | Point Positioning (metres) | Differential (metres) | Improvement Factor |
|---|---|---|---|
| 50th percentile | 142.84 | 18.57 | 7.7 |
| CPE (50%) | 147.68 | 17.70 | 8.3 |
| 95th percentile | 319.87 | 34.74 | 9.2 |
| 2drms (95%) = 2.5 CPE | 369.20 | 44.25 | 8.3 |

TABLE 6.4

Comparison Between Different Accuracy Measures.
Position corrections; time and satellite degradation;
0 km away from the monitor

combined effect of the above two aspects provides the final position uncertainty of the GPS system. Geometry can be represented by the Dilution of Precision factors, whereas the system's errors fall within two categories, i.e., the biases, and the random errors. The application of the differential mode in this simulation study achieves the following.

(1) It reduces the bias errors of the GPS system by subtracting the deviations detected at the differential monitor station from the distant user observables or solution.

(2) It reduces the random errors by including a large sample of 140 fixes over approximately 24 hours.

The sampling over 24 hours will illustrate the effectiveness of the differential operation not only when the geometry is favourable for both receivers but also when different satellite configurations cause large DOP values inducing deterioration of the final positional accuracy.

It is evident from the above that the simulation itself will isolate the geometrical effects caused by the distance of the user's position from the monitor. Errors due to the late calculation of the user's solution with respect to the monitor's solution are neglected here.

The following figures illustrate the differential GPS positional accuracy as a function of distance degradation model and azimuth to the differential monitor station where the various strategies for the application of differential corrections are employed. The results are expressed in terms of the 95th percentile error measure. Appendix III provides the same results expressed in the CPE accuracy measure.

To test the differential performance as a function of distance,

type of correction mode, type of solution, number of satellites used for the solution, type of Selective Availability and azimuth, a standard run was selected. This standard run corresponds to range corrections using common satellites from all visible, with satellite position degradation. The user is moved away from the monitor along a $135^{o}$ azimuth line at 0, 1000, 2000, 3000, 4000, and 5000 km. Every other run is compared against the above standard run.

Figure 6.9 shows the differential performance as a function of distance. It can be seen that the accuracy of the differential mode decreases as the user-monitor separation distance increases. In other words, accuracy improves as the user approaches the differential monitor station, e.g., the shore. In most cases, this is exactly what is needed.

Figures 6.8 and 6.9 show the solutions using the common satellites from all those in view at the monitor and the user test sites, but they apply different correction modes, that is, position and range corrections respectively. It can be seen that range corrections are more efficient than position corrections. This is true since application of the deviation of single ranges (e.g., $\delta\rho_i(t)$) to the user's ranges will, of course, contribute more to the efficiency of the differential mode than the combined effect of position deviation ($\delta\phi(t)$, $\delta\lambda(t)$, $\delta\Delta t(t)$) in the final solution. The maximum distance for which differential GPS navigation is still possible amounts to approximately 4000 km, when the above technique of common satellites is selected. Beyond this distance, the two receivers are not able to track more than two common satellites (three being the minimum), due to the curvature of the earth.

Figures 6.10 and 6.11 show the application of the differential GPS mode when all visible satellites are included in the monitor's solution for an unconstrained and a constrained clock at the monitor. The dramatic improvement in the clock constrained solution over the unconstrained one is because there are fewer parameters solved for, although the same number of satellites is available (stronger solution).

In the last two cases, although there is no need for the user to use exactly the same satellite constellation as the differential monitor station, the results are not as effective as the first two cases of position and range corrections using common satellites from all those in view. Accuracies provided by the differential GPS when the clock is not constrained are of the order of 300 m 95th percentile, with an effective range of about 370 km and an improvement factor of less than 1.5.

The differential mode with the constrained solution has accuracies of the order of 50 m 95th percentile, and it is still valid up to a distance of 370 km. Therefore, differential GPS, in this case, can be more appropriate and useful at close distances from the differential monitor station. The short effective range (370 km) of the differential mode is because of the curvature of the earth and the satellite selection algorithm of the user (e.g., the best set of four).

Different models of Selective Availability do not really affect the differential GPS performance. This is shown in Figures 6.12 and 6.13 where time and a combination of satellite position and time degradation is employed, respectively.

Determination of the monitor's coverage area will not only be established by situating the user at different ranges, but at different azimuth lines as well. In the first place, the user was moved away from

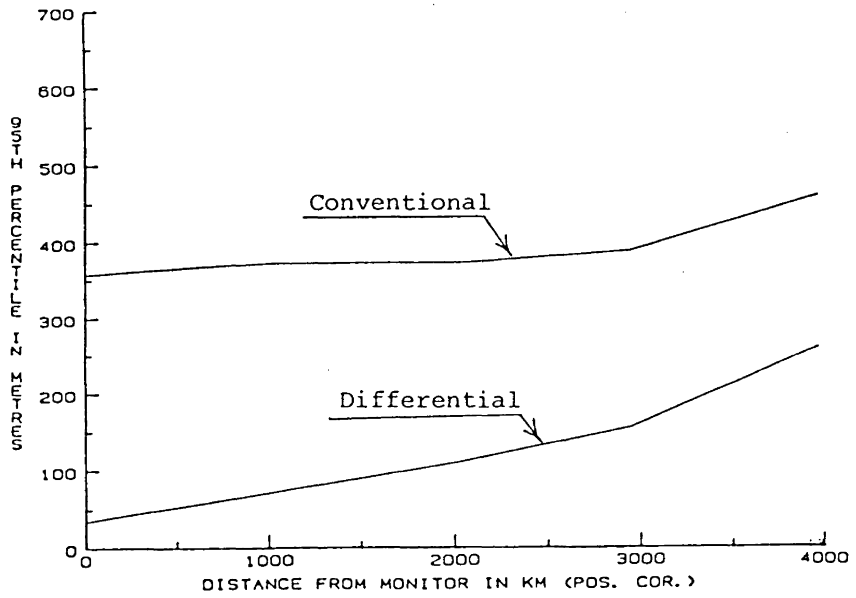


FIGURE 6.8
Position Corrections;Common Sat.;Sat. Position Degradation.

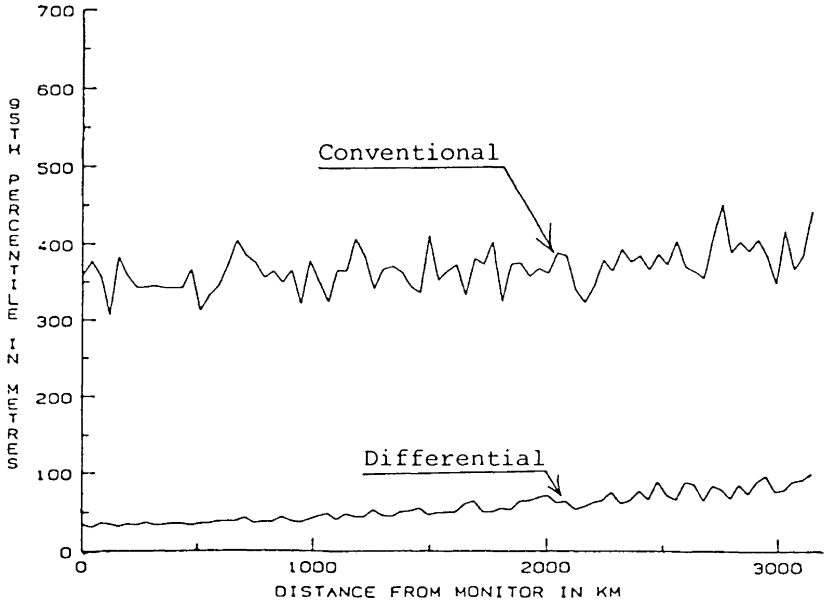


FIGURE 6.9
Range Corrections;Common Sat.;Position Degradation

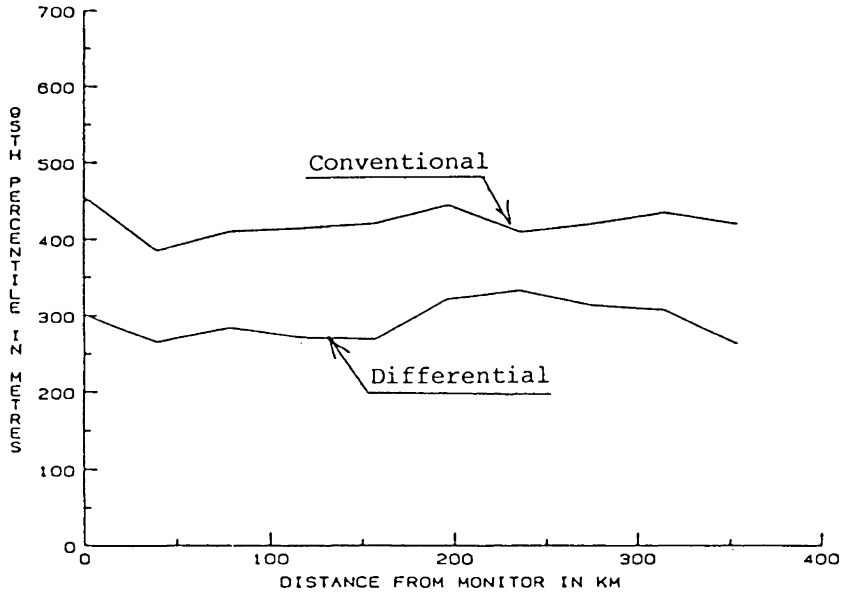


FIGURE 6.10
Range Corrections;All Visible Sat. at the Monitor;
Best at User;Sat. Position Degradation.

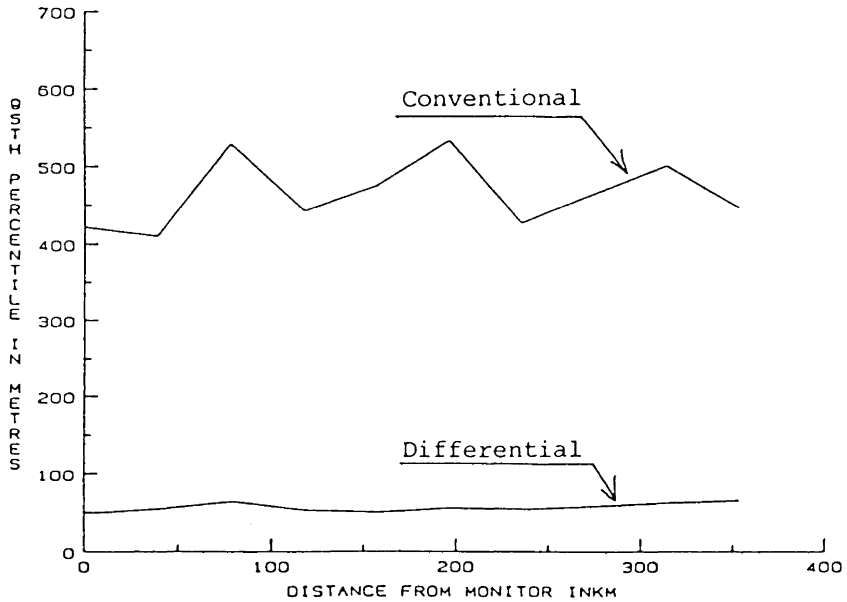


FIGURE 6.11
Range Corrections;All Visible Sat.,Clock Constrained
at the Monitor;Best at the User;Sat. Position Degradation.

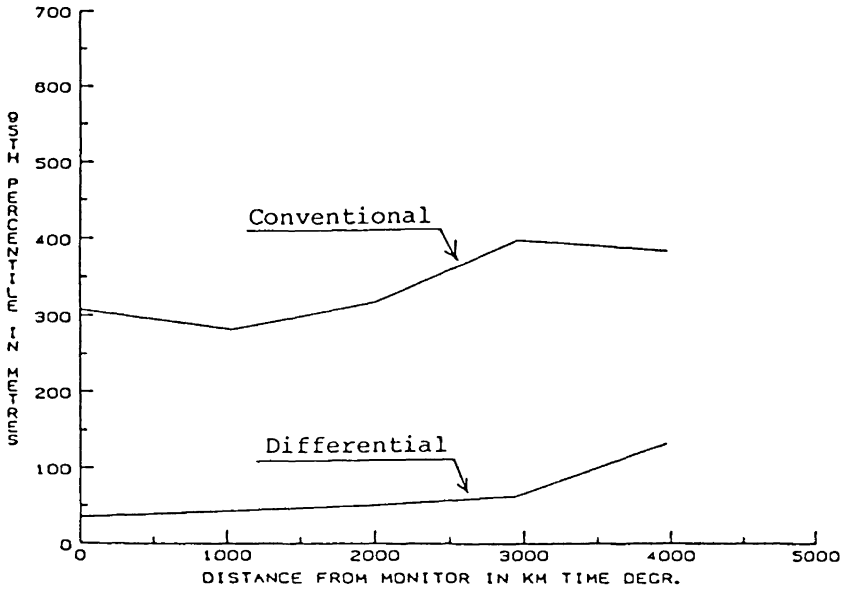


FIGURE 6.12
Range Corrections;Common Sat.;Time Degradation.

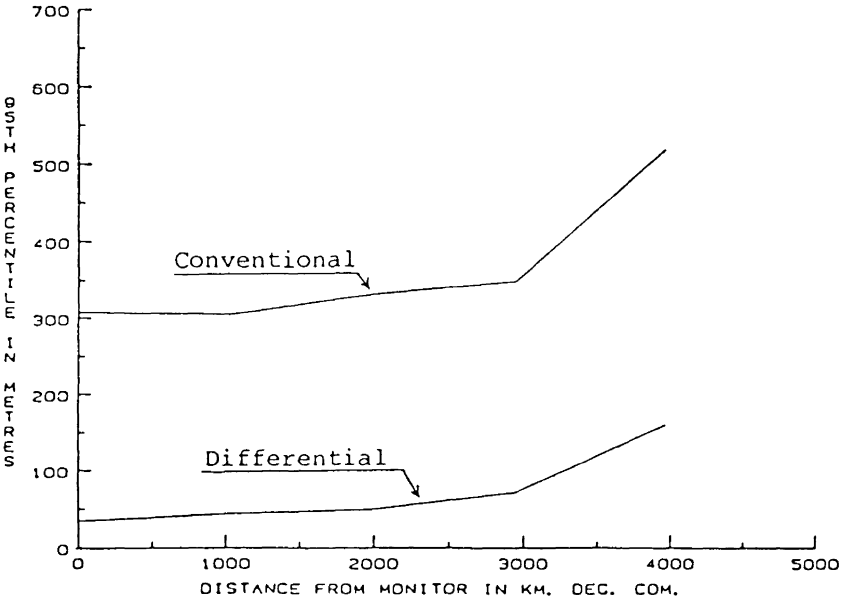


FIGURE 6.13
Range Corrections;Common Sat.;Combined Degradation.

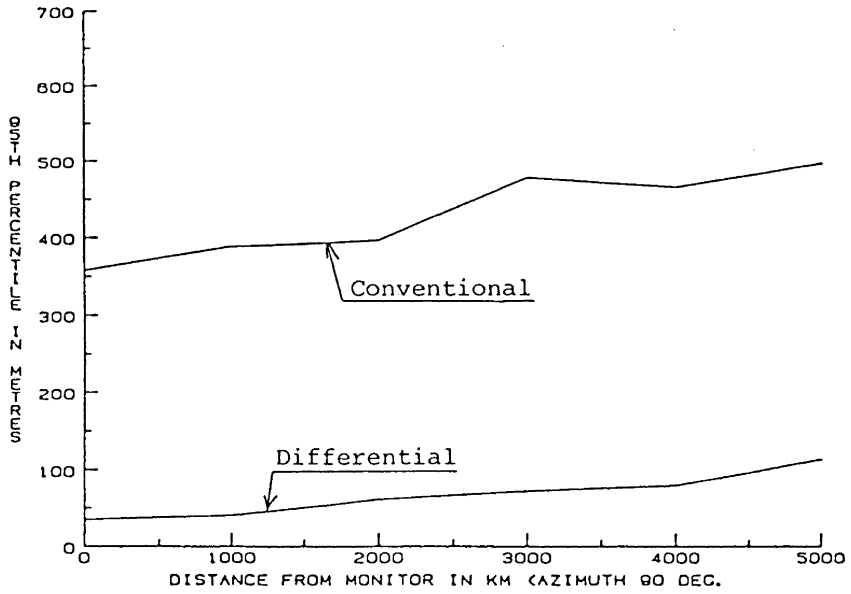


FIGURE 6.14
Range Corrections;Common Sat.;Sat. Position Degradation; 90 Degrees Azimuth.

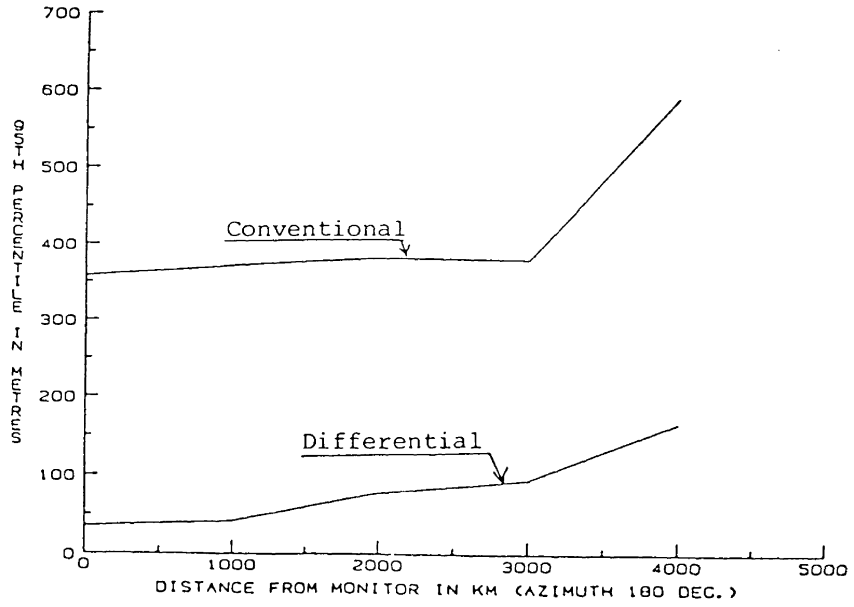


FIGURE 6.15
Range Corrections;Common Sat.;Sat. Position Degradation; 180 Degrees Azimuth.

the monitor along a $135^{o}$ azimuth line (longitude and latitude varying). Other azimuthal paths corresponding to $90^{o}$ (longitude varying) and $180^{o}$ (latitude varying) are shown in Figures 6.14 and 6.15. It is obvious that the effect of various headings is not really a significant parameter in the determination of the monitor's coverage area. However, the efficiency of the differential mode along a $180^{o}$ azimuth line appears slightly worse than the other two cases.

# 7

# Conclusions and Recommendations

Restricted access to and intentional degradation of the GPS signals spurred us to extend the conventional performance capability of the system to the differential one. Differential GPS navigation provides an opportunity to thousands of unauthorized users, who cannot gain the full benefit of the GPS system, to effectively make use of the system under intentionally degraded C/A-code conditions.

Under certain assumptions and through a simulation computer program, this study evaluated and demonstrated the validity and feasibility of the differential concept, with the main emphasis on the investigation of various geometrical aspects related to the differential operation. Inferences correspond only to marine applications (two-dimensional) of the GPS 18-satellite constellation considering hypothetical intentional degradations of the C/A-code.

To develop a conceptual approach to differential GPS navigation, the following points were brought up.

(1) Development of a would-be Selective Availability condition of the C/A-code signals. This is achieved by introducing noise models into the signals in the form of satellite position degradation, time

degradation, and a combination of both, such that an approximately 200 m CPE performance results, using four satellites for the solution.

(2) Development of various models for differential corrections. Normally, there are two ways of implementing differential corrections: position corrections ($\delta\phi(t)$, $\delta\lambda(t)$, $\delta\Delta t(t)$), and range corrections ($\delta\rho_i(t)$). Nevertheless, four different strategies for the satellite selection and receiver solution algorithms are examined. The first two cases involve position and range corrections, including common satellites, from all those in view available at the user and the differential monitor, for a three-parameter navigation solution ($\phi$, $\lambda$. $\Delta t$). The last two procedures again make use of range corrections but incorporate all visible satellites for the monitor's solution and common satellites for the user's solution among his best set of four and all those in view at the monitor. The difference between the third and fourth cases is that one uses an unconstrained clock solution ($\phi$, $\lambda$, $\Delta t$) and the other a constrained one ($\phi$, $\lambda$).

In conjunction with the above assumptions and considerations, the following conclusions were drawn.

(1) Differential GPS navigation indicates considerable promise. It can alleviate C/A-code degradation. Similar enhancement performance is expected when intentional degradation is absent but on the condition that receiver noise effects do not overcome the system's errors.

(2) Differential corrections are valid over very large distances.

(3) The most efficient way of differential corrections is range corrections using common satellites. Still, the clock constrained technique seems more suitable because of its flexibility and it

should not be overlooked.

(4) The differential GPS accuracy generally decreases as the distance between the user and the monitor increases.

(5) The effectiveness of differential corrections is almost impervious to direction and to different degradation models developed.

The following recommendations can also be made.

(1) In this thesis, all the results inferred were established on a single monitor station at Cape Race, Newfoundland. A network of differential GPS monitor stations should be considered in enhancing the differential performance.

(2) The idea of a ground-based monitor station should probably be extended to a satellite-based one. Satellites can be used either as monitor stations or as relay satellites for the transmission of differential corrections. The International Maritime Satellite Organization (INMARSAT) satellites are a possible solution that should not be overlooked.

(3) The communication data link is an area that still needs investigation. No mention was made of the data link communication problem since an appropriately configured data link was considered to be in existence. The possibility of modifying LORAN-C signals as carriers of differential corrections should be examined.

(4) Similar research on differential GPS should be conducted when intentional degradation is absent and when the current prototype satellites are used.

(5) An algorithm for the selection of those three satellites which yield the "best" navigation performance for a three-parameter

solution should be investigated.

(6) We can extend the differential concepts to aviation for supporting aerial photomapping with no need to establish accurate ground control; for conducting hydrographic surveys by aircraft, for side-looking aircraft radar surveys, etc.

(6) A proof-of-concept experiment is recommended using the STI-5010 and TI-4100 GPS receivers, owned by Nortech, mounted on a van.

## REFERENCES


Appleyard, S.F. (1980). Marine Electronic Navigation. Routledge and Kegan Paul Ltd., London.

Ashkenazi, V. and R.M. Sykes (1980). "Doppler translocation and orbit relaxation techniques." Phil. Trans. R. Soc. Lond. A 294, pp. 357-364.

Beser, J. and B.W. Parkinson (1981). "The application of NAVSTAR differential GPS in the civilian community." Proceedings of the Thirty-Seventh Annual Meeting of the U.S. Institute of Navigation, Annapolis, MD, June, pp. 60-74.

Bogen, A.H. (1974). "Geometric performance of the Global Positioning System." Aerospace Corporation, NTIS AD-783210.

Burt, A.W., D.J. Kaplan, R.R. Keenly, J.F. Reeves and F.B. Shaffer (1965). "Mathematical considerations pertaining to the accuracy of position location and navigation systems." NWRC-RM 34, NTIS AD 629-609.

Cardal, J.D. and R. Cnossen (1980). "Civil helicopter applications of the NAVSTAR Global Positioning System." Presented at the Advanced Rotorcraft Technology Workshop, NASA, Ames Research Center, Moffet Field, CA.

Cnossen, R., J. Cardall, D. DeVito, K. Park and G. Gilbert (1981). "Civil applications of differential GPS using a single sequencing receiver." Magnavox Co., NASA CR. 166168, May.

Counselman, C.G., R.J. Cappallo, S.A. Gourevitch, R.L. Greenspan, T.A. Herring, R.W. King, A.E.E. Rogers, I.I. Shapiro, R.E. Snyder, D.H. Steinbrecher and A.R. Whitney (1982). "Accuracy of relative positioning by interferometry with GPS: Double-blind test results." Proceedings of the Third International Geodetic Symposium on Satellite Doppler Positioning, Las Cruces, NM, February.

Dixon, R.C. (1975). Spread Spectrum Systems. John Wiley & Sons, New York.

Dunn, P.D. and J.W. Rees II (1980). "Hydrographic application of the Global Positioning System." Masters thesis, Naval Postgraduate School, Monterey, CA.

Fell, P.J. (1980). "Geodetic positioning using a Global Positioning System of satellites." Department of Geodetic Science Report 299, The Ohio State University, Columbus, Ohio, June.

Gay, J. (1982). "Presentation to security panel of the U.S. Secretary of Defense on the needs and requirements of the civil community for GPS." Summarized orally at the U.S. Institute of Navigation, National Marine Meeting, Boston, October.

Goddard, R.B. (1973). "Differential LORAN-C. Time stability study." U.S. Department of Transportation Report CG-D-80-74, November, NTIS AD-779 543.

Gold, R. (1967). "Optimal binary sequences for spread spectrum multiplexing." IEEE Transactions on Information Theory, pp. 615-621.

Harris, R.L. (1973). "Introduction to spread spectrum techniques." AGARD Lecture Series No. 58 on Spread Spectrum Communications, NTIS AD-766 914, July.

Hatch, R. (1982). "The synergism of GPS code and carrier measurements." Proceedings of the Third International Geodetic Symposium on Satellite Doppler Positioning, Las Cruces, NM, February.

Herman, B.R. (1981). "Formulation for the NAVSTAR Geodetic Receiver System (NGRS)." Naval Surface Weapons Center Report NSWC TR-81-348, Dahlgren, VA.

Hogg, R.V. and A.T. Craig (1978). Introduction to Mathematical Statistics. 4th ed., Macmillan Publishing Co., Inc., New York.

Hopfield, H.S. (1969). "Two-quartic tropospheric refractivity profile for correcting satellite data." Journal of Geophysical Research, Vol. 74, pp. 4487-4499.

Howel, W.E., T.N. Bundick and W.F. Hodge (1980). "Civil aviation applications of NAVSTAR/GPS through differential techniques." Presented at National Telecommunications Conference, Houston, TX, November.

Ingham, A. (1974). Sea Surveying. McGraw Hill, New York.

International Omega Association (1978). "Omega navigation system, user guide." IOA, Arlington, VA.

Johler, J.R., R.H. Doherty and L.B. Burch (1976). "Nanosecond precision for LORAN-C." U.S. Department of Commerce, OT Technical Memorandum 72-216.

Johnson, C. and P. Ward (1979). "GPS applications to seismic oil exploration." Navigation, Journal of the Institute of Navigation, Vol. 26, No. 2, Summer, pp. 109-117.

Jorgensen, P.S. (1980). "Combined pseudorange and Doppler positioning for the stationery NAVSTAR user." IEEE, PLANS, Atlantic City, NJ, December, pp. 450-458.

Jorgensen, P.S. (1980). "NAVSTAR-Global Positioning System 18-satellite constellations." Navigation, Journal of the Institute of Navigation, Vol. 27, No. 2, Summer, pp. 89-100.

Kalafus, R.M. (1982). "NAVSTAR GPS accuracy studies." Presented at Surface Transportation Navigation Users Conference, Washington, DC, November.

Kasper, J.F. Jr., and C.E. Hutchinson (1978). "The Omega navigation system: an overview. IEEE, Communications Society Magazine, May, pp. 23-35.

Klass, P.J. (1982a). "FAA seeking user's views on options for navigation." Aviation Week and Space Technology, August 23, pp. 34-35.

Klass, P.J. (1982b). "Soviets plan navigation system." Aviation Week and Space Technology, August 30, pp. 12-13.

Lachapelle, G., N. Beck and P. Heroux (1982). "NAVSTAR/GPS single point positioning using pseudo-range and Doppler observations." Proceedings of the Third International Geodetic Symposium on Satellite Doppler Positioning, Las Cruces, NM, February.

Laurila, S.H. (1976). Electronic Surveying and Navigation. John Wiley & Sons, New York.

Leppan-Angus, P.V. (1982). "NAVSTAR Global Positioning System prospects for geodesy." School of Surveying, University of New South Wales, Australia.

Martin, E.H. (1980). "GPS user equipment error model." Navigation, Journal of the Institute of Navigation, Vol. 25, No. 2, pp. 201-210.

McCaskill, T., J. Buisson and A. Buonaguro (1976). "A sequential range navigation algorithm for a medium altitude navigation satellite." Navigation, Journal of the Institute of Navigation, Vol. 23, No. 2, pp. 164.

McDonald, K.D. (1973). "A survey of satellite-based systems for navigation, position surveillance, traffic control, and collision avoidance." Navigation, Journal of the Instiitute of Navigation, Vol. 20, No. 4, pp. 301-320.

McDonald, K.D. (1975). "The satellite as an aid to air traffic control." Ch. 31, A Survey of Modern Air Traffic Control, Vol. II, NATO Advisory Group for Aerospace Research and Development, AGARDograph No. 209, July.

Mertikas, S.P. (1982). "Alert programme for the NAVSTAR Global Positioning System." Department of Surveying Engineering Technical Report 85, University of New Brunswick, Fredericton.

Mikhail, E.M. (1976). Observations and Least Squares. Harper and Row, New York.

Mikhail, E.D. and G. Gracie (1981). Analysis and Adjustment of Survey Measurements. Van Nostrand Reinhold Company, New York.

Milliken, R.J. and C.J. Zoller (1978). "Principle of operation of NAVSTAR and system characteristics." Navigation, The Institute of Navigation, Vol. 25, No. 2, pp. 95-106.

Montgomery, B.O. and Johnson, C.R. (1982). "Operation and near-term applications of the TI 4100 NAVSTAR navigator for the geophysical community." The Institute of Navigation, National Marine Meeting, Cambridge, Mass, October.

National Plan for Navigation (1977). U.S. Department of Transportation Report DOT-TST-78-4, DOT (DPB-22), Washington, D.C., November.

Oberg, E.N. (1947). "Approximate formulas for the radii of circles which include a specified fraction of a normal bivariate distribution." Annals of Mathematical Statistics, Vol. 18, pp. 442-447.

Parkinson, B.W. (1979). "The Global Positioning System (NAVSTAR)." Bulletin Geodesique, 53, pp. 89-108.

Payne, C.R. (1982). "NAVSTAR Global Positioning System: 1982". Proceedings of the Third International Geodetic Symposium on Satellite Doppler Positioning, Las Cruces, NM, February.

Roeber, J.F. (1982). "Accuracy; What is it?; Why do I need it?; How much do I need?" Presented at the Institute of Navigation, National Marine Meeting, Cambridge, Mass, October.

Rosetti, C. (1982). "Prospects for Navsat-A future worldwide civil navigation satellite system." E.S.A. Bulletin, No. 30, pp. 54-59, May.

Ruedger, W.H. (1981). "Feasibility of collision warning, precision approach and landing using the GPS." Research Tringle Institute, NASA CR 165675, March.

Rutscheidt, E.H. and B.D. Roth (1982). "The NAVSTAR Global Positioning System." Proceedings of Symposium No. 4e, IAG General Meeting, Tokyo, May.

Spilker, J.J. (1978). "GPS signal structure and performance characteristics." Navigation, Journal of the Institute of Navigation, Vol. 25, No. 2, pp. 29-54.

Stansell, T.A., Jr. (1971). "Transit, the Navy Navigation Satellite System." Navigation, Journal of the Institute of Navigation, Vol. 18, No. 1, pp. 93-109.

Stansell, T.A., Jr. (1977). "Positioning and navigation by satellite." Presented at the Joint Conference on Satellite Applications to Marine Operations, New Orleans, Lousiana, November.

Stansell, T.A., Jr. (1978). "Civil marine applications of the Global Positioning System." Navigation, Journal of the Institute of Navigation, Vol. 25, No. 2, pp. 224-235.

Stansell, T.A., Jr. (1982). "Accesss charges and related issues for civil GPS users." Navigation, Journal of the Institute of Navigation, Vol. 29, No. 2, pp. 160-175.

Surveys and Mapping Branch (1975). "Surveying offshore Canada lands for mineral resources department." Department of Energy, Mines and Resources, Ottawa.

Swanson, E.R. (1977). "Differential OMEGA." Proceedings of the Second Meeting, International OMEGA Association, Linthicum Heights, MD, November.

Swanson, E.R. (1978). "Geometric dilution of precision." Navigation, Journal of the Institute of Navigation, Vol. 25, No. 4, pp. 425-429.

Teasley, S.P., W.M. Hoover and C.R. Johnson (1980). "Differential GPS navigation." IEEE, PLANS, 1980, Texas Instruments Inc., pp. 9-16.

U.S. Coast Guard (1978). "LORAN-C user handbook." U.S.C.G. publication CG-462, (G-EEE4), Washington, D.C.

U.S. Department of Defense (1982). "Federal Radionavigation Plan." Vols. I, II, III, IV, March.

van Dierendonck, A.J., S.S. Russel, E.R. Kopitzke and M. Birnbaum (1980). "The GPS navigation message." Navigation, Journal of the Institute of Navigation, Vol. 25, No. 2, pp. 147-165.

Vanicek, P. and E. Krakiwsky (1982). Geodesy: The Concepts. North-Holland, Amsterdam.

Ward, P. (1981). "An inside view of pseudorange and delta pseudorange measurements in a digital NAVSTAR/GPS receiver." Presented at the International Telemetering Conference, GPS-Military and civil applications, San Diego, CA, October.

Wells, D.E. (1969). "Experience with satellite navigation during summer of 1968." The Canadian Surveyor, 23, pp. 334-348.

Wells, D.E. (1980). "Review of present day capabilities of satellite systems." The Hydrographic Journal, No. 18, pp. 35-51.

Wells, D.E., D. Delikaraoglou and P. Vanicek (1981). "Navigating with the Global Positioning System today and in the future." Presented at the 74th Annual Meeting of the Canadian Institute of Surveying, St. John's, Newfoundland, May.

Wells, D.E., P. Vanicek and D. Delikaraoglou (1981). "The application of NAVSTAR-GPS to geodesy in Canada. Pilot study." Department of Surveying Engineering Technical Report 79, University of New Brunswick, Fredericton.

Westerfield, E.E. and G. Worsley (1966). "Translocation by navigation satellite." Applied Physics Laboratory Technical Digest 5, No. 6, pp. 2-10, July.

Wolfe, C.A. (1976). "NAVSTAR/GPS navigation analysis and algorithm development study." Naval Electronics Laboratory Center, San Diego, CA.

APPENDIX I

## USER NAVIGATION SOLUTION

To compute a position from satellite range data measurements, the following information is required for each measurement:

(1) Position of the tracked satellites and time of signal transmission $[x_i(t_k), y_i(t_k), z_i(t_k)]$.

(2) Time of transmission of the received signal $[t_{s_i}]$.

(3) Estimates of the deterministic time delays.

The position of each tracked satellite with respect to our reference system (WGS-72) can be computed as a function of time from the six orbital elements. The most current information (taken from van Dierendonck et al. [1978]) is given as follows.

| | |
|---|---|
| $\mu = 3.986\ 008 \cdot 10^{14}\ m^3/sec^2$ | Universal Gravitational Constant (WGS-72) |
| $\omega_e = 7.292\ 115\ 147 \cdot 10^{-5}$ rad/sec | Earth's rotation rate (WGS-72) |
| $a = (\sqrt{a})^2$ | Semi-major axis |
| $n_o = \sqrt{\mu/a^3}$ | Computed mean motion |
| $t_k = t - t_{oe}$ | Time from reference epoch |
| $n = n_o + \Delta n$ | Corrected mean motion |
| $M_k = M_o + nt_k$ | Mean anomaly |
| $M_k = E_k - e \sin E_k$ | Kepler's equation for eccentric anomaly |
| $\cos V_k = (\cos E_k - e)/(1 - e \cos E_k)$<br>$\sin V_k = \sqrt{1-e^2}\ \sin E_k/(1 - e \cos E_k)$ | True anomaly |
| $\phi_k = V_k + \omega$ | Argument of latitude |

| | | |
|---|---|---|
| $\delta u_k = C_{uc} \cos 2\phi_k + C_{us} \sin 2\phi_k$ | Correction to argument of latitude | 2nd Harmonic Perturbations |
| $\delta r_k = C_{rc} \cos 2\phi_k + C_{rs} \sin 2\phi_k$ | Correction to orbit radius | |
| $\delta i_k = C_{ic} \cos 2\phi_k + C_{is} \sin 2\phi_k$ | Correction to inclination angle | |
| $u_k = \phi_k + \delta u_2$ | Corrected argument of latitude | |
| $r_k = a(1 - e \cos E_k) + \delta r_k$ | Corrected orbit radius | |
| $i_k = i_o + \delta i_k$ | Corrected inclination | |
| $x_k = r_k \cos u_k$ | Position in orbital plane | |
| $y_k = r_k \sin u_k$ | | |
| $\Omega_k = \Omega_o + (\dot{\Omega} - \omega_e)t_k - \omega_e t_{oe}$ | Corrected longitude of ascending node | |
| $X_k = x_k \cos\Omega_k - y_k \cos i_k \sin\Omega_k$ | Earth fixed coordinates | |
| $Y_k = x_k \sin\Omega_k + y_k \cos i_k \cos\Omega_k$ | | |
| $Z_k = y_k \sin i_k$ | | |

The above satellite ephemeris, along with system time, satellite clock behaviour data, and transmitter status information, is supplied by means of the GPS navigation message [van Dierendonck, 1978].

Let us consider the Jth ground station and the ith satellite. The position vector of the ground station is

$$\underline{R}_j = [X_j, Y_j, Z_j]^T.$$

The position vector and Cartesian coordinates of the ith satellite, at some epoch $t_k(\tau)$ (a function of the conventional GPS time) are

$$\underline{r}_i(t_k(\tau)) = [x_i(t_k), y_i(t_k), z_i(t_k)]^T \quad .$$

The Cartesian coordinates of the geometric range vector between the ith satellite and the jth ground station are

$$\underline{\rho}_{ij} = [\xi_{ij}, \eta_{ij}, \zeta_{ij}]^T \quad .$$

The length of $\underline{\rho}_{ij}$ is denoted by $\rho_{ij}$. From Figure 3.6, the geometric

range vector is

$$\underline{\rho}_{ij} = \underline{r}_i(t_k) - \underline{R}_j \quad . \tag{AI.1}$$

The pseudorange $\tilde{\rho}$, which a receiver can measure, is defined as

$$\tilde{\rho}_{ij} = \rho_{ij} + c(\Delta t_{u_j} - \Delta t_{s_i}) + c \cdot \Delta t_{A_i} \quad , \tag{AI.2}$$

where

$\tilde{\rho}_{ij}$ = pseudorange (metres)

$\rho_{ij}$ = geometric (true) range (metres)

$c$ = speed of light (metres/second)

$\Delta t_{u_j}$ = user clock time bias (seconds)

$\Delta t_{s_i}$ = satellite i clock time bias (seconds)

$c \cdot \Delta t_{A_i}$ = atmospheric delays (ionospheric, tropospheric)(metres).

The atmospheric delays $c \cdot \Delta t_{A_i}$ are introduced by propagation error due to the atmosphere, specifically the ionospheric and tropospheric delay.

Ionospheric delays are estimated by the user (j) by measuring pseudoranges $\tilde{\rho}_{ij}$ at two different frequencies ($L_1$ = 1575 MHz; $L_2$ = 1227 MHz). This is done because the ionosphere has a delay effect which is approximately inversely proportional to the square of the frequency ($\sim 1/f^2$) [van Dierendonck et al., 1978]. For single channel receivers, ionospheric delays are modelled. Coefficients of a polynomial approximation are provided by means of the navigation satellite message.

Tropospheric delays are frequency-independent. Estimation models for the troposphere are based on geometry and altitude. Approximation models for the estimation of ionospheric and tropospheric delays are given in Ward [1981].

The satellite clock time bias $\Delta t_{s_i}$ is again provided by the satellite message, whereas the user clock time bias $\Delta t_{u_j}$ is considered unknown and is solved for through the navigation solution.

The mathematical model $F(\underline{X}, \underline{L}) = 0$ for an observation of pseudorange is in the form

$$F(\underline{X}, \underline{L}) = \rho_{ij} + c \cdot (\Delta t_{u_j} - \Delta t_{s_i}) + c \cdot \Delta t_{A_i} - \tilde{\rho}_{ij} = 0 \quad , \text{(AI.3)}$$

where i designates the satellite and j the ground station.

The geometric (true) range at some epoch $t_k$ is

$$\rho_{ij}(t_k) = \sqrt{\{X_j - x_i(t_k)\}^2 + \{Y_j - y_i(t_k)\}^2 + \{Z_j - z_i(t_k)\}^2} \quad . \text{(AI.4)}$$

Substituting the above in the general mathematical model of the pseudorange:

$$F(\underline{X},\underline{L}) = \sqrt{\{X_j - x_i(t_k)\}^2 + \{Y_j - y_i(t_k)\}^2 + \{Z_j - z_i(t_k)\}^2} + c \cdot (\Delta t_{u_j} - \Delta t_{s_i}) + c \cdot \Delta t_{A_i} - \tilde{\rho}_{ij} = 0 \quad . \quad \text{(AI.5)}$$

Expanding the above equation of pseudorange observation in a Taylor series about an initial approximate user's position and clock bias

$$\underline{X}_j^{(o)} = [X_j^{(o)} \; Y_j^{(o)} \; Z_j^{(o)} \; \Delta t_{u_j}^{(o)}]^T \quad ,$$

and using the measured values of the observation vector

$$\underline{L}^{(o)} = [\tilde{\rho}_{1j}^{(o)} \; \tilde{\rho}_{2j}^{(o)} \; \tilde{\rho}_{3j}^{(o)} \; \tilde{\rho}_{4j}^{(o)} \; \ldots]^T \quad ,$$

we get

$$\{\frac{\partial F}{\partial \underline{X}_j}\Big|_{\underline{X}_j^{(o)}}\}(\underline{X}_j - \underline{X}_j^{(o)}) + (-I)(\underline{\tilde{\rho}}_{ij} - \underline{\tilde{\rho}}_{ij}^{(o)}) + F(\underline{X}_j^{(o)}, \underline{\tilde{\rho}}_{ij}^{(o)}) = 0. \quad \text{(AI.6)}$$

In our familiar notation of surveying, the above can be written as

$$A \cdot \underline{\delta X} + B \cdot \underline{V} + \underline{W} = \underline{C} \quad , \quad \text{(AI.7)}$$

where

$$A = \left\{\frac{\partial F}{\partial \underline{X}_j}\Big|_{\underline{X}_j}(o)\right\} = \text{design matrix}$$

$$\underline{\delta X} = \underline{X}_j - \underline{X}_j^{(o)} = \text{correction vector}$$

$$B = -I = \left\{\frac{\partial F}{\partial \underline{\rho}_{ij}}\Big|_{\underline{\rho}_{ij}}(o)\right\} = \left\{\frac{\partial F}{\partial \underline{L}}\Big|_{\underline{L}}(o)\right\} = \text{design matrix}$$

$$\underline{V} = \underline{L} - \underline{L}^{(o)} = \text{residual vector;}\quad \tilde{\rho}_{ij} = \tilde{\rho}_{ij}^{(o)} = v_i$$

$$\underline{W} = F(\underline{X}_j^{(o)}, \tilde{\underline{\rho}}_{ij}^{(o)}) = \text{misclosure vector.}$$

The above equation (AI.7) is the linearized equation which relates pseudorange measurements to the desired user navigation information, either $[X_J, Y_J, Z_J]$ or $[\phi_j, \lambda_j, h_j]$, as well as the user clock bias $\Delta t_{u_j}$.

When four satellites are available (i=1,2,3,4), the linearized equations can be written as

$$A \cdot \underline{\delta X} + B \cdot \underline{V} + \underline{W} = \underline{0} \quad , \tag{AI.8}$$

where

$$A=\text{design matrix}=\left\{\frac{\partial F}{\partial \underline{X}_j}\Big|_{\underline{X}_j}(o)\right\}=\begin{vmatrix} \frac{X_j^{(o)}-x_1(t_k)}{\rho_{1j}^{(o)}} & \frac{Y_j^{(o)}-y_1(t_k)}{\rho_{1j}^{(o)}} & \frac{Z_j^{(o)}-z_1(t_k)}{\rho_{1j}^{(o)}} & c \\ \frac{X_j^{(o)}-x_2(t_k)}{\rho_{2j}^{(o)}} & \frac{Y_j^{(o)}-y_2(t_k)}{\rho_{2j}^{(o)}} & \frac{Z_j^{(o)}-z_2(t_k)}{\rho_{2j}^{(o)}} & c \\ \frac{X_j^{(o)}-x_3(t_k)}{\rho_{3j}^{(o)}} & \frac{Y_j^{(o)}-y_3(t_k)}{\rho_{3j}^{(o)}} & \frac{Z_j^{(o)}-z_3(t_k)}{\rho_{3j}^{(o)}} & c \\ \frac{X_j^{(o)}-x_4(t_k)}{\rho_{4j}^{(o)}} & \frac{Y_j^{(o)}-y_4(t_k)}{\rho_{4j}^{(o)}} & \frac{Z_j^{(o)}-z_4(t_k)}{\rho_{4j}^{(o)}} & c \end{vmatrix} \tag{AI.9}$$

$$\underline{\Delta X}_j = \text{correction vector} = \underline{X}_j - \underline{X}_j^{(o)} = \begin{vmatrix} X_j - X_j^{(o)} \\ Y_j - Y_j^{(o)} \\ Z_j - Z_j^{(o)} \\ \Delta t_{u_j} - \Delta t_{u_j}^{(o)} \end{vmatrix} \quad \text{(AI.10)}$$

$$\underline{V} = \text{residual vector} = \underline{L} - \underline{L}^{(o)} = \begin{vmatrix} \tilde{\rho}_{1j} - \tilde{\rho}_{1j}^{(o)} \\ \tilde{\rho}_{2j} - \tilde{\rho}_{2j}^{(o)} \\ \tilde{\rho}_{3j} - \tilde{\rho}_{3j}^{(o)} \\ \tilde{\rho}_{4j} - \tilde{\rho}_{4j}^{(o)} \end{vmatrix} \quad \text{(AI.11)}$$

$$B = \text{design matrix} = \left\{\frac{\partial F}{\partial \underline{L}}\Big|_{\underline{L}^{(o)}}\right\} = \begin{vmatrix} -1 & 0 & 0 & 0 \\ 0 & -1 & 0 & 0 \\ 0 & 0 & -1 & 0 \\ 0 & 0 & 0 & -1 \end{vmatrix} = -I \quad \text{(AI.12)}$$

$$\underline{W} = \text{misclosure vector} = F(\underline{X}^{(o)}, \underline{L}^{(o)}) = \begin{vmatrix} \rho_{1j}^{(o)} + c\cdot(\Delta t_{u_j}^{(o)} - \Delta t_{s_1}) + c\cdot\Delta t_{A_1} - \tilde{\rho}_{1j}^{(o)} \\ \rho_{2j}^{(o)} + c\cdot(\Delta t_{u_j}^{(o)} - \Delta t_{s_2}) + c\cdot\Delta t_{A_2} - \tilde{\rho}_{2j}^{(o)} \\ \rho_{3j}^{(o)} + c\cdot(\Delta t_{u_j}^{(o)} - \Delta t_{s_3}) + c\cdot\Delta t_{A_3} - \tilde{\rho}_{3j}^{(o)} \\ \rho_{4j}^{(o)} + c\cdot(\Delta t_{u_j}^{(o)} - \Delta t_{s_4}) + c\cdot\Delta t_{A_4} - \tilde{\rho}_{4j}^{(o)} \end{vmatrix} \quad \text{(AI.13)}$$

$$\text{where } \rho_{ij}^{(o)} = \sqrt{(X_j - x_i(t_k))^2 + (Y_j - y_i(t_k))^2 + (Z_j - z_i(t_k))^2} \quad \text{(AI.14)}$$

The quantities to be computed ($\delta X_j$, $\delta Y_j$, $\delta Z_j$, $\delta \Delta t$ ) are corrections that the user will make to his current estimate of position ($X_j^{(o)}$, $Y_j^{(o)}$,

$Z_j^{(o)}$) and his clock bias $\Delta t_{u_j}^{(o)}$ .

It should be noted that the coefficients in the first three columns of the design matrix A are the negative direction cosines of the line of sight from the user (j) to the satellite (i). For all four elements, the coefficient of $\Delta t_{u_j}$ is the speed of light c.

Let $\underline{U}_i = (u_i, v_i, w_i)^T$ be the unit vector from the user position (j) to the ith satellite. $u_i$, $v_i$, and $w_i$ are the x, y, and z components of this unit vector $\underline{U}_i$, as shown in Figures I.1 and I.2. It is known from analytical geometry that the components of the unit vector $\underline{U}_i$ are:

$$\left(\frac{x_i(t_k) - X_j}{\rho_{ij}}, \frac{y_i(t_k) - Y_j}{\rho_{ij}}, \frac{z_i(t_k) - Z_j}{\rho_{ij}}\right)^T = (u_i, v_i, w_i)^T \quad .$$

Therefore the design matrix

$$A = \left\{\frac{\partial F}{\partial \underline{X}_j}\Big|_{\underline{X}_j^{(o)}}\right\}$$

can be expressed in an equivalent form with direction cosines as

$$\begin{vmatrix} -u_1 & -v_1 & -w_1 & c \\ -u_2 & -v_2 & -w_2 & c \\ -u_3 & -v_3 & -w_3 & c \\ -u_4 & -v_4 & -w_4 & c \end{vmatrix} = A = \left\{\frac{\partial F}{\partial \underline{X}_j}\Big|_{\underline{X}_j^{(o)}}\right\} \quad . \qquad \text{(AI.15)}$$

Assuming that the weight matrix of the observations is known, an estimate of the correction vector $\underline{\delta X} = \underline{X}_j - \underline{X}_j^{(o)}$, besed on the principle of least squares, is given by:

$$\underline{\delta X} = \underline{X}_j - \underline{X}_j^{(o)} = (A^T P A)^{-1} A^T P \cdot \underline{W} \quad . \qquad \text{(AI.16)}$$

The final solution vector is

$$\underline{X}_j = \underline{X}_j^{(o)} + \underline{\delta X} = \underline{X}_j^{(o)} + (A^T P A)^{-1} A^T P \underline{W} \quad . \qquad \text{(AI.17)}$$

It is obvious that the above process is iterative and this final vector

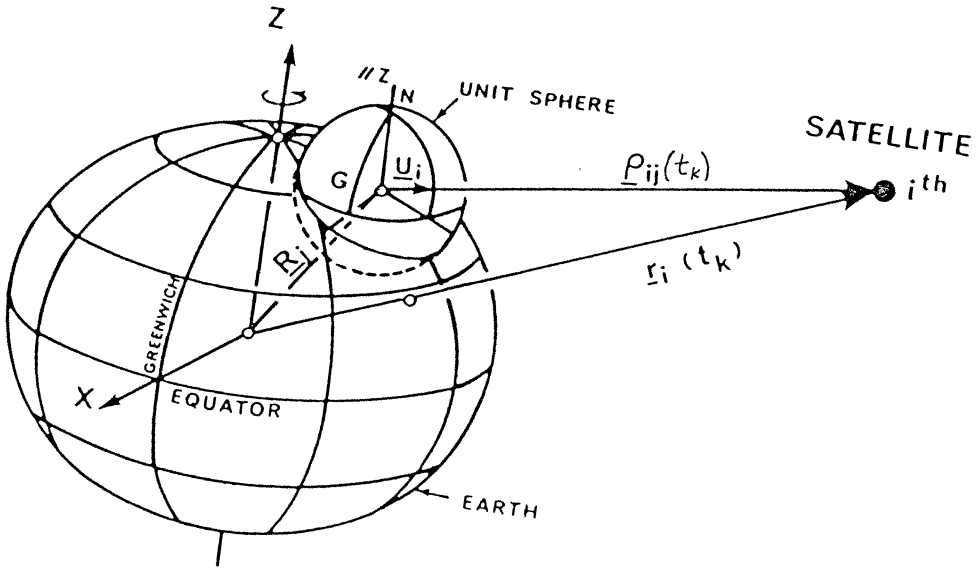


FIGURE I.1
Satellite Geometry.

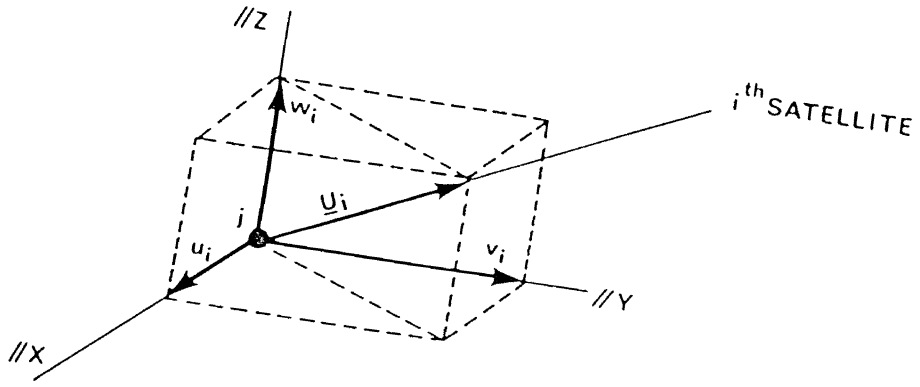


FIGURE I.2
Unit Vectors $\underline{U}_i$.

$\underline{X}_j$ can be used as a new approximation for another iteration. The number of iterations depends on an error criterion. Usually three iterations are adequate.

When a solution in latitude ($\phi$), longitude ($\lambda$), and height (h) of the user position is required, either a simple comversion of the ($X_j$, $Y_j$, $Z_j$, $\Delta t_{u_j}$) is applied into a ($\phi_j$, $\lambda_j$, $h_j$, $\Delta t_{u_j}$) solution after the above procedure is performed, or the design matrix should have rows of four elements such that

$$A_\ell = \left[\frac{\partial F_\ell}{\partial \phi} \quad \frac{\partial F_\ell}{\partial \lambda} \quad \frac{\partial F_\ell}{\partial h} \quad \frac{\partial F_\ell}{\partial \Delta t_u}\right] \quad , \quad (\ell = 1,2,3,\ldots) \quad . \qquad \text{(AI.18)}$$

For marine navigation, we can consider our height as known (usually it is taken as equal to 10 metres), and determine only two coordinates of position and the user clock bias. In such a case, the sought receiver solution would be

$$\underline{X}_j = \begin{vmatrix} \phi_j \\ \lambda_j \\ \Delta t_{u_j} \end{vmatrix} \quad , \qquad \text{(AI.19)}$$

and the design matrix $A = \left\{\frac{\partial F}{\partial \underline{X}_j}\Big|_{\underline{X}_j}(o)\right\}$

$$A = \begin{vmatrix} \frac{\partial F_1}{\partial \phi} & \frac{\partial F_1}{\partial \lambda} & \frac{\partial F_1}{\partial \Delta t_u} \\ \frac{\partial F_2}{\partial \phi} & \frac{\partial F_2}{\partial \lambda} & \frac{\partial F_2}{\partial \Delta t_u} \\ \frac{\partial F_3}{\partial \phi} & \frac{\partial F_3}{\partial \lambda} & \frac{\partial F_3}{\partial \Delta t_u} \\ \frac{\partial F_4}{\partial \phi} & \frac{\partial F_4}{\partial \lambda} & \frac{\partial F_4}{\partial \Delta t_u} \end{vmatrix} \qquad \text{(AI.20)}$$

The partial derivatives of the general mathematical model F with respect

to $\phi$, $\lambda$, and $\Delta t_u$ are

$$\frac{\partial F}{\partial \phi} = \frac{\partial F}{\partial X} \cdot \frac{\partial X}{\partial \phi} + \frac{\partial F}{\partial Y} \cdot \frac{\partial Y}{\partial \phi} + \frac{\partial F}{\partial Z} \cdot \frac{\partial Z}{\partial \phi}$$

$$\frac{\partial F}{\partial \lambda} = \frac{\partial F}{\partial X} \cdot \frac{\partial X}{\partial \phi} + \frac{\partial F}{\partial Y} \cdot \frac{\partial Y}{\partial \lambda} + \frac{\partial F}{\partial Z} \cdot \frac{\partial Z}{\partial \lambda}$$

$$\frac{\partial F}{\partial \Delta t_u} = c \quad ,$$

or in matrix notation

$$\begin{vmatrix} \frac{\partial F}{\partial \phi} \\ \frac{\partial F}{\partial \lambda} \\ \frac{\partial F}{\partial \Delta t_u} \end{vmatrix} = \begin{vmatrix} \frac{\partial X}{\partial \phi} & \frac{\partial Y}{\partial \phi} & \frac{\partial Z}{\partial \phi} & 0 \\ \frac{\partial X}{\partial \lambda} & \frac{\partial Y}{\partial \lambda} & \frac{\partial Z}{\partial \lambda} & 0 \\ 0 & 0 & 0 & 1 \end{vmatrix} \cdot \begin{vmatrix} \frac{\partial F}{\partial X} \\ \frac{\partial F}{\partial Y} \\ \frac{\partial F}{\partial Z} \\ c \end{vmatrix} \quad . \qquad \text{(AI.21)}$$

The partial derivatives involved are given in McCaskill et al [1976] as

$$\frac{\partial X}{\partial \phi} = \left[\frac{a}{(1-e^2\sin^2\phi)^{1/2}} + h\right]\sin\phi\cdot\cos\lambda + \frac{a\cdot e^2\cdot\sin\phi\cdot\cos^2\phi\ \cos\lambda}{(1-e^2\sin^2\phi)^{3/2}} \qquad \text{(AI.22)}$$

$$\frac{\partial Y}{\partial \phi} = -\left[\frac{a}{(1-e^2\sin^2\phi)^{1/2}} + h\right]\sin\phi\cdot\cos\lambda + \frac{a\cdot e^2\cdot\sin\phi\cdot\cos^2\phi\ \sin\lambda}{(1-e^2\sin^2\phi)^{3/2}} \qquad \text{(AI.23)}$$

$$\frac{\partial Z}{\partial \phi} = \left[\frac{a}{(1-e^2\sin^2\phi)^{1/2}} + h - \frac{a\cdot e^2}{(1-e^2\sin^2\phi)^{1/2}}\right]\cos\phi + \frac{a\cdot e^2(1-e^2)\sin^2\phi\cdot\cos\lambda}{(1-e^2\sin^2\phi)^{3/2}} \qquad \text{(AI.24)}$$

$$\frac{\partial X}{\partial \lambda} = \left[\frac{a}{(1-e^2\sin^2\phi)^{1/2}} + h\right]\cos\phi\cdot\sin\lambda \qquad \text{(AI.25)}$$

$$\frac{\partial Y}{\partial \lambda} = \left[\frac{a}{(1-e^2\sin^2\phi)^{1/2}} + h\right]\cos\phi\cdot\cos\lambda \qquad \text{(AI.26)}$$

$$\frac{\partial Z}{\partial \lambda} = 0 \quad . \qquad \text{(AI.27)}$$

APPENDIX II

LIST OF SUBROUTINES USED

1. ANMLY

   Computes satellite eccentric and true anomalies from mean anomaly.

2. AREA

   Defines the physical size of a plotting area.

3. CEPRMS

   Transforms rms values to along ellipse axes and computes the CEP and 2drms quantities.

4. CION

   Makes the ionospheric correction to the dual frequency carrier phase observation.

5. CLKAN

   Applies corrections for secular relativistic effects on the broadcast clock correction coefficients.

6. CLKERR

   Simulates clock error due to bias, drift, aging and random frequency fluctuations.

7. CLKRCV

   Defines the receiver's clock parameters for simulation of pseudoranges.

8. CLZCT

   Calculates the z-count for a given time of the week.

9. DASET

Performs input/output buffer operations.

10. DATUM

Defines reference ellipsoid parameters.

11. DERIV

Computes ranges to satellite, its derivatives with respect to latitude and longitude, and satellite elevation and azimuth.

12. ERRBDG

Defines error model budget for simulation of pseudorange observables.

13. FIXAPR

Reads approximate solution fix in the geodetic coordinates ($\phi$, $\lambda$, h) of a receiver and converts them into Cartesian ones (x, y, z).

14. GAUSS

Computes a normally distributed random number with a given mean and standard deviation.

15. GDOPR

Calculates the geometrical dilution of precision factors (GDOP, HDOP, VDOP, TDOP).

16. HPFLD

Computes tropospheric refraction using Hopfield's model.

17. IONDLY

Computes the ionospheric delay in terms of the maximum possible delay error.

18. IONRG

Computes the first-order ionospheric correction for range data.

19. LOGS

Locates the maximum and the minimum value from a data set.

20. LSA

Least-squares approximation for the solution of

$\delta \underline{x} = (P_x + A^T P\ A)^{-1}\ A^T\ P\ \ \underline{W}$.

21. NEPHM

Extracts satellite orbital parameters from the ephemeris record.

22. NCLOK

Extracts satellite clock coefficients from the ephemeris record.

23. OPTION

Defines various simulation processing options.

24. PLHXYZ

Computes the Cartesian coordinates x, y, z given the ellipsoidal coordinates $\phi$, $\lambda$, h.

25. PPLOT

Plots the results of two vectors on either Gould or Zeta line plotters.

26. PRES

Computes partial vapour pressure based on Hopfield's model from relative humidity and temperature.

27. READEF

Reads input satellite ephemeris.

28. SATEPH

Reads the GPS satellite ephemeris for all observed satellites, storing the values in an ephemeris vector.

29. SEARCH

Searches for those satellite identities and number which are common to a differential monitor station and a user at the same time.

30. SIMRNG

Simulates GPS $L_1$ and $L_2$ pseudoranges.

31. SORTD

Arranges a set of data in ascending or descending order.

32. STXYZ

Computes GPS satellite earth-fixed Cartesian coordinates from broadcast ephemeris parameters.

33. TRPRG

Computes tropospheric correction based on Black's tropospheric model.

34. VISIB

Determines the number and identity of all visible satellites with their direction cosines and the four satellites which yield the best navigational performance.

35. VOLUME

Calculates the volume of a special tetrahedron formed by four satellites and the receiver.

APPENDIX III

ADDITIONAL PLOTS

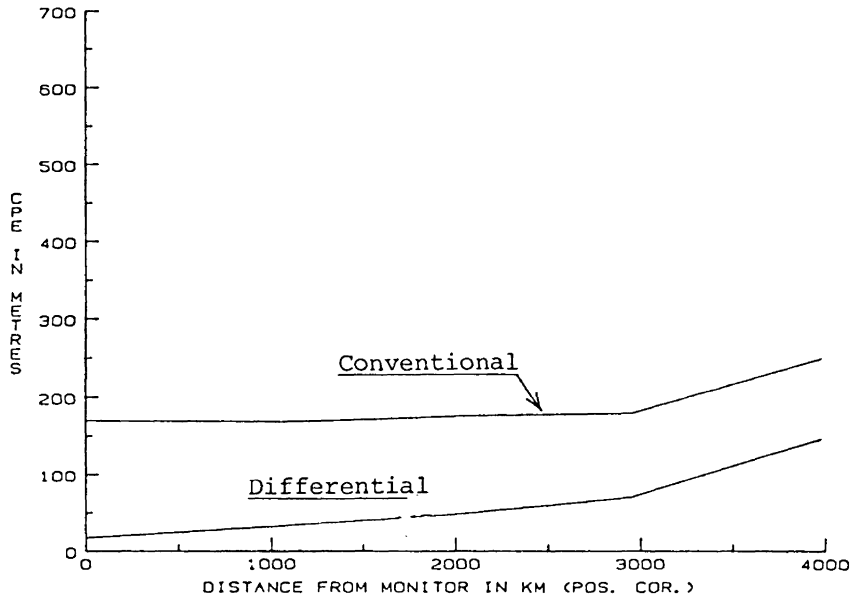


FIGURE III. 1
Position Corrections;Common Sat.;Sat. Position Degradation.

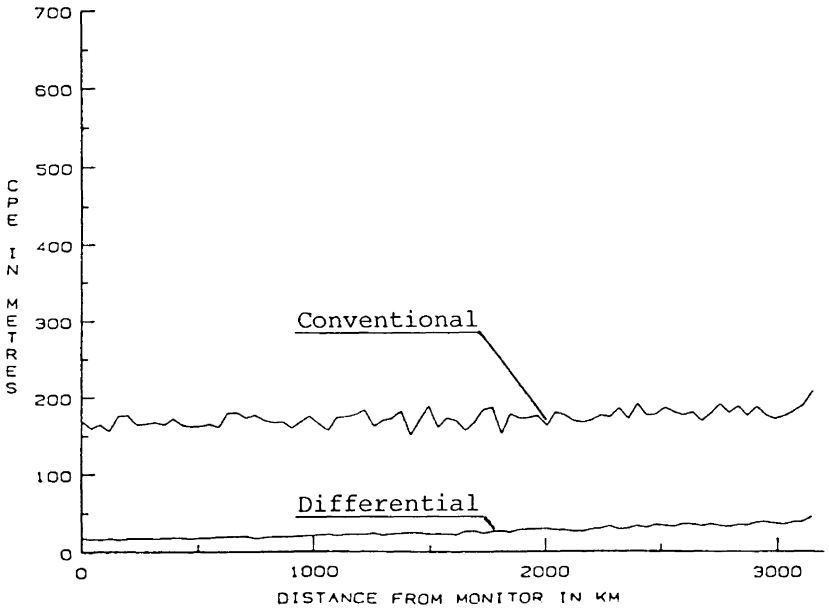


FIGURE III. 2
Range Corrections;Common Sat.;Sat. Position Degradation.

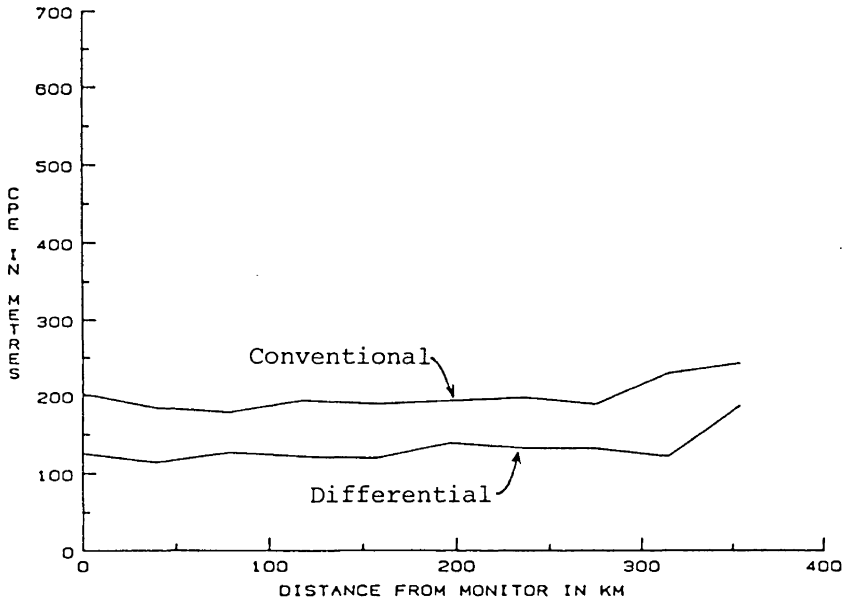


FIGURE III. 3
Range Corrections;All Visible Sat. at the Monitor;
Best at User;Sat. Position Degradation.

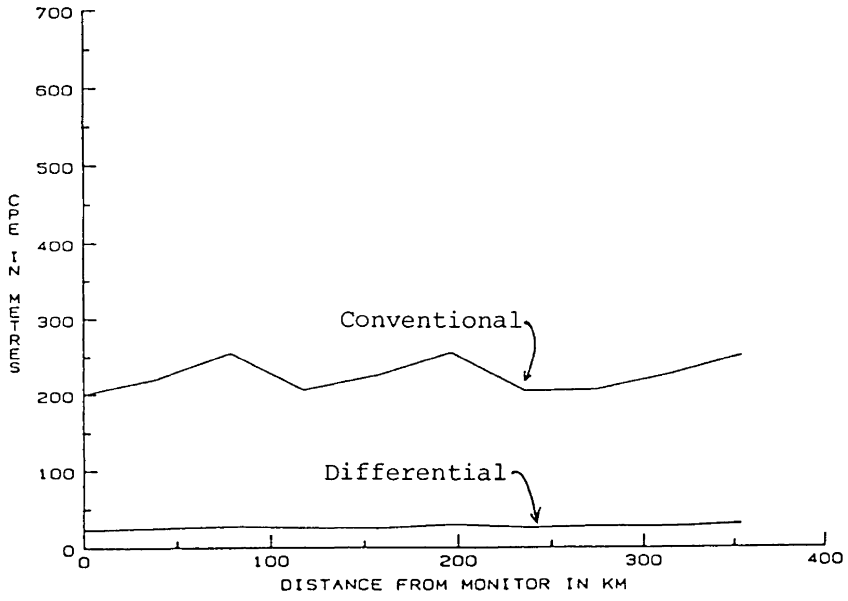


FIGURE III. 4
Range Corrections;All Visible Sat.,Clock Constrained
at the Monitor;Best at the User;Sat. Position Degradation

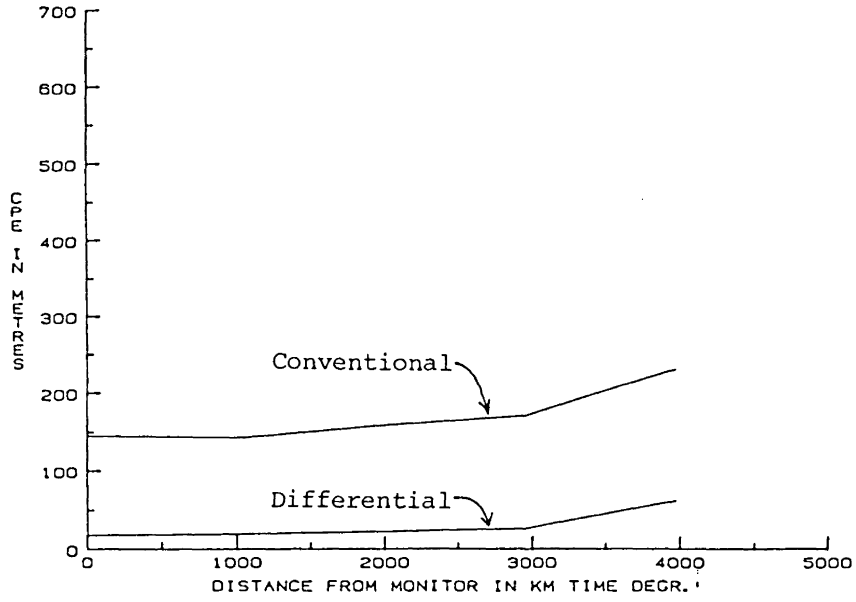


FIGURE III. 5
Range Corrections;Common Sat.;Time Degradation.

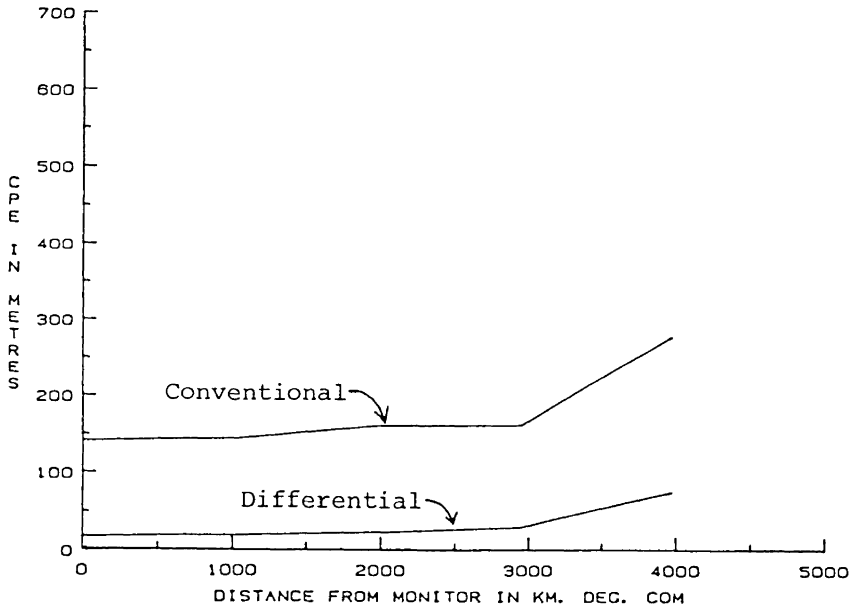


FIGURE III. 6
Range Corrections;Common Sat.;Combined Degradation.

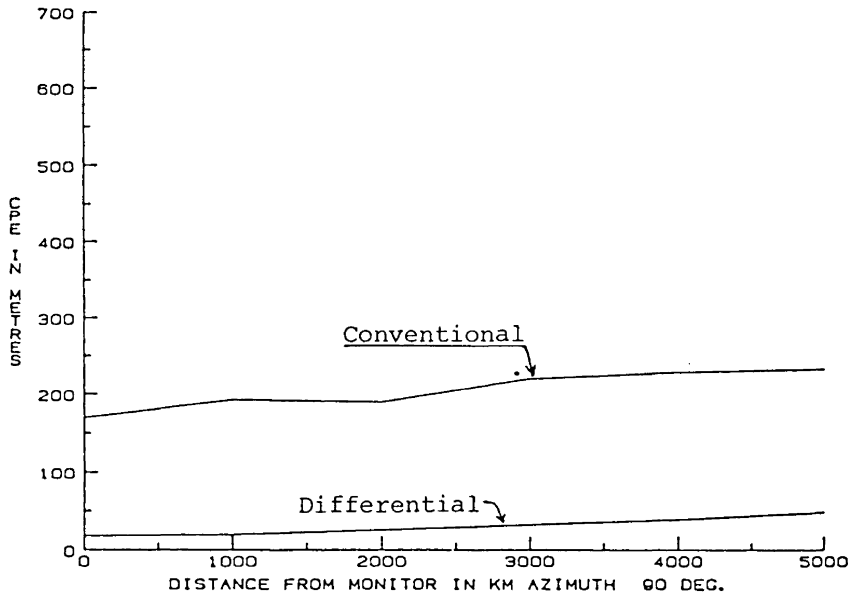


FIGURE III 7

Range Corrections;Common Sat.;Sat. Position Degradation; 90 Degrees Azimuth.

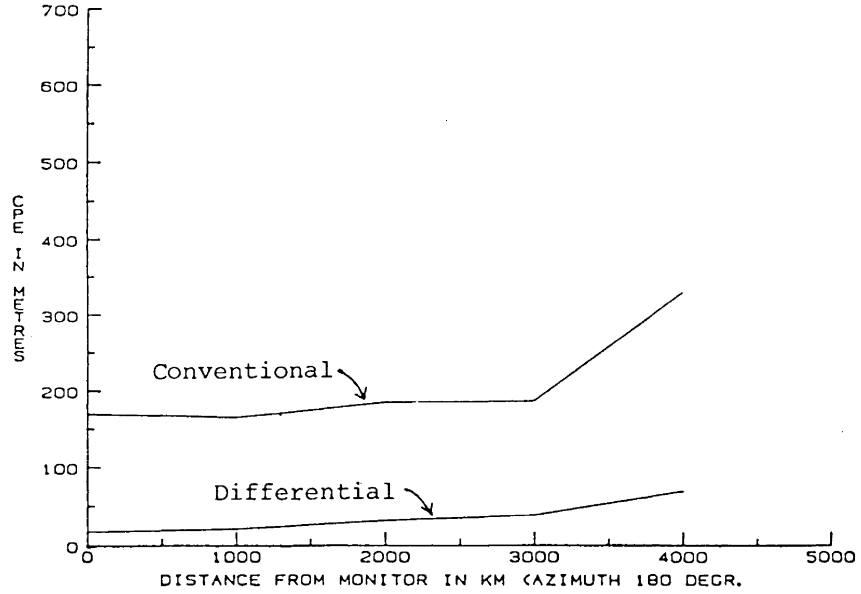


FIGURE III- 8

Range Corrections;Common Sat.;Sat Position Degradation; 180 Degrees Azimuth.